SUSPENSION HYDROGEN REDUCTION OF IRON ORE CONCENTRATE

by

Moo Eob Choi

A dissertation submitted to the faculty of
The University of Utah
in partial fulfillment of the requirements for the degree of

Doctor of Philosophy

Department of Metallurgical Engineering

The University of Utah

August 2010

The University of Utah Graduate School

STATEMENT OF DISSERTATION APPROVAL

The dissertation of **Moo Eob Choi**

has been approved by the following supervisory committee members:

Hong Yong Sohn	, Chair	**May 14** Date Approved
Michael L. Free	, Member	**May 14** Date Approved
Zhigang Zak Fang	, Member	**May 14** Date Approved
Michael S. Moats	, Member	**May 14** Date Approved
Milind Deo	, Member	**May 14** Date Approved

and by **Jan D. Miller**, Chair of the Department of **Metallurgical Engineering**

and by Charles A. Wight, Dean of The Graduate School.

ABSTRACT

A new ironmaking technology is under development at the University of Utah. This process produces iron directly from fine iron ore concentrate by a gas-solid suspension reduction, utilizing hydrogen as the main reducing agent for high reactivity and for the elimination of carbon dioxide emissions during ironmaking operation and also pursuing the direct use of concentrate to bypass the problematic pelletization/sintering and cokemaking steps in the steel industry. The technology is aimed at producing iron as a feed to the steelmaking process, eventually replacing the blast furnace.

The purpose of this research was to perform the feasibility tests of the proposed process in terms of the material and energy balances and the kinetics of concentrate particle reduction by hydrogen, together with preliminary scale-up tests. The material and energy balance calculations have shown that the process would drastically reduce energy consumption compared with that required by the blast furnace and lower environmental pollution, especially CO_2 emission, from the steel industry. The kinetic feasibility tests have also verified that the reduction rate of concentrate particles by hydrogen is sufficiently fast for a suspension reduction process and forms the most important basis for the new technology. Finally, the preliminary scale-up tests have shown that the scale-up of the proposed process is plausible if a proper method of heat supply is applied.

TABLE OF CONTENTS

LIST OF TABLES

LIST OF FIGURES

NOMENCLATURE

Symbol	Unit	Definition
A_p	m^2	Surface area of the particle
b	-	Stoichiometric coefficient
d_p	m	Particle size
D	m	Inner diameter of tubular reactor
D_e	$m^2 \cdot s^{-1}$	Effective diffusivity of H_2-H_2O in porous iron
D_{ij}	$m^2 \cdot s^{-1}$	Binary diffusion coefficient of H_2-H_2O
$(\%Fe)_o$	%	% iron in the concentrate before reduction
$(\%Fe)_t$	%	% iron in the concentrate after reduction
g	$m \cdot s^{-2}$	Gravitational acceleration
$\Delta G°$	cal	Standard Gibbs free energy
k	$s^{-1} \cdot kPa^{-1}$	Reaction rate constant
k_{app}	$m^{-2} \cdot s^{-1} \cdot kPa^{-1}$	Global apparent rate constant
k_m	$m \cdot s^{-1}$	Mass transfer coefficient
K_e	-	Equilibrium constant

K_{R2}	-	Equilibrium constant of FeO-H_2 reaction
L	m	Length of the reaction zone
m	-	Reaction order of iron oxide reduction by hydrogen
m_t	g	Mass of a reduced sample used for chemical analysis collected after reaction for time t
m_o	g	Mass of the unreduced dry concentrate calculated by Equation (17)
n_{H2}	mol	Amount of hydrogen
n^e_{H2}	mol	Amount of hydrogen at equilibrium
n_{H2O}	mol	Amount of water vapor
n^e_{H2O}	mol	Amount of water vapour at equilibrium
$n_{H2,min}$	mol	Minimum amount of hydrogen to reduce iron oxide to metallic iron including the amount to satisfy the equilibrium condition
$n_{H2,supplied}$	mol	Total amount of hydrogen fed into the reactor
n^i_o	mol	Amount of hydrogen used to remove the oxygen from iron oxide
$(\%O)_o$	%	% oxygen combined with iron in the concentrate before reduction
$(\%O)_t$	%	% oxygen combined with iron in the concentrate after reduction
p_{H2}	kPa	Partial pressure of hydrogen

p^e_{H2}	kPa	Partial pressure of hydrogen at equilibrium
p_{H2O}	kPa	Partial pressure of water vapor
p^e_{H2O}	kPa	Partial pressure of water vapor at equilibrium
Q	$m^3 \cdot s^{-1}$	Volumetric flow rate of gas through V
r	m	Radial position in the drop-tube reactor
r_i	m	Inner radius of the drop-tube reactor
r_p	m	Radius of the solid particle
R	$mol \cdot m^{-2} \cdot s^{-1}$	Reaction rate of iron oxide
Re	-	Reynolds number
Sh	-	Sherwood number
t	s	Reaction time
T	^oC, K	Temperature
u_g	$m \cdot s^{-1}$	Centerline gas velocity at furnace temperature
$u_{g,avg}$	$m \cdot s^{-1}$	Average linear velocity of gas up to η
$u_{g,max}$	$m \cdot s^{-1}$	Maximum linear velocity of gas along the centreline
u_p	$m \cdot s^{-1}$	Particle velocity relative to tube wall
u_t	$m \cdot s^{-1}$	Terminal velocity of a falling particle
V	m^3	Volume of the reaction zone ($0 \sim \eta$)

V_p	m^3	Volume of the particle
X	-	Degree of reaction

Greek Symbol

η	-	Normalized radial distance from the centreline (= r/r_i)
μ	$kg \cdot m^{-1} \cdot s^{-1}$	Viscosity of gas
ρ_B	$mol \cdot m^{-3}$	Molar density of solid B
ρ_g	$kg \cdot m^{-3}$	Gas density
ρ_O	$mol \cdot m^{-3}$	Moles of oxygen atom per unit volume of the particle
ρ_p	$kg \cdot m^{-3}$	Particle density
τ	s	Residence time of particles in the reaction zone
τ_{avg}	s	Average residence time of gas up to η

ACKNOWLEDGMENTS

I am sincerely grateful to my advisor, Professor Hong Yong Sohn, for his guidance, suggestion, encouragement and patience throughout this project.

Considerable thanks are due to Professor Michael L. Free, Zhigang Zak Fang, Michael S. Moats, and Milind Deo for many helpful discussions as committee members. Special thanks are due to Dr. Hang Goo Kim for his invaluable and sincere help, and to many fellow students, especially Yao Zhang, Josh E. Ramos, and Haitao Wang, for their support and help, and also to many other faculty and staff members, especially Karen Haynes and Kay Argyle for their help throughout the course of my graduate program.

Special thanks are extended to Mr. H.R. Kokal and Dr. P.C. Chaubal of ArcelorMittal and R. Viramontes B. of Ternium for providing the iron ore concentrates used in this work and technical discussion. I would also like to take this opportunity to acknowledge the financial support by the American Iron and Steel Institute under Project TRP 0403C for services with respect to its Technology Roadmap Program under Cooperative Agreement No. DE-FC36-97ID13554 with the U.S. Department of Energy.

Finally, I wish to express my gratitude to wife, Myung Hee, and our parents for their unselfish support and encouragement over the years.

CHAPTER 1

INTRODUCTION

More than 90% of iron is currently produced via the blast furnace (BF) process, while the balance is produced by the direct reduction (DR) processes.[1] Despite the improvements of the modern BF process in the productivity, furnace efficiency, and the campaign life, it still suffers from drawbacks. The process requires the feed in the form of sinters or pellets and coke manufactured from high-grade coking coal which is problematic from an environmental perspective. The BF process is also highly capital and energy intensive, requiring large-scale infrastructure and operation. Those constraints limit the flexibility of the BF process in terms of operation and the choice of materials.[2,3] Thus, BF iron production is projected to decrease by 15-20% between 1998 and 2015.[4] The main factors for this are the environmental regulations and the high capital investment cost.[5]

A large number of new ironmaking technologies have been developed or are under development.[6] Most of these processes, however, are not sufficiently intensive to replace the blast furnace because they cannot be operated at high temperatures due to the sticking and fusion of particles. Especially, the shaft furnace processes, being dominant types among others, require pelletization steps of iron ore concentrate accompanied by additional cost and environmental problems, and also suffer from pellet disintegration

problems.

Thus, a new technology is under development at the University of Utah[7] for producing iron directly from fine concentrate by a gas-solid suspension technology, which would reduce energy consumption by about 40% of the amount required by the blast furnace and drastically lower environmental pollution, especially CO_2 emissions, from the steel industry. Sohn,[8] who originally proposed the suspension ironmaking technology, indicates that the proposed process has a high potential for a high-intensity alternative ironmaking technology. The following is a quotation from a project report[8]:

> This is accomplished by adopting H_2-based reductant, together with bypassing pelletization/sintering and cokemaking steps of conventional ironmaking processes. Unlike other gas-based alternative ironmaking processes based on shaft furnaces or fluidized-bed reactors, the suspension reduction technology is a high-intensity process because it will not suffer from the problems associated with other processes when operated at high temperatures, mainly from the sticking and fusion of particles. Low-temperature disintegration problems encountered in the processes using pellets can also be avoided.

CHAPTER 2

SUSPENSION REDUCTION PROCESS

2.1 Current Ironmaking Technologies

A modern large-capacity blast furnace (BF) represents an extremely efficient chemical reactor, capable of stable operation and high thermal efficiency. It is suitable for handling almost all naturally occurring iron ores, and its product, the molten pig iron, can be used directly without further treatment in the existing processes for steel manufacture.[9] Furthermore, there have been countless improvements[3,10,11] in the productivity, furnace efficiency, and the campaign life of modern blast furnace operations. Much of the improvement has been the result of better preparation and charging of burden materials, the use of increased blast preheat, the oxygen enrichment of the blast, the injection of hydrocarbons and steam, the decrease of coke dependence by increasing coal injection, the development of improved cokemaking processes, and so on. Therefore, in 2007, more than 90% among about 950 million metric tons of iron production per year worldwide was produced via the BF process, with the balance produced by alternative ironmaking processes, mainly the direct reduction (DR) processes.[1,12] The production of molten iron from the blast furnace has held the predominant position to the present day as the method of supplying iron for oxygen steelmaking.

Despite its improvement and predominance, the BF process has been facing great

challenges toward innovation and development[5, 13 , 14] from serious environmental problems including CO_2 emission, tighter regulations on the agglomeration and coke plants, and the depleting reserve of coking coal. Another critical factor affecting the use of the blast furnaces is the capital and energy intensities that demand large infrastructure and operation.[2,3] A blast furnace is reported to be economical when annual hot metal production is of the order of 3 million tons.[15] These constraints limit the flexibility in operation and choice of materials. Operated at less than full capacity, the blast furnace/basic oxygen furnace (BF/BOF) route becomes less efficient than the minimills whose electric arc furnaces (EAF) can be operated efficiently at lower capacities. Such large production rates and high capital requirements make developing countries, whose steel outlets are limited, and developed countries reluctant to build new blast furnaces in the near future. Accordingly, many researchers[14] have projected a tremendous decrease in the BF iron production. Fruehan,[4] for example, expected the hot metal production via BF process to decrease by 15-20% from 1998 to 2015.

In addition to the above-mentioned factors, the shutdown of aging coking operations and older, smaller blast furnaces have driven the development of new ironmaking technologies to complement or replace the blast furnace. New ironmaking processes have been extensively explored with a view to saving resources and energy, as well as reducing environmental pollution.[6] A number of new technologies have been developed or are under development to take advantage of lower cost raw materials and lower capital cost for smaller scale equipment. These technologies aim to allow EAF to produce high quality steels utilizing alternative solid and/or liquid iron as scrap substitutes.

Processes that produce iron by reduction of iron ore below the melting point of

iron are generally classified as DR processes and the products referred to as direct reduced iron (DRI). A temperature of 1200^{o}C is considered the upper limit for the DR processes, above which the metallic iron formed absorbs carbon resulting in fusing and melting of the solid. The processes that produce a molten product, similar to blast furnace hot metal, directly from ore are classified as direct smelting processes. The direct smelting processes thus operate with product temperatures higher than 1300^{o}C because carbon is absorbed rapidly and a liquid hot metal forms. In some of the more ambitious projects, the objective is to produce liquid steel directly from ore and these processes are classified as direct steelmaking processes.[16]

The gaseous reduction of iron oxide, which is the predominant alternative process, can be further grouped by the nature of the iron-bearing feed material into two broad types: shaft furnace and fluidized-bed processes. The shaft-furnace alternative ironmaking processes have been dominated by the MIDREX[17] and HYL[18-20] processes. This additional ironmaking capacity has primarily served the EAF industry, providing an alternative to high quality and expensive scrap as a source of clean, low residual iron units. The COREX[21-24] and FINEX processes[24-29] are so far the only smelting processes to be operated on a commercial scale. Although they have a high capital cost relative to the shaft-furnace DR processes, these coal-based iron reduction processes have a notable advantage in regions where an abundant and inexpensive source of natural gas is not available. FINMET[24,30] and the earlier FIOR,[31] the natural gas-based Circored and the coal-based Circofer,[32-34] and Iron Carbide processes[35] are the representative fluidized bed processes categorized as DR technology and producing hot briquetted iron (HBI). Recently they have been extended to direct smelting process as the FINEX process emerges.

Any alternative processes that can replace the blast furnace must be sufficiently intensive to meet the large production rates required for economic competitiveness. Most of the above processes, however, are not sufficiently intensive because they cannot be operated at high temperatures due to the sticking and fusion of particles.[36,37] Especially, the shaft furnace processes, being the dominant type among others, require pelletization steps of iron ore concentrate accompanied by additional cost and environmental problems, and also suffer from pellet disintegration problems.[38-41] Therefore, a new technology for alternate ironmaking has been proposed[7] to utilize concentrate from low-grade iron ores and to reduce global environmental problems and energy consumption.

2.2 Technology Description of Suspension Reduction Process

The suspension ironmaking technology is defined by Sohn[8] as follows:

> This technology is based on the suspension reduction of iron ore concentrate by hydrogen-based reductants although reformed natural gas, a reducing gas generated by partial combustion of coal or waste plastics, or a combination thereof can also be used. Here, the term ‘suspension’ is used to represent processes such as the ‘flash’, ‘flame reaction’, or ‘cyclone’ processes. In addition to the ultimate objective of significantly reducing energy consumption and environmental pollution in the steel industry, the suspension process presents a high-intensity process, especially by starting with the finely-sized concentrate. As an example of production rate of such a suspension process, a flash smelting furnace (significantly smaller than what would be used for iron flash reduction) produces 0.3-0.4 million tons of copper per year.

The technology description, advantages, and technical issues of the proposed process will be discussed further with the research objectives at the end of this chapter.

2.2.1 Direct Use of Iron Ore Concentrate

An important factor in the development of the suspension reduction technology is the large quantities of fine iron ore concentrates currently produced in the United States and elsewhere that are well-suited for suspension reduction.

In 2008, the gross iron ore production in the U.S. was 54 million metric tons equivalent to about 3% of world total production. Minnesota (Mesabi Range) and Michigan (Marquette Range) taconite mines account for almost all U.S. iron ore production meeting about 80% of domestic demand.[42,43] The ore types from the Lake Superior district include (1) direct shipping ores and lump ores, (2) beneficiated ores which can be upgraded easily by gravity methods, (3) magnetite taconite which is concentrated by magnetic methods after fine grinding, (4) hematite bearing jaspers which can be concentrated by flotation techniques. Magnetite taconite, the principal iron ore in the U.S., is a hard, dense, compact, fine-grained rock, commonly containing from 40-55% silica and 15-35% iron in the form of magnetite and thus requires beneficiation prior to commercial use.[44,45]

Beneficiation is accomplished by a variety of processes whereby extracted ore from mining is reduced to particles that can be separated into mineral and waste, the former suitable for further processing or direct use. As-mined taconite ore is transported to a crushing plant for size reduction and then to a beneficiation plant for fine grinding and concentration. The iron ore materials of the Mesabi Range are mainly magnetite taconites being -37 μm (-400 mesh) out of the magnetic separation and those from the Marquette Range are magnetic and nonmagnetic taconites requiring even finer grinding at -25 μm (-500 mesh) for the liberation of minerals by selective flotation or magnetic methods or a combination of both.[44] The finely-sized concentrates are usually

agglomerated into 6-10 mm balls and fired into hard durable pellets to produce a suitable feed for shaft-type ironmaking furnaces as the fines cause plugging of the bed and sticking at reduction temperatures.[46]

However, iron ore agglomeration processes such as pelletizing and sintering cause considerable energy consumption, pollution problems and additional costs to the ironmaking processes. Fuel supply for pelletizing typically ranges from 0.5 to 1 GJ/metric ton of pellets. Although it is noted that the oxidation of magnetite to hematite during pelletizing magnetite concentrate provides a considerable portion of the heat requirement,[44] the balance is still significant and also the oxidation generates another problem by lowering the relative iron content in the feed materials. Binders generally used to raise the wet strength of green pellets are also a significant cost element and add to the silica content of the final product. Therefore, the unit price for pellets is about 40% higher than that for concentrates according to the prices of iron ores imported to the U.S. in 2007.[43] The requirement of fuel supply in the form of oil, natural gas, and coke breeze and binders such as limestone and dolomite contributes to the release of large amount of hazardous and greenhouse gases (GHGs) into the atmosphere. The waste gases from pellet plants include CO_2, CO, CH_4, NO_x, and SO_2. Recent concerns about global warming have seen the operators of iron ore agglomeration plants come under increased pressure to reduce the consumption of fossil fuel-based energy, and in turn, greenhouse gas (GHG) emissions.[47] In addition, the current processes using pellets cannot take advantage of the fact that concentrates are in the form of very fine particles with large surface area which would allow rapid reduction by a gas. The specific surface area of fine concentrates is drastically diminished by fusion between particles during agglomeration processes.

Therefore, there have been tremendous efforts toward improving the existing ironmaking processes[23,48,49] or developing alternative technologies to take advantage of direct use of iron ore fines or concentrates without agglomeration for environmental and economical considerations.[50]

The fluidized bed process is used in direct reduction or smelting processes with iron ore fines. The FIOR, FINMET, Circored/Circofer, Iron Carbide and the recent FINEX processes are the representative large-scale application of the technology. Here, it should be noted that iron ore fines are defined as iron ore with the majority of individual particles measuring less than 10 mm diameter, which is completely different from concentrates whose sizes are less than 100 μm.

The early process with the direct use of iron ore concentrates was the Höganäs process,[51] a tunnel kiln ironmaking technology invented in 1908. Concentrate particles are directly charged with coal or coke dust as the reductant and the metallized iron tube is produced. The tube is crushed for sale as high purity iron powder used in powder metallurgy or as high grade scrap for producing special steels. Although the process is still in commercial use, the production capacity is very low at about 38,000 metric tons annually since the total retention time in the tunnel kiln is approximately 80 hours.

Fine iron ore concentrates are well-suited for flash reactors which have been adopted widely for smelting and converting sulfide concentrates. The application of a flash reaction process to the reduction of iron oxides has been considered, but it was stated that the reduction rate would be too slow for such a process to be feasible.[52] The in-flight processes have mostly been investigated by the use of gas burner or plasma torch, or a combination thereof to enhance mass and heat transfer in a turbulent gas-particle flow.

The use of a cyclone for the partial reduction and melting of iron ore concentrate was performed by Bartlett et al.[53,54] While axially injecting the taconite feed (5 to 45 μm), a natural gas burner port and a nontransferred arc plasma torch port using an Ar-N_2 mixture as the plasma gas were tangentially situated. Because of concerns over the rapid erosion of the torch electrodes, the natural gas burner was used only to preheat the cyclone to 1000-1200^{o}C prior to operating the plasma system to maintain an average cyclone temperature of 1500^{o}C or higher. Carbon monoxide as reductant was fed along the taconite feed line and the degree of reduction ranged from 80 to 95%.

The earliest attempt of flash reaction systems to the reduction of iron ore concentrate by the use of a burner was conducted by Johnson and Davison[55] who investigated the feasibility of producing metallic iron from a prereduced iron ore in a vertical cyclone furnace. A pulverized fuel burner was applied by burning fine coal partially with air or oxygen to produce a highly reducing, high-temperature atmosphere which reduced concentrate falling through the center of the burner. Although over 98% Fe was obtained at 1500^{o}C of operating temperature, greater than 35% prereduction was required considering the slow reaction time and the practical reactor dimensions.

Unlike the previous technologies, the jet smelting technology developed by Cavanagh[56-58] employs only a gas burner for producing molten iron directly from iron ore concentrate using natural gas as the preferred fuel and reductant. The 80-90% complete combustion of natural gas with pure oxygen makes a high temperature flame in which the concentrate particles are rapidly heated up to a high temperature. The ore used was a magnetite concentrate ground to -250 μm (-60 mesh) and contained 5-10% -74 μm (-200 mesh) fraction. Secondary natural gas is supplied to provide a reducing gas mixture of hydrogen and carbon monoxide. The hot ore particles promotes cracking of the

secondary gas and is rapidly reduced by the concurrent flow of hot reducing gas. The high velocity stream of reduced ore particles is blown vertically downwards into a bath of molten metal and slag. The carbon content of the molten phase after reduction was low, being in the range of 0.1%, indicating that very little carbon is derived from reaction with the reducing gas. The bath is maintained at a high carbon content by injecting powdered graphite so that the final reduction takes place in the slag layer. When the particle velocity is sufficiently high, very little dusting occurs if the exhaust velocity is regulated. The flame temperature drops from 1980^{o}C at the top to 1540^{o}C at the bottom. The reduction takes place at atmospheric pressure. Although the jet smelting technology is a good example of applying a flash reaction system with a gas burner to ironmaking process, the degree of reduction was still low. Only 70% conversion from ore toward metal was reported as the maximum value. This is likely due to the larger ore particles (-250 μm) than the typical concentrates and low hydrogen content (less than 55%) in the reducing gas streams resulting in lower reactivity than pure hydrogen.

The early try of converting iron ore concentrate directly to metallic iron in-flight is found in the work done by Kazonich et al.[59] They built a prototype reactor incorporating rocket technology in which -44 μm (-325 mesh) magnetite concentrate from taconite ore could be reduced to iron metal in less than 50 ms in a high temperature (1200-2500^{o}C) flow through high pressure (1300-1700 kPa) reactor. Fuel rich mixtures of propane (C_3H_8) and oxygen were burned to produce highly turbulent reducing gases whose composition was roughly 66% H_2 and 33% CO. Although they successfully acquired fully reduced metallic iron, the maximum iron recovery was very low (less than 50%) due to the low controllability of high temperature and pressure reducing gas stream and the inefficiency in the cyclonic separator of the quenched iron particle product.

The suspension reduction process under development[7] is essentially the first flash-type ironmaking process converting iron ore concentrate directly to metallic iron in-flight that would be possible to be adopted in a large industrial scale. The intent of the proposed process is to produce iron directly from fine concentrate without going through pelletization or sintering and thus avoiding the need for coke. In addition to the numerous benefits by avoiding the agglomeration and cokemaking steps, this process concept allows intensive operation unlike other alternative ironmaking routes. For example, direct reduction (DR) and fluidized bed processes cannot be operated at high temperatures because they suffer problems of sticking and fusion. This problem will be greatly diminished in the dilute particle suspension in a suspension process and thus the proposed process can be operated at high temperature, which allow the process more intensive.

Another benefit is that the direct use of fine concentrates can avoid the environmentally problematic and energy-intensive cokemaking step. Coke is produced by baking coal in the absence of oxygen to remove the volatile hydrocarbons contained in coal. The resulting coke is mechanically strong, porous, and chemically reactive, which are all critical properties for stable blast furnace operation. In addition to supplying carbon for heat and the reduction of iron ore, coke must also physically support the burden in the blast furnace shaft and remain permeable to the hot air blast entering from the bottom.

However, cokemaking is extremely problematic from an environmental perspective as many of the hydrocarbons driven off during coking process are hazardous. The coal dust generated during the transportation, and the charging of coal and the discharging of coke also represent a significant environmental problem. In addition to tightened pollution control requirements and associated production cost increase, the

necessity for replacing the aging coking facilities and the coke price increase due to the depletion of coking coal have made cokemaking step an economical liability. Therefore, the supply of coke becomes more critical and the decreasing of the coke rate has been a major focus of the development in the blast furnace for several decades. The injection of pulverized coal, natural gas, oil, and recycled plastics to the blast furnace has been the major efforts to replace a portion of the metallurgical coke.

However, extensive experimentation in the U.S. and elsewhere has found that the lowest coke rates (tons of coke consumed per ton of blast furnace iron produced) at an optimum combination of fuels is still higher than 0.4 due to the requirements on the mechanical strength to support the iron ore burden and the permeability for the flows of the hot air blast and the reducing gas stream in a blast furnace.[3,60] The alternative methods also suffer from other problems such as the build-up of partially combusted coal char at high coal injection rates. Thus, all the problems associate with the use of coke can be resolved only in an alternative ironmaking process that does not require it.

2.2.2 Hydrogen as a Reductant and Fuel

An additional factor to consider is the expectation of the development of hydrogen economy in the U.S. and the availability of inexpensive hydrogen.[7,61,62] In the proposed process, iron ore concentrates are reduced to a high degree of metallization in suspension by hydrogen-based reductants. Ironmaking processes using hydrogen as the reductant and/or fuel would have several technical advantages such as (1) generated gases are essentially composed of H_2O and H_2, thus avoiding the release of CO and CO_2 (2) rapid reduction rate compared to CO_2 reduction, (3) low carbon content of the produced iron, (4) replacement of the expensive and pollution-prone metallurgical coke.[63]

The steel industry is faced with a wide range of environmental concerns that are fundamentally related to CO_2 emissions, high energy requirement, material usage, and byproducts associated with large amount of steel production worldwide. The impact of environmental regulations on steel companies is largely in the ironmaking area because more than 80% of energy is consumed and most pollutants are created in these operations.[64] As climate changes, reportedly accelerated by manmade carbon emissions, have become a significant global issue, increasing demand to minimize greenhouse gas (GHG) emissions has intensified the pressure on steel makers and certainly impacted the direction of the development of steel industry. The mitigation of CO_2 emission, having the highest global warming effects and accounting for half the effect of all GHGs[14,65] in the steel industry, has been performed by modifying and integrating currently available technologies, especially more efficiently utilizing the heavily fossil-oriented energy sources. Examples include less energy-consuming bonding technology for pelletization, prolonging coke-oven life and reducing pollutant emission in coke-making, and increasing the campaign life of BF and the pulverized coal injection (PCI) rate.[66]

Although CO_2 emission per ton steel has been noticeably reduced due to such efforts during the past decades, the steel industry still contributes around 5-7 % to total anthropogenic emission of CO_2.[67-69] Since modern steel plants operate very close to the limits of what is technically possible, even a major cooperative R&D initiative, such as, ULCOS (Ultra-low carbon dioxide steelmaking)[70,71] launched by a consortium of 48 companies and organizations from 15 European countries can only suggest alternative technologies with the aim of a 50% reduction of today's CO_2 emissions inevitably in combination with carbon capture and storage (CCS) technology. It is obvious that further reduction of CO_2 emission is not possible without drastic technological change and, in the

long term, the steel industry will eventually reduce the CO_2 emission by introducing carbon-free energy and reducing agents - the use of hydrogen, renewable energy – and/or storing CO_2 securely or converting CO_2 into a harmless substance. One of the most attractive aspects of using hydrogen as an alternative fuel/reductant source is that there are no carbon-containing products. Ideally, hydrogen reduction would imply zero CO_2 emissions.

The replacement of blast furnaces requires the new process to be highly intensive. Bogdandy and Engell[72] pointed out that the H_2 reduction times of fine iron oxide particles should be less than 5 seconds at the mean temperature of 1150^{o}C in the concurrent reaction vessel in order to overcome the blast-furnace throughput performance. Starting with fine concentrate and taking advantage of the high reactivity of hydrogen toward iron oxide, the suspension process has proven to meet the high intensity requirement in the present work and thus shown the highest potential for a high-intensity alternative ironmaking technology.

Other expected benefits include the fact that hydrogen reduction yields iron that does not contain carbon, and thus the iron can directly go through refining without requiring the converting step.[7,73] The highly reducing environment of the blast furnace produces hot metal or carbon saturated iron (~5 wt.% C). However, most steel products have a carbon content of less than 1 wt.% C and even lower carbon content is required for the ultra low carbon steel in the automobile industry.[3,74] Due to the difficulties in controlling the reduction of iron ore to low-carbon iron in a highly productive and cost-effective process, the capability of producing steel or low carbon iron directly became an important condition in the development of a new ironmaking process.

Besides, carbon-based fuels and reductants contain ash and sulfur that influence the product quality.[46] Employing hydrogen as the main reductant and fuel can minimize the degradation of the reduced iron ore and avoid the environmental and economical problems coming from the cokemaking step in the current ironmaking process.

To take advantage of the use of hydrogen as fuel/reductant, there has been many developments of hydrogen-based ironmaking processes. Most of the development was made in direct reduction (DR) processes to utilize hydrogen's higher reactivity as compared to carbon monoxide toward iron oxide at lower operating temperatures than in the BF process. MIDREX and HYL processes are the main examples. Although reformed natural gas is the main reductant for those processes at present, they are capable of reducing iron ore with any combination of H_2 and CO, even with 100% H_2.[69] In addition to the shaft furnace processes, the fluidized bed processes have long been developed to utilize hydrogen. POSCO's FINEX and Lurgi's Circored processes use hydrogen-rich gas and pure hydrogen, respectively, for the reduction of fine ore. However, the total amount of hydrogen-reduced iron remains a very small fraction of the total world iron production.

Hydrogen can be produced either from fossil media or from carbon-free sources. At present, hydrogen production from fossil sources in the form of coal, oil, and natural gas is predominant due to the high cost and premature technology of hydrogen production from nonfossil sources. However, the necessity for sustainable hydrogen production for environmental compatibility and energy security is compelling. There have been tremendous amounts of efforts to develop carbon-free hydrogen production technologies utilizing solar-derived, wind, nuclear, or geothermal energy.[75] Among others, nuclear energy is cited as the best resource for economically producing large quantities of hydrogen.[76-80] Not surprisingly, the possibilities of applying nuclear energy

to ironmaking by the use of hydrogen as the main reducing gas and energy carrier have been sought for several decades to compensate the large material and energy consumption rate and to move toward an environmentally benign process. In addition to the development of DR processes coupled with a nuclear reforming process, for example, the CSM (Centre Sperimentale Metallurgico, Rome) process[81] was designed to use nuclear energy for hydrogen production via a steam reforming process and for superheating the reducing gas to utilize it in a fluidized bed reactor. More recently, South Korea's POSCO, the world's fourth largest steel producer as of 2008, announced plans to eventually halt CO_2 emission by switching to a nuclear energy-based hydrogen steelmaking process.[82,83] Massive hydrogen production is anticipated to be obtained from small or mid-sized nuclear reactors, for example, the SMART (System-integrated Modular Advanced ReacTor) nuclear reactor under development through collaborative efforts with the Korea Atomic Energy Research Institute.[84,85]

As the development of ultrasafe nuclear power plants that can provide electric power for the production of inexpensive hydrogen is in progress, the steel industry must be ready with technologies to take advantage of energy alternatives when available. This is where the suspension reduction technology, which can take full advantage of using hydrogen as fuel/reductant, becomes extraordinarily attractive and promising.

2.2.3 Advantages and Applications of the New Technology

The new technology will have the following advantages according to Sohn[8]:

- Elimination of the coke oven and the pelletization or sintering step with the associated considerable energy consumption, pollution problems and costs by the direct utilization of the large quantities of fine iron ore concentrates produced in the United States and elsewhere.

- Significant reduction, or even complete elimination, of carbon dioxide emission from the steel industry, depending on the choice of the reducing agent and fuel used in the proposed suspension reduction technology. (The calculated details will be presented subsequently.)
- Energy savings of up to 40 % of the amount required in the blast furnace technology. (Detailed calculations to reach this conclusion will be presented subsequently.)

Sohn[8] also indicates the possible application of the suspension reduction process as either an independent ironmaking step or a direct steelmaking process.

> The proposed technology is to be applied either as an ironmaking step or as an integral part of a possible direct steelmaking process from iron ore concentrate. When applied as an ironmaking unit, the product from the suspension process can be collected either in the solid state or in the molten state.

The solid state product could be briquetted for easy and safe handling prior to shipment. When the steelmaking unit is adjacent, the product iron could be transferred either to a coal-based or an electric melter for producing a molten metal feed or directly to the secondary steelmaking units such as an electric arc furnace (EAF). Furthermore, the direct transport of hot product is also attractive. This will save the reheating energy and reduce the reoxidation of the produced iron. The efficiency of hot charging of direct reduced iron (DRI) for mills with direct reduction (DR) plants on-site has already been verified, for example, by HYTEMP iron from the HYL process.[20] Hot charging of iron product from this process is expected to be more efficient than DRI pellets because the smaller size makes the pneumatic transport easier and takes shorter time to be melted in the subsequent steelmaking unit.

It is also promising to apply the proposed technology for a direct steelmaking in a single unit as illustrated in Figure 1.[8] In the nonferrous industry, a flash furnace similar

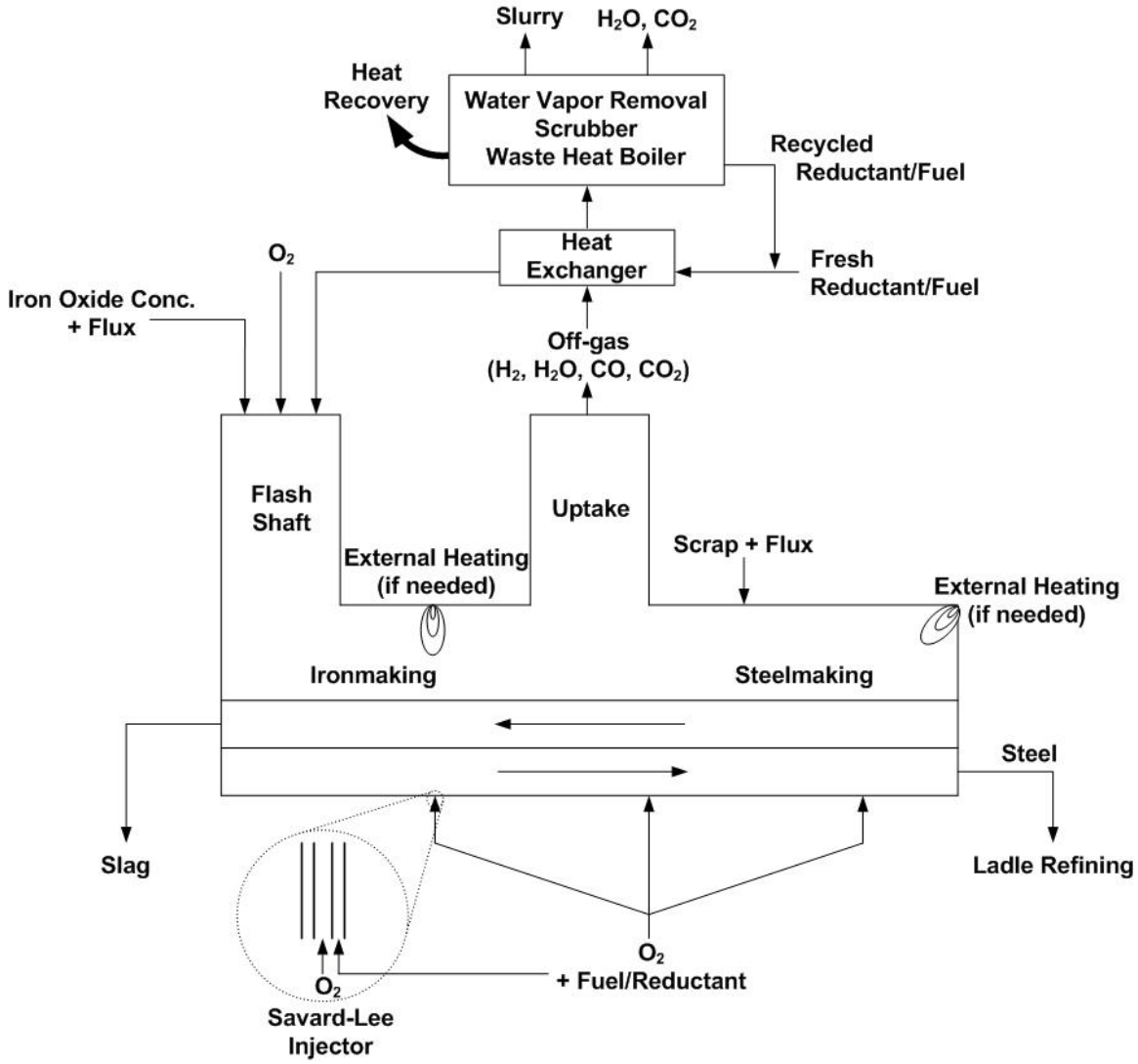

Figure 1. A schematic diagram of a possible direct steelmaking process in a single unit. (updated diagram of similar drawing in Ref. 8)

to what is shown in the figure has been the most widely used smelting furnace, in which fine concentrate particles are oxidized, form molten droplets, and collected as a bath in the settler. Using modern monitoring and control technologies and expanded fundamental knowledge of reaction thermodynamics and kinetics, a new process capable of producing steel or low-carbon iron in a single continuous reactor might be possible. Then, the conventional unit processes of the coke plant, sinter or pelletizing plant, blast furnace, and oxygen steelmaking furnace could be replaced by a single reactor.

2.3 Technical Issues to be Overcome

The ultimate goal in the development of the suspension ironmaking technology is presented by Sohn[8] as follows:

> The primary objective of the proposed research is to develop an ironmaking process based on hydrogen and fine iron ore concentrates with the ultimate objective of eliminating or drastically reducing the generation of CO_2 in the steel industry. Before an industrially viable process can be developed, a number of technical hurdles must be overcome.

In the quoted paragraph, the ‘proposed research’ means the entire project covered by the U.S. DOE-AISI research program. The main issues are discussed individually here.

2.3.1 Rate of Reduction

An important condition for the proposed process is whether iron ore concentrate can be reduced by hydrogen-based gaseous reductants to a high metallization degree within a few seconds of the residence time typically available in a suspension reduction process. Although there has been a great deal of work carried out on the hydrogen reduction of iron oxide, little has been published on the hydrogen reduction of fine

concentrate particles of -37 μm (-400 mesh) size. Most rate data on iron oxide reduction have been obtained typically with pellets or lump ores of millimeter and larger sizes, much larger than the concentrate particles to be used in the suspension reduction process. Furthermore, previous work has also been done at relatively lower temperatures because pellets in shafts or in fluidized beds are reduced at those temperatures and suffer problems of sintering and fusion at higher temperatures.

Further, there are conflicting assessments as to whether the rate of iron oxide reduction is sufficiently rapid for the generally short residence times available in a suspension reactor. Based on the rate data obtained using pellets of 70 to 42,000 μm in diameter at temperatures ranging from 600-1000^{o}C, Themelis and Gauvin[86] concluded that the process is controlled by the rate of reaction. The linear rate of Fe_2O_3 reduction in pure hydrogen was estimated to be 1.7 μm/s at 800^{o}C and 2 μm/s at 1000^{o}C.[52,86,87] Davis and Feld[88] studied the flash reduction of fine low-grade iron ore (monosized by passing -100, -200, or -400 mesh size equivalent to -149, -74, or -37 μm, respectively) by hydrogen and reformed natural gas in a dilute-phase system at 500 to 900^{o}C. Concurrently flowing with the reducing gases, Alabama brown iron ore and Mesabi semitaconite ore were observed to be reduced rapidly. However, the maximum reduction extent was only 77% by hydrogen and the reduction rates were equivalent to a linear rate of 1-2 μm/s. At this rate, in accordance with Themelis and Gauvin's results, a particle of 40 μm size would take 10 seconds or longer to react completely in pure hydrogen. This rate may be too slow for a suspension reduction process, especially a flash reduction process.

Based on careful examination of the methodology and reasoning used to reach this conclusion,[52,86] however, Sohn[89] noted a number of uncertain factors in this

calculation as to the validity of extrapolation to very small particles: Firstly, the particle shape was assumed to be spherical in this extrapolation whereas naturally occurring fine particles have irregular, nonspherical shapes with sharp edges, corners, elongations and various degrees of flatness. The reaction rates of particles are dependent on the surface area to volume ratio or the size of the smallest dimension rather than their nominal screen size. Thus, fine concentrate particles are expected to react faster than estimated based on a spherical shape which has the lowest surface area of any other shapes with the same screen size and reacts most slowly.[8,89] Ezz and Wild's work[90] on the hydrogen reduction of fine hematite ore particles sized between 50 and 260 μm indicated that the most influential characteristics of particles on the reduction rate are particle size and specific surface area and the angular particles were more rapidly reduced than sub-angular particles due to their larger specific surface area. Secondly, judging from the low activation energy (3,000 cal/mol), Sohn[89] further noted that Themelis and Gauvin's kinetic data[86] mostly based on large pellets are likely to have included mass transfer effects. Mass transfer controlled conversion rate has a much stronger dependence on particle size than chemically controlled rate, except in the case of an initially nonporous particle reacting under the control of external mass transfer between the bulk gas and particle surface. In the latter case, which is encountered very infrequently, the particle size effect is the same as when chemical reaction controls the overall rate.[91] Contrary to the above estimated rate, Fuji et al.[92] stated in a preliminary report that the hydrogen reduction of particulate Fe_2O_3 to FeO had an activation energy of 26,000 cal/mol and that of FeO to Fe 41,000 cal/mol. They further observed 90% conversion of Fe_2O_3 (9 μm particle) to Fe in 0.6 second in pure hydrogen at 1000°C. Hayashi and Iguchi[93] investigated the final stage of iron oxide reduction from FeO (58 μm particle) to Fe at

1500-1600^{o}C and reported about 80% fractional reduction in less than 0.5 seconds with N_2-30% H_2 reducing gas mixture and about 26,000 cal/mol of activation energy. More recently, Nomura et al.[94,95] observed that the fraction reduction of fine iron ore particles (32-45 μm) by N_2-11% CH_4, which decomposes into carbon and hydrogen at temperatures above 500^{o}C, reached over 90% at 1300^{o}C within 1 second.

Based on the examination of the rather limited amount of literature, it is clear that the reduction rates of the concentrate-size particles might be significantly higher than the extrapolated values and thus a carefully designed and performed investigation of the kinetics of hydrogen reduction of concentrates particles is warranted. Additionally, tests in simulated suspension-reduction conditions are needed as a necessary step toward a comprehensive evaluation of the feasibility of an industrial process.

2.3.2 Heat Supply

Unlike sulfide smelting reactions, which are highly exothermic and thus need little or no external heating, the hydrogen reduction of iron oxide requires an external heat supply. The heat may be generated internally by burning a portion of the reducing agents, or supplied by plasma or burning of other fuels. These types of processes in which hot reducing gas environment is created internally are used in numerous industrial operations.[8] Examples include the reforming of natural gas and coal gasification by partial combustion,[17] and the gas-fired Flame Reactor Process for treating electric arc furnace (EAF) dusts.[96,97] Preheating concentrates before injection might be considered for supplying additional energy just like scrap preheating at EAF mills for energy conservation, shorter cycle times, and reduced operating costs.[3,5] The preheating energy can be obtained by recovering sensible heat from the exhaust gas and the post-

combustion of the flammable gas in the off-gas. This issue is raised here to indicate that it is an important item of consideration but has a likely solution based on existing technologies.

This is why the feasibility tests have to be performed in terms of the material and energy balance on the proposed process in addition to the kinetics. The reduction temperature will be one of the main interests during the kinetic feasibility tests and the energy requirement of the proposed process compared with the conventional ironmaking routes such as the blast furnace (BF) and direct reduction (DR) processes will also be emphasized.

2.3.3 Equilibrium Hydrogen Utilization

Another important technical issue to be addressed in fully developing the proposed ironmaking method into an industrial process is the equilibrium limitation of iron oxide reduction.[8] The hydrogen reduction of hematite to magnetite is essentially irreversible and that of magnetite to wüstite also has a large equilibrium constant. Thus, the equilibrium gas products of these reactions contain little reducing gas, i.e. the degree of equilibrium utilization is very high. However, the final stage of the reduction, i.e. the reaction of FeO with H_2 or CO, is considerably limited by equilibrium. For example at 1400°C,

$$FeO\ (s) + H_2\ (g) = Fe\ (s) + H_2O\ (g)\ ; \qquad \Delta G^\circ \approx +90\ \text{cal}\ (1400^\circ C)^{98} \qquad (1)$$

This reaction has a slightly positive standard Gibbs free energy, and the equilibrium gas product has a H_2/H_2O molar ratio of 1.0 at 1400°C, i.e., 50 % H_2 and 50

% H_2O excluding any inert gas. Hydrogen compared with CO is the better reducing agent in terms of the degree of utilization at temperatures over 800^oC.[99] With pure CO, at 1400^oC, only 22 % is utilized at equilibrium. However, some of the remaining CO can be used to form hydrogen in the presence of water vapor (the water-gas shift reaction). Thus, the product gas from this reaction will contain a substantial amount of unutilized reducing gas. This will require the removal of water from the off-gas and recycling of hydrogen. Therefore, it is necessary to determine the amount of excess hydrogen in the reducing gas to obtain a high reduction degree within a few seconds of residence time and the effect of water vapor with low excess hydrogen.

2.4 Research Objectives

The goal of this study is to determine the basic feasibilities of the proposed ironmaking technology based on the direct gaseous reduction of fine iron ore concentrates in a suspension reduction process. These include reaction kinetics and material/energy balances. Based on the above discussion, the following specific objectives were established:

(1) Perform detailed material and energy balances, with special attention to carbon dioxide generation from the possible use of carbon-containing fuels such as natural gas or coal.

(2) Determine the kinetics of gaseous reduction of iron ore concentrates as a function of temperature and gas composition including water vapor and CO/CO_2.

(3) Perform preliminary scale-up tests on simulated suspension reduction process by the use of a large laboratory flash reactor.

CHAPTER 3

MATERIAL AND ENERGY BALANCES

3.1 Material Balance and Calculation of CO_2 Emission

The input and output streams and quantities for the proposed technology using various types of fuel/reductant used, i.e. hydrogen, natural gas (considered as CH_4), and bituminous coal (considered as $C_{1.4}H$) are given in Table 1, together with those for the conventional blast furnace (BF) operation.[60,100] Methane and coal were assumed to be used as precursors for syngas (H_2 + CO).

The basis for the balance calculation was set to be 1 metric ton of molten Fe at 1600^oC instead of hot metal because the compositions of hot products in different processes will not be the same. The hot metal from the BF process was assumed to be composed of 95.5% Fe and 4.5% C whereas that from other processes were 100% Fe. All processes were based on Fe_2O_3 for the purpose of comparison although the proposed processes would largely depend on Fe_3O_4 when applied to taconite ores.

The amount of SiO_2 in the proposed process was assumed to be 70% of that for the BF operation, considering that the proposed process does not require coke and coal which contribute about 30% of SiO_2 input into the BF. All the silica goes into slag as $CaSiO_3$ after being combined with CaO which comes from the decomposition of limestone ($CaCO_3$). The amount of fuel/reductant and the corresponding amount of

Table 1. Material balance comparison between the proposed technology and the blast furnace (for 1 metric ton of molten Fe). (updated results of similar calculation in Ref. 8)

		BF [kg/mtFe]	Prop'd(H_2) [kg/mtFe]	Prop'd(CH_4) [kg/mtFe]	Prop'd(Coal) [kg/mtFe]
Input	Fe_2O_3	1430	1430	1430	1430
	SiO_2	110	77	77	77
	$CaCO_3$	184	128	128	128
	O_2(g)	677	238	429	474
	N_2(g)	2209	777	1399	1547
	C(coke)	462			
	H_2(g)		84		
	CH_4(g)			215	
	Coal ($C_{1.4}H$)				305
	Subtotal	5072	2734	3678	3961
Output	Fe	1000	1000	1000	1000
	$CaSiO_3$	213	149	149	149
	C	47			
	CO_2(g)	**1603**	**56**	**647**	**1111**
	H_2O		752	483	154
	N_2(g)	2209	777	1399	1547
	Subtotal	5072	2734	3678	3961

* The values for the BF feedstock preparation such as cokemaking and pelletization/sintering were not included in this calculation.

** C in BF hot metal should be included in CO_2 comparison as CO_2 since it needs to be burnt off eventually.

oxidant, assuming the use of air, were determined from the energy balance calculation. And the amounts of water vapor and N_2 in the off-gas were obtained accordingly.

Of particular interest is the greatly reduced generation of CO_2 for the new technology. The CO_2 emissions from the proposed processes significantly decreased to about 4 % (H_2), 40 % (CH_4), and 70 % (coal) of that for the BF process assumed to use only coke as fuel and reductant. In a more comprehensive comparison, CO_2 emissions associated with the production of additional energy required for the feedstock preparation in the BF process and the preparation for the fuel/reductant in the proposed processes should be considered.

3.2 Energy Balance

Table 2 lists the energy requirements per metric ton of molten Fe for the blast furnace (BF) and the proposed technology using different types of fuel (H_2, CH_4, and coal). The energy requirement to produce molten Fe in the proposed processes significantly decreased to about 62% of that for the BF process. The energy savings are largely due to the elimination of the feedstock preparation steps such as pelletization/sintering and cokemaking. The energy requirement values for the proposed processes are almost the same as those for direct reduction (DR) processes typically requiring 10 to 14 GJ per metric ton of solid direct reduced iron (DRI).[69] It is noted that the proposed process could produce solid iron, but for a fair comparison it was assumed to produce molten iron just as the blast furnace. The proposed process is more energy efficient than COREX (16.9-20.2 GJ/mtHM), and comparable to MIDREX (13.3 GJ/mtHM) and HYLIII (12.3 GJ/mtHM) in which the heat to melt solid products has been added.[101,102]

Table 2. Energy requirement comparison between the proposed technology and the blast furnace (for 1 metric ton of molten Fe). (updated results of similar calculation in Ref. 8)

	BF [GJ/mtFe]	**Prop'd (H_2) [GJ/mtFe]**	**Prop'd (CH_4) [GJ/mtFe]**	**Prop'd (coal) [GJ/mtFe]**
Energy required (feed at 25°C to products)				
1) Enthalpy of iron-oxide reduction (25°C)[a] (assumed to produce H_2O and CO_2)[b]	2.08	-0.31	1.39	1.72
2) Sensible heat of molten Fe (1600°C)	1.35	1.35	1.35	1.35
3) Slag making	-0.16	-0.11	-0.11	-0.11
4) Sensible heat of slag (1600°C)	0.36	0.25	0.25	0.25
5) Limestone ($CaCO_3$) decomposition	0.33	0.23	0.23	0.23
6) Carbon in pig iron[c]	1.55			
7) Heat loss and unaccounted-for amounts (assumed the same for all processes)	2.60	2.60	2.60	2.60
8) Sensible heat of off-gas (90°C)[d]	0.24	0.26	0.26	0.21
Subtotal	**8.35**	**4.27**	**5.97**	**6.25**
Energy value for reductant				
Heating value of feed used as reductant	5.30	7.70	5.99	5.66
Total for Iron oxide reduction	**13.65**	**11.97**	**11.96**	**11.91**
Preparation[e]				
1) Pelletizing	3.01			
2) Sintering	0.65			
3) Cokemaking	2.02			
Subtotal for preparation	**5.68**			
Total for molten Fe making	**19.33**	**11.97**	**11.96**	**11.91**

a: The values may be slightly different when Fe_3O_4 is used.

b: This assumption is equivalent to giving full energy credit to CO in the BF off-gas.

c: Carbon in pig iron represents the heating value of dissolved C. It is noted that its heating value is used in subsequent converting, but it was decided to leave it in as an energy item because the carbon removal is an added required step that requires other energy and costs. Further, a large portion of the heat generated by burning this C content is lost and not utilized. Even if this item is removed from the BF numbers, the proposed process has much lower energy requirement than the BF process.

d: The temperature 90°C represents the assumption of recovery of sensible heat from the off-gas down to this temperature in all cases.

e: The values were compiled based on data from Refs. 103 and 104.

In the table, the amounts of silica in the proposed processes were assumed to be 70% of that for the BF operation during the material balance calculation and thus the same ratios were reflected in ‘slagmaking’, ‘sensible heat of slag’, and ‘limestone decomposition’ values. ‘Carbon in pig iron’ represents the heating value of dissolved C. It is noted that its heating value is used in subsequent converting, but it was decided to leave it in as an energy item because the carbon removal is an added required step that requires other energy and costs. Further, a large portion of the heat generated by burning this C content is lost and not utilized. Even if this item is removed from the BF numbers, the proposed process has much lower energy requirement than the BF process. A rigorous comparison must include energy balances for the entire integrated steel plant using different ironmaking technologies, which is out of the scope of this work.

C and H_2 were assumed to be converted to CO_2 and H_2O, equivalent to crediting their heating values. It is seen that even with the assumption of full combustion of CO to CO_2 in the blast furnace, equivalent to giving full credit for the heating value of the BF off-gas, the proposed technology using any of the three possible reductants and fuels requires a much smaller amount of energy with ~40% less consumption. Further, the energy required for grinding ore to the concentrate size is not included because 70-80% of iron production in the U.S. by the BF process already depends on such concentrates. Furthermore, there is a large amount of low-grade iron ores requiring concentration and the industry trend is to upgrade even many of the higher-grade ores by comminution and impurity removal. It is noted that the proposed technology compares favorably with the BF process as well as other commercial alternate ironmaking processes.

CHAPTER 4

EXPERIMENTAL APPARATUS AND PROCEDURE

The kinetic feasibility tests of the proposed process have proceeded through three steps; preliminary experiments, kinetic measurements, and scale-up tests. In this chapter, the equipment and the experimental procedure for each step will be described in detail as well as the basic information on the material used throughout the experiments and the methods for the analysis and characterization.

4.1 Materials

The iron ore concentrates were provided by Ternium (Monterrey, Mexico) and by ArcelorMittal (East Chicago, USA). The concentrate particles are irregularly shaped and angular as shown in Figure 2. The chemical composition of each concentrate is presented in Table 3. In both cases, most of the iron oxide was magnetite, which was confirmed by X-ray diffraction patterns as shown in Figure 3, and the total iron content ranged from 68 to 71%. Figure 4 shows the particle size distribution analyzed with a Beckman Coulter LS Particle Size Analyzer. The median and mean sizes were 23.4 and 34.4 μm, respectively, and 94.4% of the total volume were less than 100 μm. For reaction rate measurements, the Ternium concentrate screened to 22-30 μm was utilized for preliminary experiments and the ArcelorMittal concentrate screened to 25-32 μm was

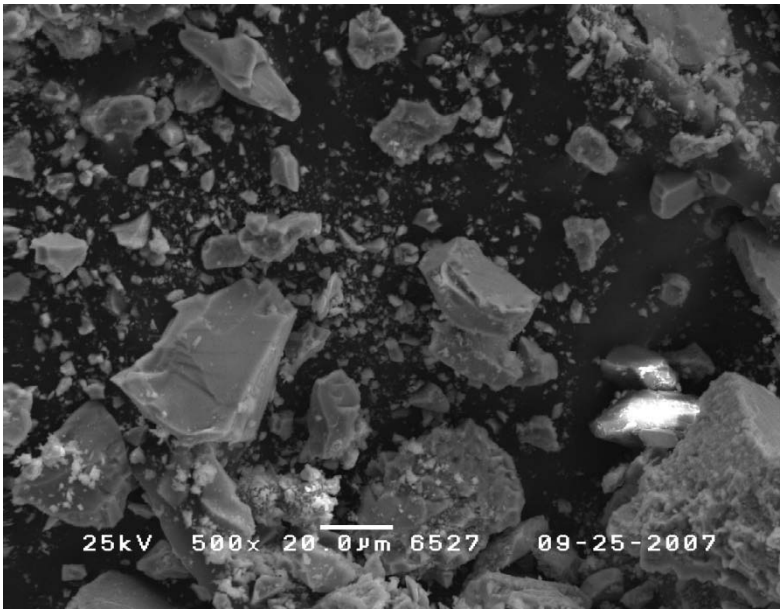

(a)

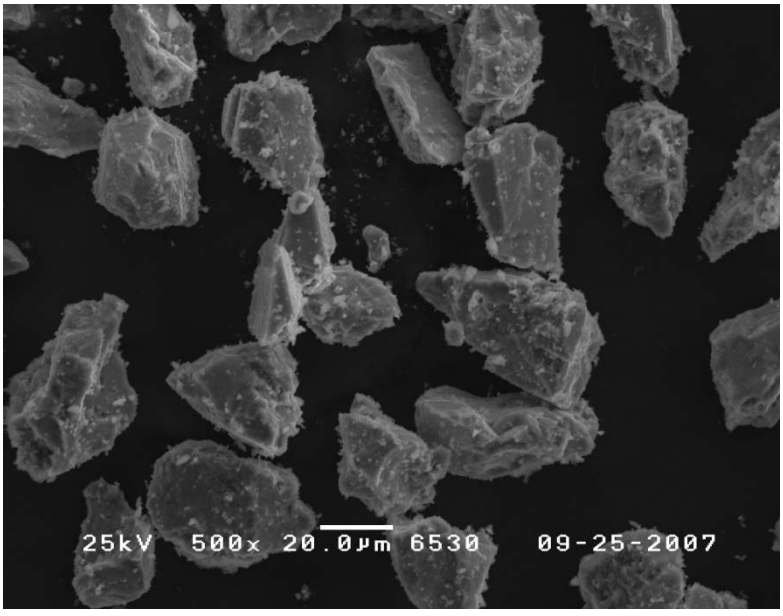

(b)

Figure 2. SEM micrographs: (a) unscreened Ternium concentrate; (b) screened ArcelorMittal concentrate.

Table 3. Chemical composition (wt %) of iron ore concentrates from Ternium and ArcelorMittal.

Component	**Ternium**	**ArcelorMittal**
Total Iron	68.4	70.65
FeO	20.9	30.53
P	0.029	0.01
S	0.0055	0.02
C	N/A	0.24
Sr	N/A	0.01
SiO_2	1.73	1.87
Al_2O_3	0.55	0.13
CaO	0.68	0.27
MgO	0.40	0.13
MnO	0.075	0.11
Cr_2O_3	N/A	0.11
K_2O	N/A	0.01
Na_2O	N/A	0.10
TiO_2	N/A	0.01
ZrO_2	N/A	0.03
CuO	0.021	N/A

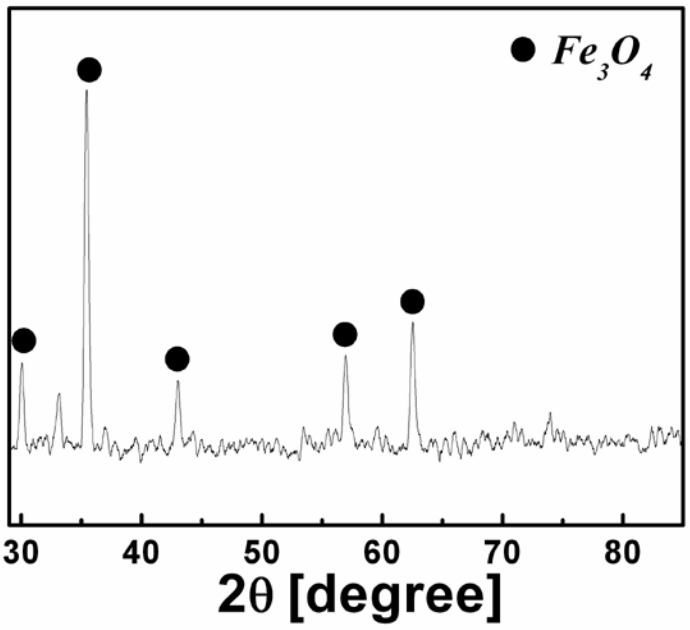

(a)

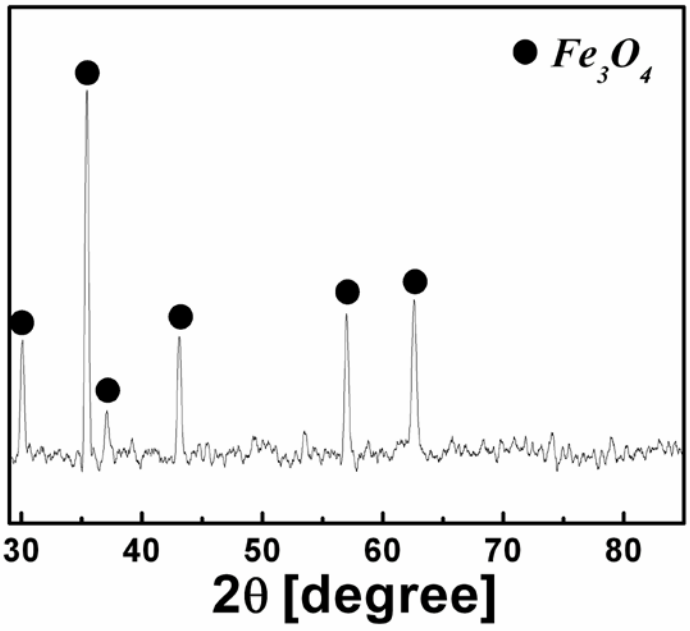

(b)

Figure 3. X-ray diffraction patterns: (a) Ternium concentrate; (b) ArcelorMittal concentrate. (using Cu-Kα radiation)

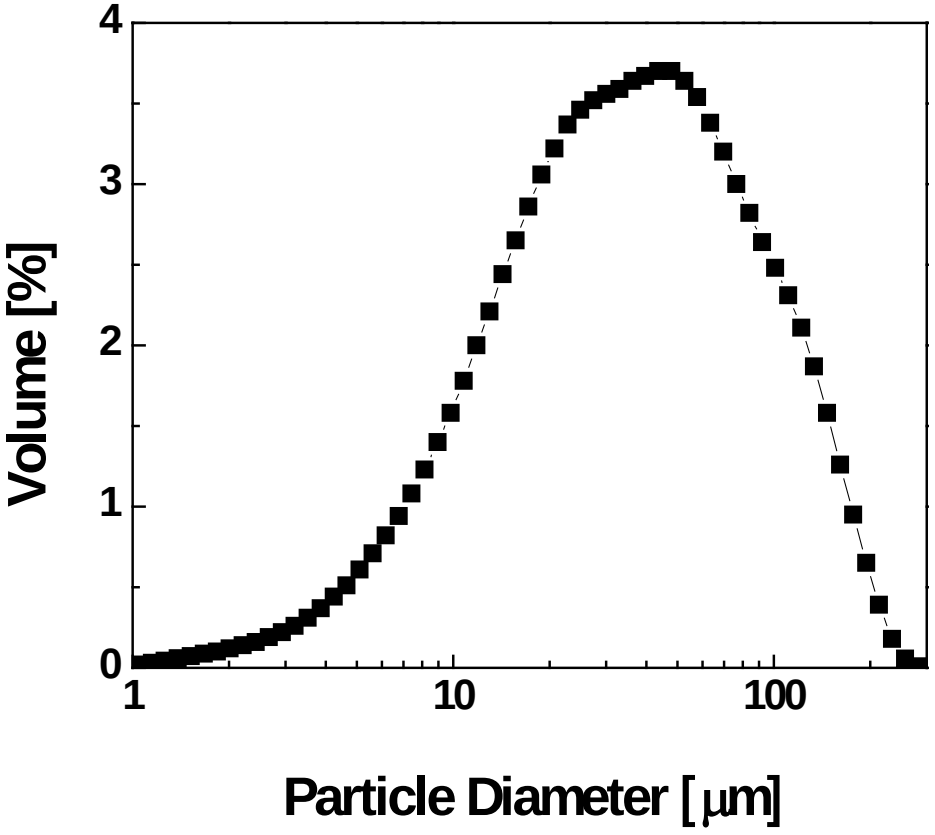

Figure 4. Particle size distribution of Ternium concentrate. (Note: abscissa in logarithmic scale)

used for kinetics measurements with a drop-tube reactor. Unscreened Ternium concentrate was used as a solid feed material for scale-up tests in the Utah flash reactor. It should be noted that the reaction rate of a particle assemblage of which the particle size has a normal or log-normal distribution is similar to the reaction rate of uniform particles of the mass average size, based on Mcllvried and Massoth's mathematical evaluation.[105]

4.2 Preliminary Experiments

At the beginning of this study, it was uncertain if individual concentrate particles could be reduced by hydrogen within a few seconds of reaction time that would be available in a suspension reduction process. To get a very approximate idea of the reduction rate, the experiments in a rather simple facility were designed to test the kinetic feasibility of the proposed process, before more elaborate and accurate measurements were made. The reasoning was that the latter type of measurements would be unnecessary if these simple tests revealed that the rate is much too slow for a suspension process.

The apparatus consisted of a horizontal tube furnace, a gas delivery system, a bed of copper turnings, and an off-gas system as shown in Figure 5. Only a small amount of concentrate were sprinkled loosely and spread thinly on top of a Kaowool compact held in a shallow ceramic tray in order to remove the effect of inter-particle diffusion of the gaseous species and thus to mimic the conditions of a suspension reaction.

The experiments were conducted by measuring the weight change of the Ternium concentrate screened to 22-30 μm over time at three different temperatures 900^{o}C, 1000^{o}C, and 1100^{o}C in pure hydrogen flowing into the reactor (2 cm ID) at the rate of 2 NL/min when the desired temperature was reached. The per cent reduction of the product was calculated from the ratio of the weight loss of sample to the weight of oxygen in the

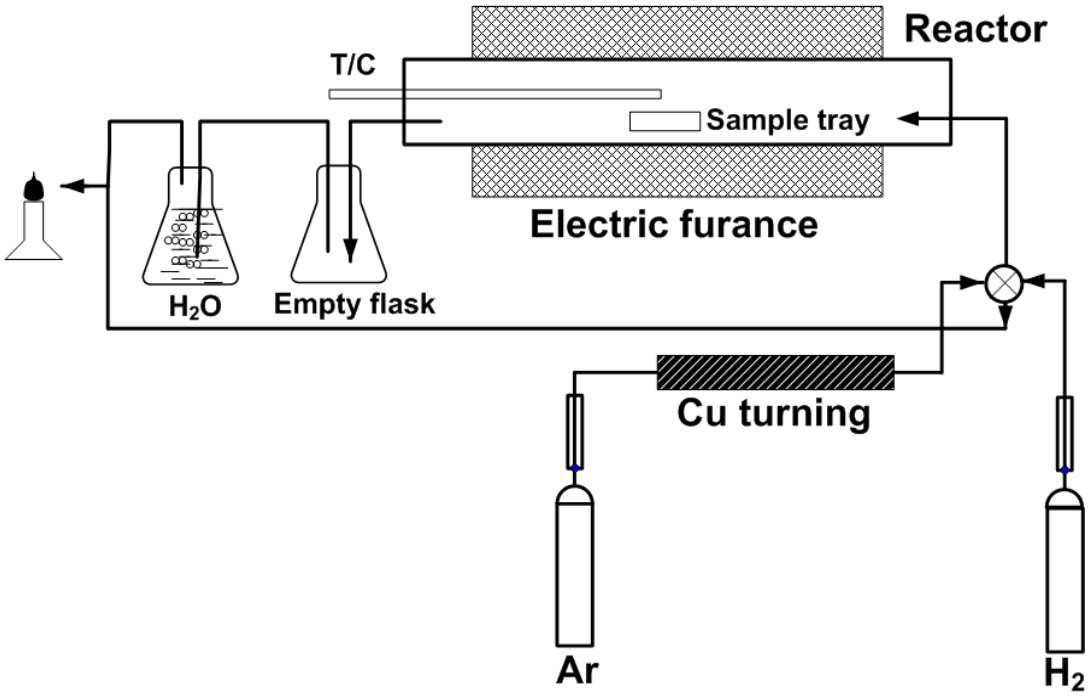

Figure 5. Schematic diagram of horizontal furnace system for preliminary experiments.

iron ore concentrate. It was assumed that the weight loss during the reduction occurred only due to the loss of oxygen associated with iron because the amount of oxygen in the gangue materials which could be reduced by hydrogen in the experimental temperature range was negligible and the weight change due to the possible volatile species such as phosphorus and sulfur was also neglected based on the small contents as given in Table 3. Weight loss by heating alone was also negligible, confirming this assumption.

4.3 Kinetics Measurements

Encouraged by the reasonably rapid kinetics measured by the preliminary tests, a high temperature drop-tube reactor system was fabricated for accurate determination of the rate of individual concentrate particles. Unlike the standard experimental technique of reducing a stationary particle in a stream of gas, this system utilizes a dilute fine particles-gas conveyed system to measure the chemical reaction rate of fine particles entrained in a reducing gas and reduced in flight. The advantages of such a system are: firstly, the rate measurement of the rapid in-flight reduction of fine particles is possible. Secondly, high mass and heat transfer between gas and particles is expected. Thirdly, there is no contamination from external parts because no crucible is used.[87,93,95]

As shown in Figure 6, this apparatus consisted of a vertical high temperature drop-tube furnace, a pneumatic powder feeder, gas delivery lines, a powder cooling and collecting system, and an off-gas outlet. The furnace system was made up of a vertical split tube furnace with a maximum working temperature of 1540^{o}C and a cylindrical alumina tube (5.6 cm ID, 193 cm long). A reaction zone was maintained at a constant temperature between 900 and 1500^{o}C by bar-type SiC elements. Carefully measured reaction zone was 91 cm long within ± 20 K for typical downward gas flow conditions.

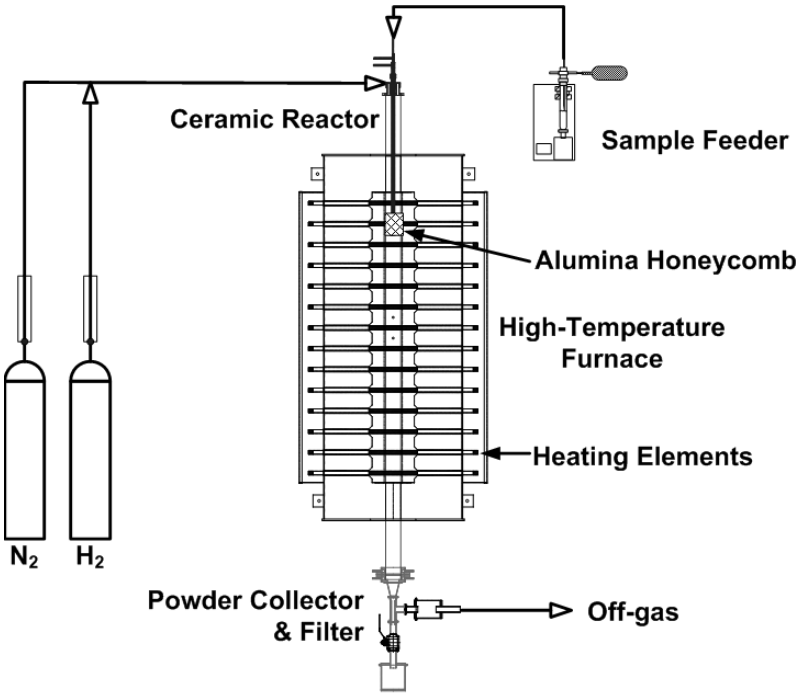

(a)

(b)

Figure 6. A high temperature drop-tube reactor system: (a) schematic diagram; (b) photograph.

During experiments, temperatures at the beginning and the center of the reaction zone were measured by two B-type thermocouples (platinum + 6% rhodium vs. platinum + 30% rhodium). A cylindrical alumina honey-comb was inserted in the tube and hung right above the beginning of the reaction zone as a flow straightener and a heat exchanger for the reducing gas. The concentrate particles were injected through a tube of 0.12 cm ID carried by a hydrogen flow of 200 NmL/min. The reacted powder was collected in a powder collector at the bottom of the reactor, as shown in Figure 7, and the unreacted hydrogen and water vapor were discharged through the off-gas outlet that included a backflow prevention device for safety.

4.3.1 Pneumatic Powder Feeding System

Figure 8 shows the pneumatic powder feeding system which consisted of a syringe pump, a vibrator, a carrier gas line, a powder container, and a powder delivery line. Dried concentrate was charged in a powder container, a Pyrex vial, which was held by a bore-through Swagelok and sealed with an O-ring. Hydrogen was fed as the carrier gas at 200 NmL/min into the vial (0.9 cm ID) and passed through the powder delivery line (0.12 cm ID) at the top of the powder feeder continuously entraining a small amount of the powder. The feeding tube was vibrated by an electric vibrator to prevent clogging. The vial was pushed up by a motor at a constant target advancing rate which was determined based on the calibration data between the advancing rate of the syringe pump and the powder feed rate, as shown in Figure 9. During the experiments, the concentrate feed rate was controlled from 100 to 600 mg/min.

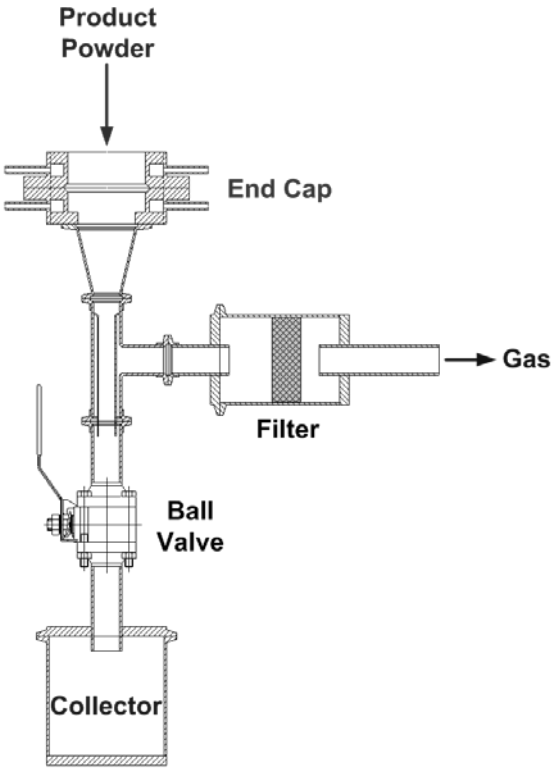

(a)

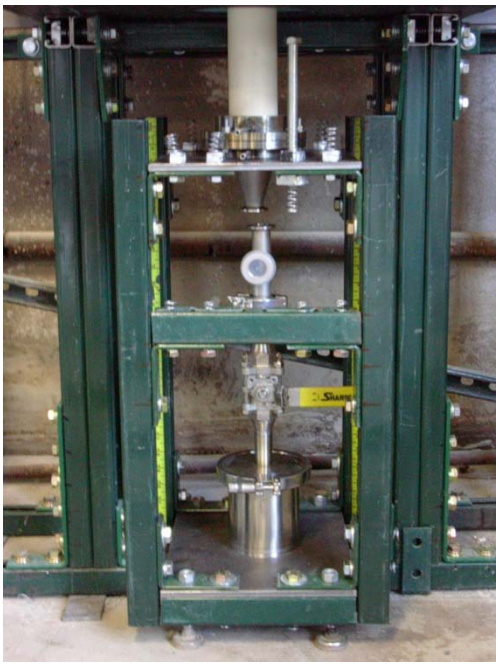

(b)

Figure 7. Powder collection system: (a) schematic diagram; (b) photograph.

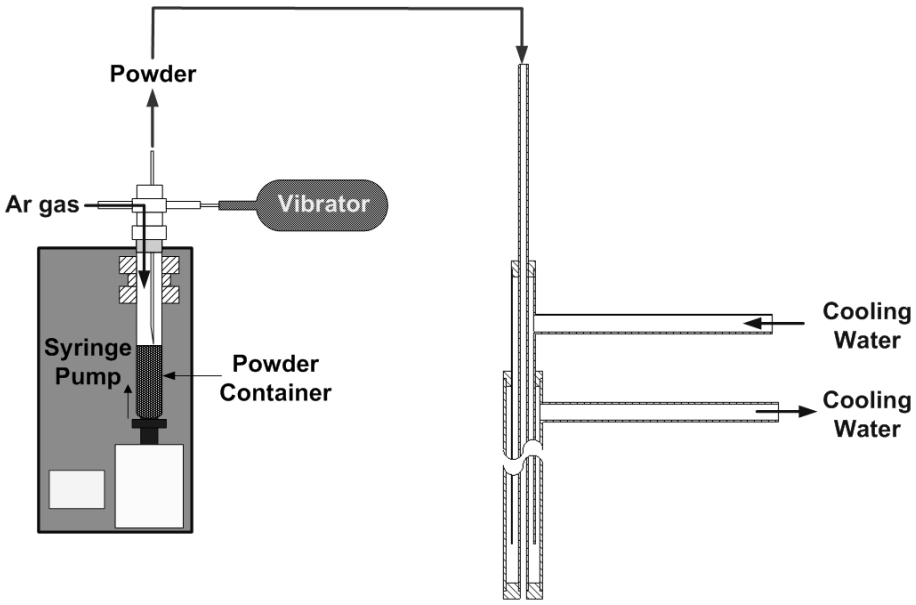

(a)

(b)

Figure 8. Pneumatic powder feeding system and the powder feeding probe with a water cooling jacket: (a) schematic diagram (b) photograph.

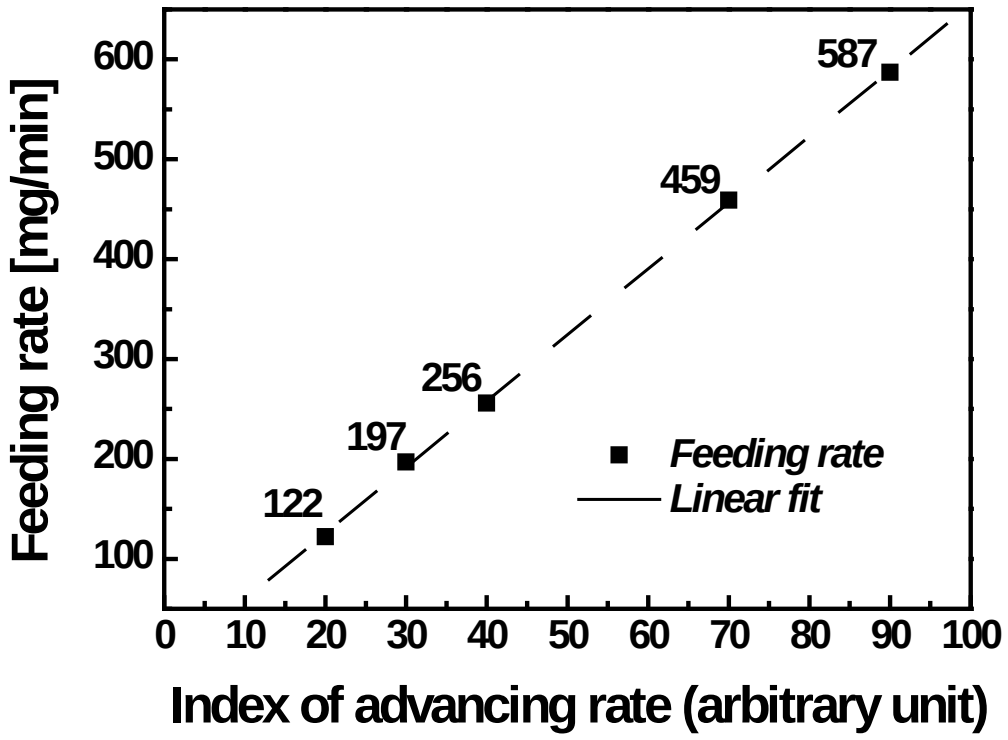

Figure 9. Powder feed rate vs. advancing rate of the syringe pump.

A powder feeding tube system shown on the right side of Figure 8-(a), comprising a stainless steel powder delivery line and a water cooling jacket, was inserted into the main reactor tube. The tip of the feeding tube was located at the beginning of the reaction zone where the heating of the concentrate particles and mixing with reducing gases began. Although every effort was made to improve the heating and mixing of the solid and gaseous species, the zone where the reduction reaction occurs at the designated temperature can in fact be only shorter than the zone designated as isothermal. Thus, the reduction extent presented in this work could be attained in shorter residence time than the calculated value.

4.3.2 Residence Time Determination

The duration of hydrogen reduction of fine iron ore concentrate particles was determined by the residence time (τ) of particles in the reaction zone. The value of the residence time was calculated from the length of the reaction zone, which starts from the tip of the powder feeding probe, the linear velocity of the gas, and the terminal falling velocity of particles in a creeping flow region expressed by the Stokes' law assuming that particles fall at a constant velocity in the reaction zone.[106] The assumption on the creeping flow mode was reasonable over the entire experimental conditions because the Reynolds number was always less than 0.1.

As the gas flows downward after the flow straightener, the flow mode changes from a plug flow to a fully developed laminar flow due to the entrance effects in pipe flow is expected over a very short length of the circular tube. From the normalized development length relationship suggested by Durst et al.[107] as indicated in Equation (2), it was found that the fully developed state of the flow is reached in less than 5% of the

reaction zone length.

$$L/D = [(0.619)^{1.6} + (0.0567Re)^{1.6}]^{1/1.6} \quad (2)$$

where L = length of the reaction zone, D = inner diameter of tubular reactor, Re = Reynolds number.

Since the solid particles fall mainly near the centerline, the residence time in this work was calculated by taking the maximum velocity, which is twice the average velocity (= volumetric flow rate divided by cross-sectional area), as the linear velocity of gas. The residence time, calculated by including the terminal velocity of the solid particles, ranged from 1.0 to 7.0 seconds for all the experimental conditions. The relevant equations for the residence time calculation are:

$$u_t = d_p^2 g(\rho_p - \rho_g)/18\mu \quad (3)$$

$$u_p = u_g + u_t \quad (4)$$

$$\tau = L/u_p \quad (5)$$

where all in consistent units, d_p= particle size, g = gravitational acceleration, ρ_p = particle density, ρ_g = gas density, μ = viscosity of gas, u_p = particle velocity relative to tube wall, u_g = centerline gas velocity at furnace temperature, and u_t = terminal velocity of a falling particle.

The terminal velocity depends not only on the particle size but also the temperature due to its effect on the gas density and the viscosity of gas. As temperature increases, the gas density decreases and the gas viscosity increases and then the terminal velocity decreases, as shown in Figure 10. This makes the residence time, namely the

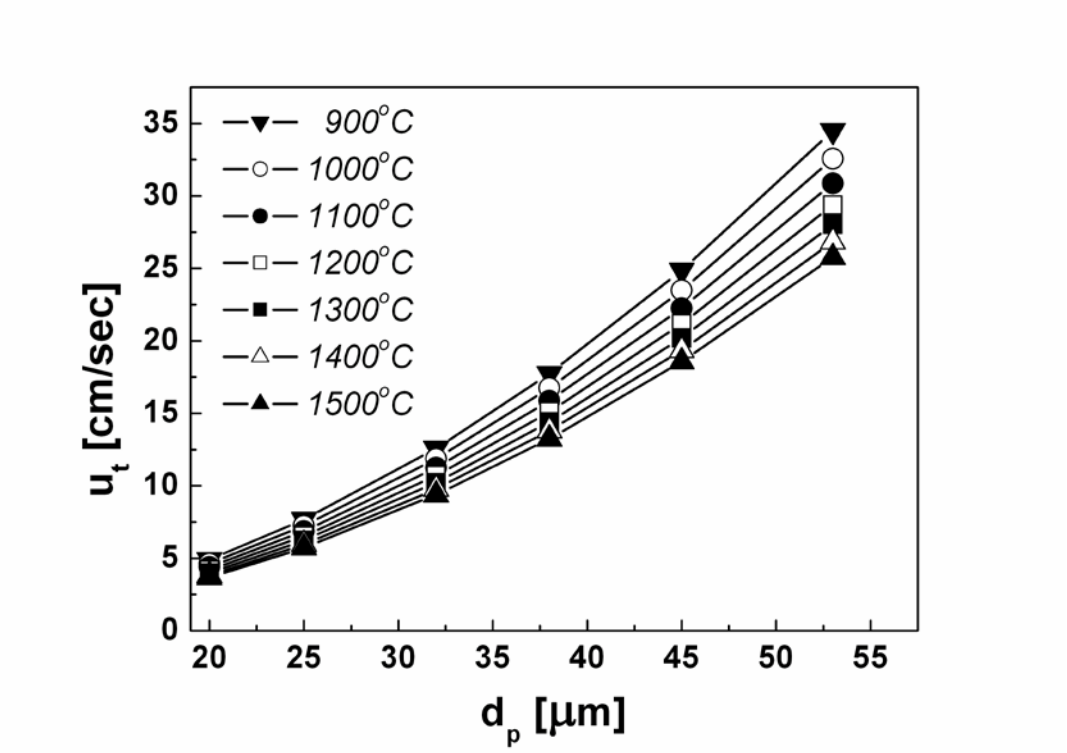

Figure 10. Terminal velocity of a falling spherical particle vs. the particle size

reduction time, longer in the same length of the reaction zone when other parameters are fixed. On the other hand, a higher temperature causes the gas velocity to increase at the same molar rate of gas input, which in turn decreases the residence time. Thus, all these factors must be taken into consideration when interpreting the effect of temperature on the reduction rate.

As the particle-laden gas stream enters the reaction zone through 0.12 cm ID tubing, the stream expands like a jet and the particles are expected to be spread over the cross section. It becomes necessary to verify if the use of centerline gas velocity in the residence time calculations is justified. Thus, error analyses were performed by examining the effect of radial variation of velocity on the average residence time. The relevant equations are:

$$u_g(\eta) = u_{g,\max}\left(1-\eta^2\right) \text{ in a fully developed laminar flow} \tag{6}$$

$$\tau_{avg}(\eta) = V(\eta)/Q(\eta) = \int_0^{\eta} 2\pi\eta L d\eta \Big/ \int_0^{\eta} 2\pi\eta u_g(\eta) d\eta = L/u_{g,avg}(\eta) \tag{7}$$

$$u_{g,avg}(\eta) = \int_0^{\eta} \eta u_g(\eta) d\eta \Big/ \int_0^{\eta} \eta d\eta = \int_0^{\eta} \eta u_{g,\max}\left(1-\eta^2\right) d\eta \Big/ \int_0^{\eta} \eta d\eta = u_{g,\max}\left(2-\eta^2\right)/2 \tag{8}$$

$$\tau_{avg}(\eta)/\tau(0) = 2/\left(2-\eta^2\right) \tag{9}$$

where all in consistent units, η = normalized radial distance from the centerline defined as the radial distance from the centerline (r) divided by the radius of tubular reactor (r_i), V = volume of the reaction zone (0~η), Q = volumetric flow rate of gas through V, τ_{avg} = average residence time of gas up to η, $u_{g,max}$ = maximum linear velocity of gas along the centerline, and $u_{g,avg}$ = average linear velocity of gas up to η.

As shown in Figure 11 plotted with Equation (9), the change in the average residence time of the gas is only about 10% of that at the centerline even if we assume that the particles are spread over the cross section within the inner half of the reactor radius. Besides, although the particle-laden gas stream expands like a jet, particles are gradually dispersed radially as shown in Figure 12. The particles flow around the centerline in most of the length of the reaction zone. Particles may disperse more widely when the gas flow rate is very low, but in this case the effect of the terminal velocity of particles on the residence time becomes stronger and thus the effect of radial velocity variation on the estimation of the average residence time becomes small. This error analysis confirms that, under the experimental conditions used in this work, the use of the centerline gas velocity is justified. Further, the actual residence time can only be longer, which makes the real reaction rate only faster if the error is significant.

4.3.3 Percent Excess Hydrogen

A hydrogen-containing gas mixture was fed as the reductant into the reactor concurrently with the pneumatically transported concentrate particles. To accurately determine the kinetics, it is best to carry out the experiment under a condition in which the gaseous reactant concentration remains constant over the entire reactor length, which requires a sufficiently large excess of the gaseous reactant over the stoichiometric amount. This is also necessary to achieve a high degree of reduction, especially taking into consideration the fact that the final stage of the iron oxide reduction, i.e., the reaction of FeO with H_2 or CO is significantly limited by equilibrium whereas the equilibrium concentration of H_2 and CO for the reduction of magnetite to wüstite is essentially zero, i.e., H_2 and CO are completely utilized for the reduction reaction. The equilibrium

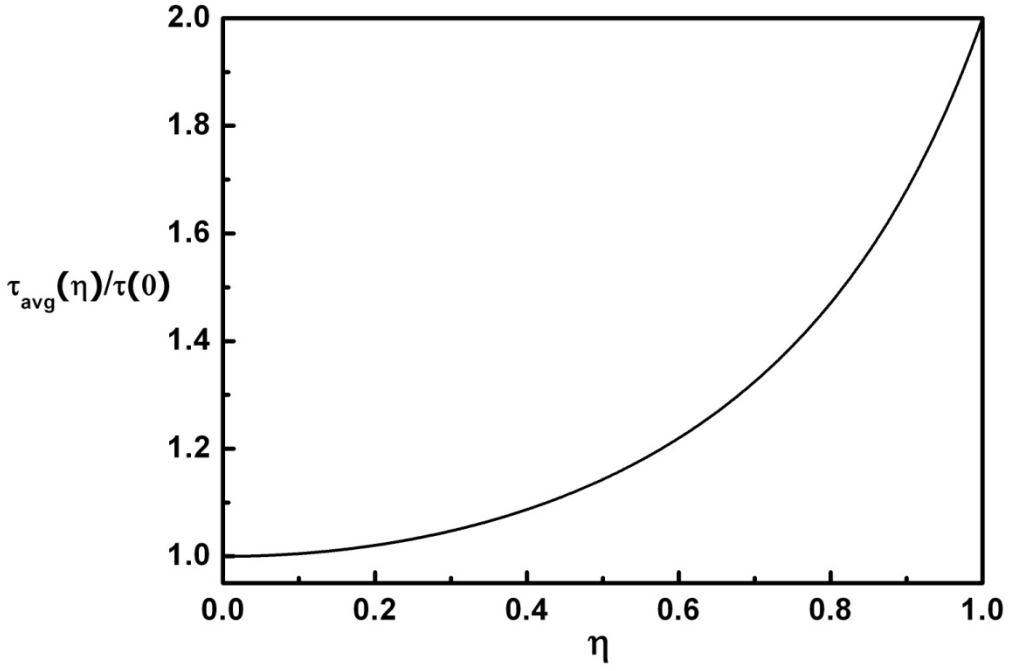

Figure 11. The deviation of the average residence time of gas in the radial direction with respect to the normalized radial distance from the centerline (η).

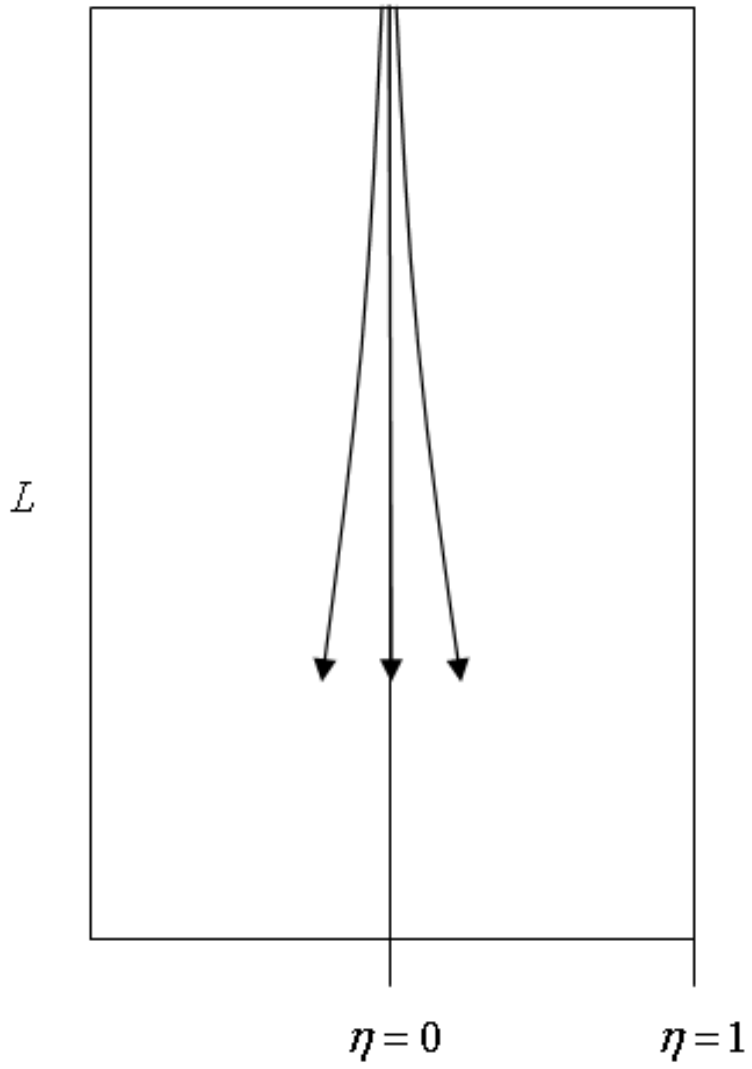

Figure 12. Schematic flow diagram of particle-laden gas jet in the reaction zone.

percentages of H_2 in a mixture with H_2O and CO with CO_2 as well as their equilibrium constants are plotted in Figure 13 for the FeO-H_2 and FeO-CO reactions against temperature. It is shown that the equilibrium gas ratio changes somewhat with temperature and the % H_2 decreases and levels off as temperature increases while the % CO increases.

Taking the equilibrium composition into consideration, the term % excess H_2 was defined as follows:

$$Fe_3O_4 + H_2 = 3FeO + H_2O \tag{10}$$

$$FeO + H_2 = Fe + H_2O \tag{11}$$

$$\text{Overall:} \quad Fe_3O_4 + 4H_2 = 3Fe + 4H_2O \tag{12}$$

$$K_{R2} = \left[\frac{p_{H_2O}}{p_{H_2}}\right]_{eq} = \left[\frac{n_{H_2O}}{n_{H_2}}\right]_{eq} \tag{13}$$

$$n_{H_2,\min} = n_o^i + \frac{n_o^i}{K_{R2}} = \left[1 + \frac{1}{K_{R2}}\right] n_o^i \tag{14}$$

$$\%\ \ excess\ \ H_2 = \frac{n_{H_2,\sup plied} - n_{H_2,\min}}{n_{H_2,\min}} \times 100 \tag{15}$$

Reaction (10), the hydrogen reduction of magnetite to wustite, has a large equilibrium constant, i.e. essentially irreversible, whereas Reaction (11) is considerably limited by chemical equilibrium. Thus, the amount of hydrogen in equilibrium with the water vapor present in the gas was used for the equilibrium constant of Reaction (11) represented by Equation (13). The minimum amount of hydrogen, $n_{H2,min}$, then is the

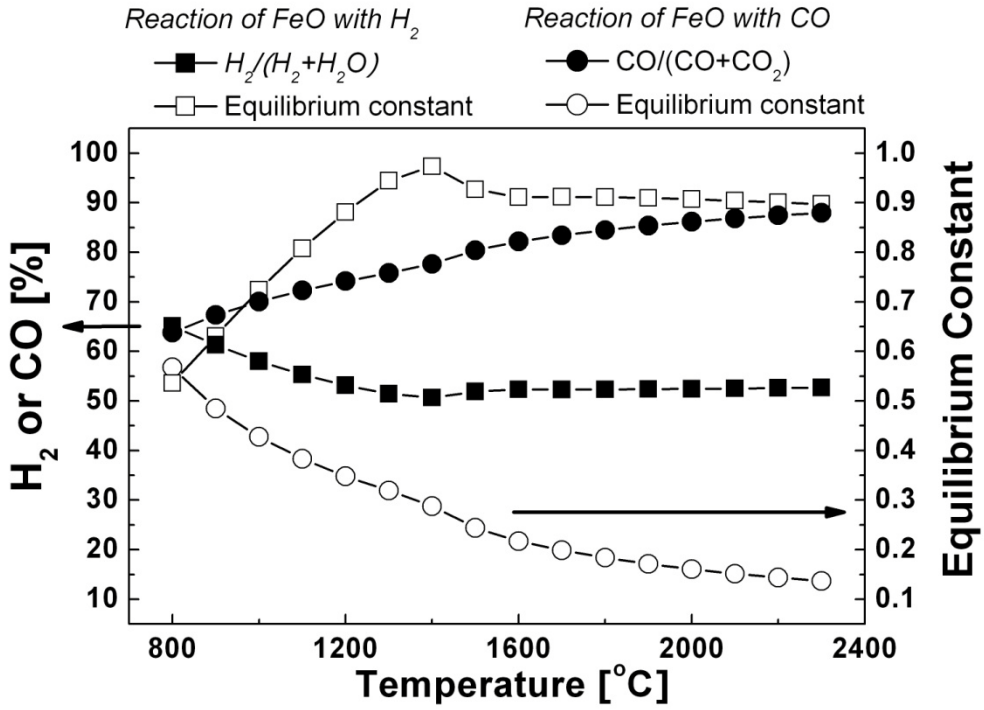

Figure 13. Equilibrium gas compositions and constants vs. temperature for the FeO-H_2 and FeO-CO reactions.

amount of hydrogen used to remove the oxygen from the iron oxide, n^i_o, plus the hydrogen required by equilibrium to be present with the water vapor produced by the reduction reaction, n^i_o / K_{R2}. The % excess H_2 was then calculated from the total amount of hydrogen fed into the reactor, $n_{H2,supplied,}$ compared with the minimum amount of hydrogen, $n_{H2,min}$, as indicated in Equation (15).

4.3.4 Degree of Reduction

The concentrate particles were transported downward, heated, reduced in-flight, and collected. The total iron content in the particles after reduction was determined by titration methods and/or with an inductively coupled plasma (ICP) emission spectrometer (Perkin Elmer, Plasma 400). The percent reduction was calculated as follows.

$$\text{Reduction [\%]} = \frac{m_o(\%O)_o - m_t(\%O)_t}{m_o(\%O)_o} \times 100 \tag{16}$$

where

$$m_o = m_t(\%Fe)_t/(\%Fe)_o \tag{17}$$

Here, $(\%O)_o$ and $(\%O)_t$ are % oxygen combined with iron in the concentrate before and after the reduction. m_t and m_o are, respectively, the mass of a reduced sample used for chemical analysis, collected after reaction for time *t*, and the corresponding mass of the unreduced dry concentrate calculated by Equation (17). $(\%O)_o$ was obtained as the difference between 100 and the sum of the total iron content and the total gangue content, which was 3.05% in the ArcelorMittal concentrate as seen in Table 3. The amount of oxygen in the gangue materials which could be reduced by hydrogen in the experimental

temperature range was negligible and the weight change due to the possible volatile species such as phosphorus and sulfur was also neglected based on the small contents as given in the same table and the fact that weight loss by heating alone was also confirmed to be negligible. $(\%O)_t$ was calculated from $(\%Fe)_t$, assuming the same weight ratio of iron to gangue.

4.4 Scale-Up Tests

Based on the kinetic measurements, larger-scale suspension reduction tests were conducted in a large laboratory flash reactor, as shown in Figure 14, which was prepared by modifying the flash reactor from the previous project in this laboratory on flash smelting of sulfide minerals.[108,109]

The apparatus consists of five subsystems; a vertical furnace, an electric power controller, gas delivery lines, a preheater, and a pneumatic powder feeder. A tubular steel reactor (20.3 cm ID, 244 cm long) was electrically heated by six SiC heating elements, which were grouped into two and managed by two SCR power controllers. Limited by the materials of the reactor, the maximum temperature obtained with the set-up was 1150^{o}C in 76 cm of reaction zone. The temperatures were measured by a K-type thermocouple (nickel-chromium vs. nickel-aluminum) close to the centerline. It is noted that the reaction zone has a temperature gradient in the radial direction by the way of heating method unlike the drop-tube reactor system for kinetic measurements in which the temperature of the isothermal zone was the same as that of heating elements. For example, to maintain the isothermal zone at 1150^{o}C, the heating elements had to be heated up to about 1250^{o}C, which introduced temperature gradient in the radial direction of the tubular reactor and thus the temperature near the inner wall of the tube was higher

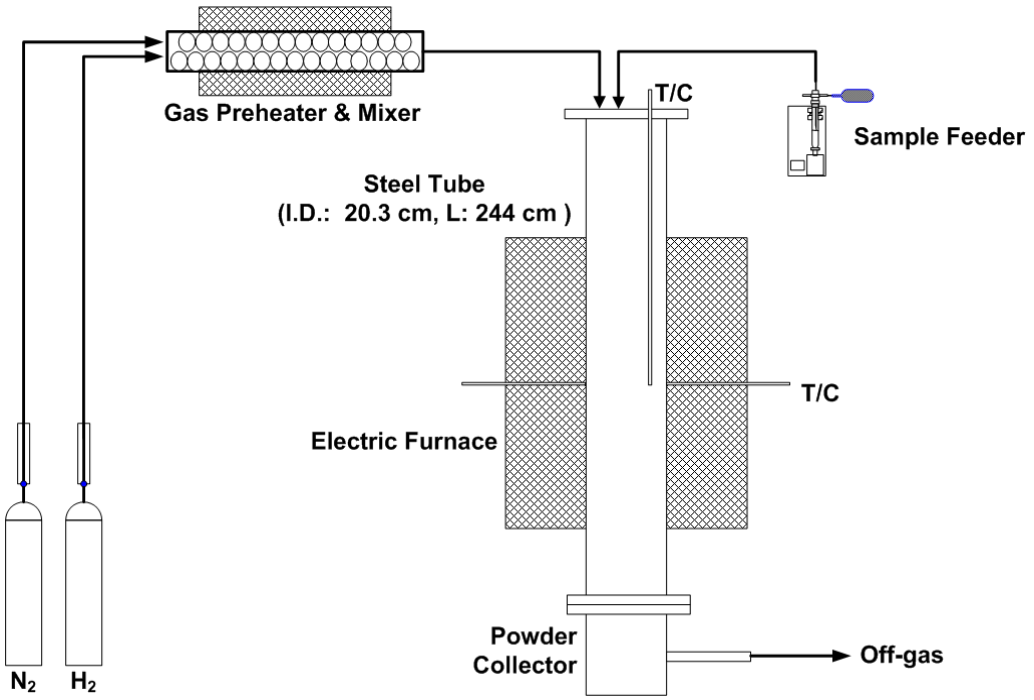

(a)

(b)

Figure 14. Utah flash furnace for testing suspension hydrogen reduction of iron ore concentrate: (a) schematic diagram; (b) photograph.

than 1150^{o}C.

The flow rates of all the gaseous species were carefully controlled by flowmeters with high-resolution valves and provided at ambient pressure. It should be noted that the average barometric pressure of Salt Lake City is 86.1 kPa. The input gas was preheated to about 500^{o}C in a horizontal tube (6.4 cm ID, 122 cm long) furnace packed with ceramic Raschig rings to improve mixing and heating of the gas species before entering the main reactor. To prevent the heat loss from preheated gas, a pack of Kaowool wrapped around the end-cap of the preheater and the gas delivery line connecting the preheater and the main reactor was covered by a high temperature heating tape (760^{o}C max) as shown in Figure 15.

The iron ore concentrate provided by Ternium was dried and fed into the reactor by a pneumatic powder feeding system, which was a similar type as the one used for the kinetic measurements but had larger capacity, at about 1.5 g/min of feed rate. A powder feeding tube from the pneumatic feeder was connected to a powder and gas injector on the top metal flange as shown in Figure 15. To improve the distribution of the particle-laden gas stream, a cone-shape distributor was inserted at the beginning of injection as shown in Figure 16. The concentrate was not screened because the scale-up tests were not for accurate kinetic measurements but to simulate an actual suspension reduction process.

The duration of reduction of the particles was determined by the nominal residence time of particles in the reaction zone. The value of the residence time was calculated from the length of the reaction zone, the average linear velocity of the gas (= olumetric flow rate divided by cross-sectional area), and the terminal falling velocity of particles. In the present work, the nominal residence time varied from 3.5 to 5.5 seconds and percent excess H_2 from 0 to 860%. The product was collected in the powder collector

Figure 15. Reducing gas preheating system.

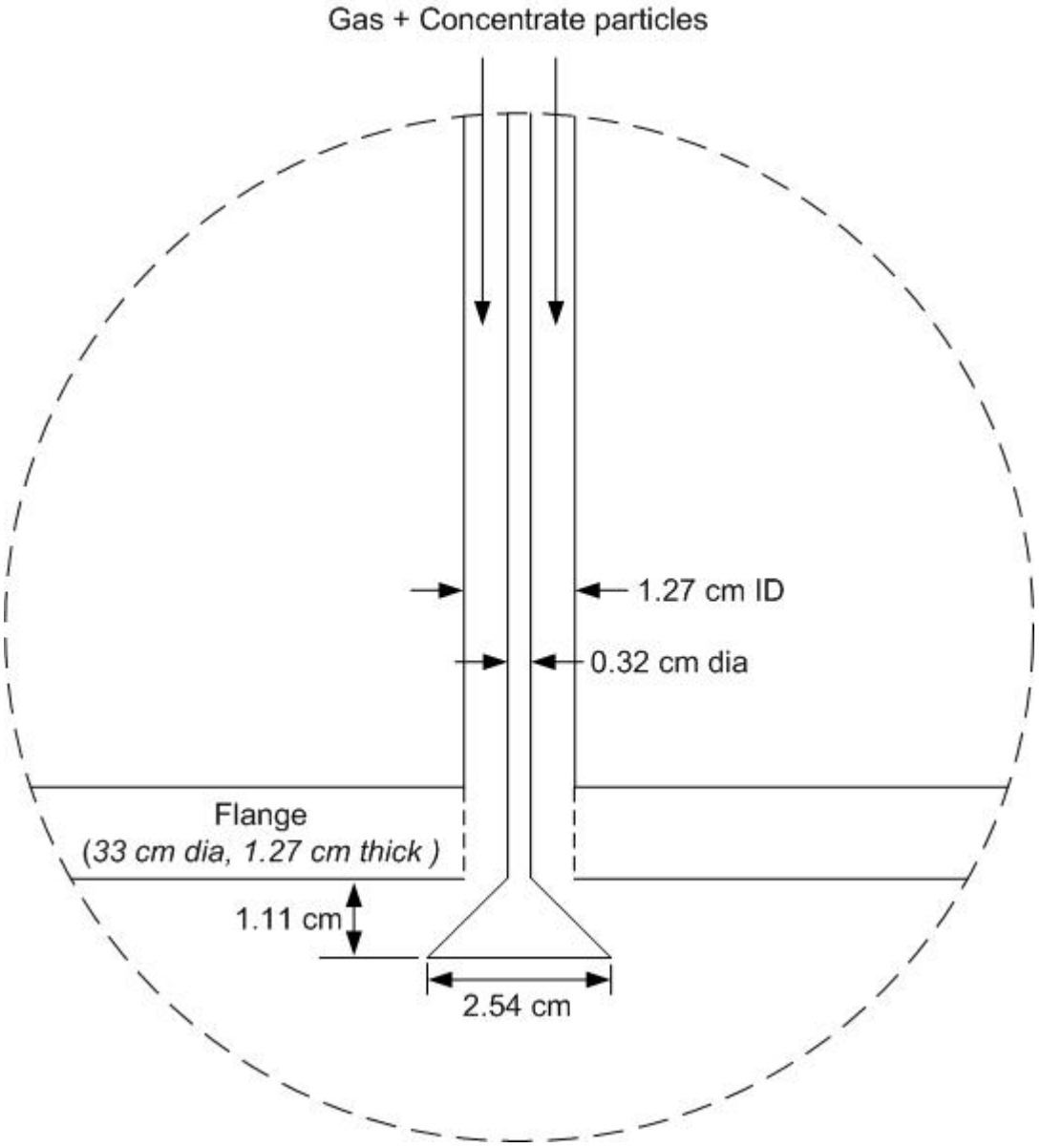

Figure 16. Cone-shape distributor.

at the bottom of the reactor and sent to further analysis.

4.5 Analytical Techniques

The determination of the conversion extent from raw concentrate (Fe_3O_4) to metallic iron (Fe) in the reaction product was the major concern in the analysis during this study. While applying the definition on the degree of reduction introduced previously, the total iron content in the product was determined by titration methods based on international standard on the determination of metallic iron in direct reduced iron (DRI)[110] and/or with an inductively coupled plasma (ICP) emission spectrometer (Perkin Elmer, Plasma 400). For both cases, the sample was dissolved in an aqua regia solution prepared by mixing concentrated hydrochloric acid (36.5-38.0% HCl) and concentrated nitric acid (68.0-70.0% HNO_3) in a volume ratio of 3:1. For example, 1 L (801 g) of aqua regia solution contains 750 mL of hydrochloric acid (636 g, 6.62 moles of HCl) and 250 mL of nitric acid (165 g, 1.78 moles of HNO_3). To confirm the analytical procedure, either hematite or iron powder with over 99% purity supplied by Alfa Aesar was also analyzed along with the samples.

For further characterization, a Siemens D5000 X-ray diffractometer was used for the compositional analysis of samples. A TOPCON SM-300 Scanning Electron Microscope (SEM) equipped with an energy dispersive spectrometer (EDS) was used to examine the microstructure of concentrate and the quantitative elemental analysis. A Beckman Coulter LS230 Particle Size Analyzer was used to obtain the particle size distribution and the mean particle size of samples.

CHAPTER 5

EXPERIMENTAL RESULTS AND DISCUSSION

5.1 Preliminary Experiments

Figure 17 indicates that about 80% reduction of iron ore concentrate was achieved in 5 seconds at 1100^{o}C in a flowing hydrogen stream and the reduction was almost completed in 10 seconds. The reduction proceeded from Fe_3O_4 to FeO and to Fe in succession, as shown in Figure 18. The presence of FeO as the intermediate product of concentrate reduction were consistently observed in the range of temperature investigated in the present study because FeO is stable above 570^{o}C[111] and the reduced sample was quenched before collection. SEM micrographs in Figures 19-21 show that the products became porous as the hydrogen reduction proceeded and that the porosity increased with the reaction temperature leaving a series of small interconnected grains.

Because certain conditions were not fully controlled to accurately determine the fast reduction rate of very fine particles, this experiment must be considered as an approximate representation of the actual reduction rates of individual particles in suspension reduction conditions. Possible uncertainties included the effect of radiation from the furnace wall and the sample holder, which would affect the measurement of real temperature of the reacting particle, the effect of mass transfer between the bulk gas and

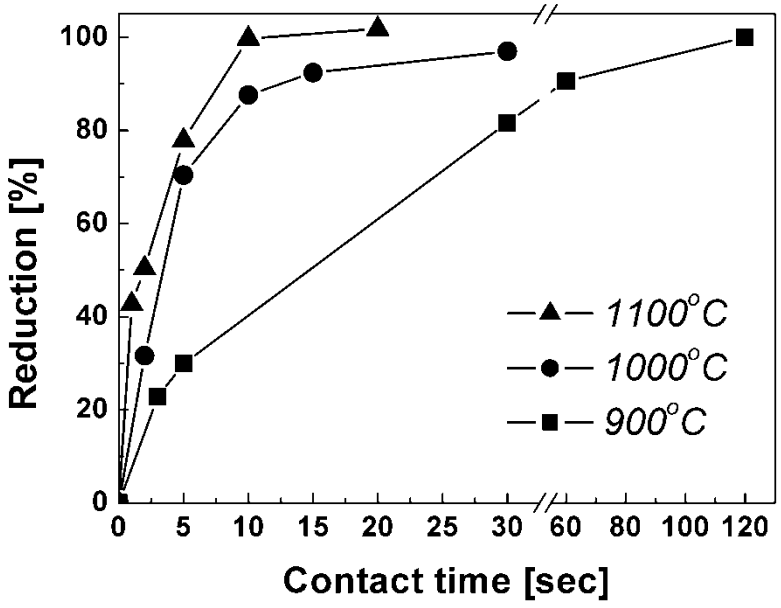

Figure 17. Approximate hydrogen reduction rate of iron ore concentrate vs. reaction time at different temperatures. (particle size: 22-30 μm)

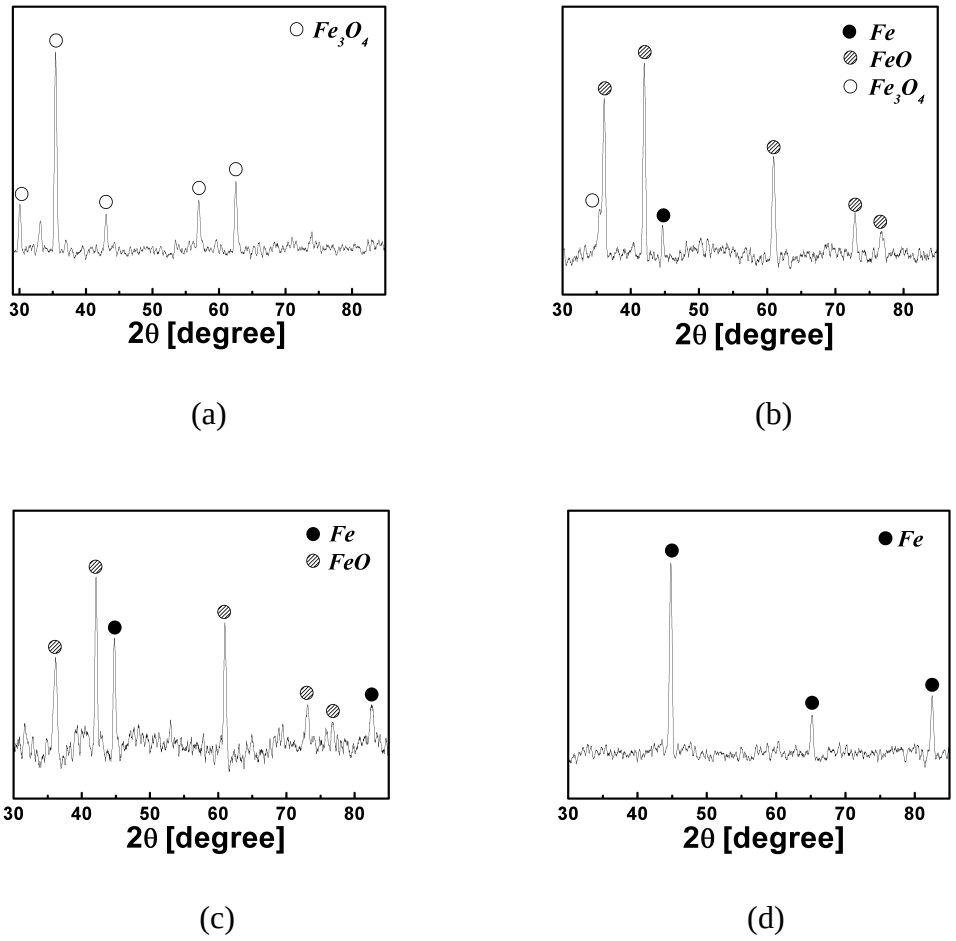

Figure 18. X-ray patterns: (a) initial iron ore concentrate (0% reduction); (b) 30% reduction at 900^{o}C for 5 seconds; (c) 50% reduction at 1100^{o}C for 2 seconds; (d) 100% reduction at 1100^{o}C for 10 seconds. (using Cu-Kα radiation)

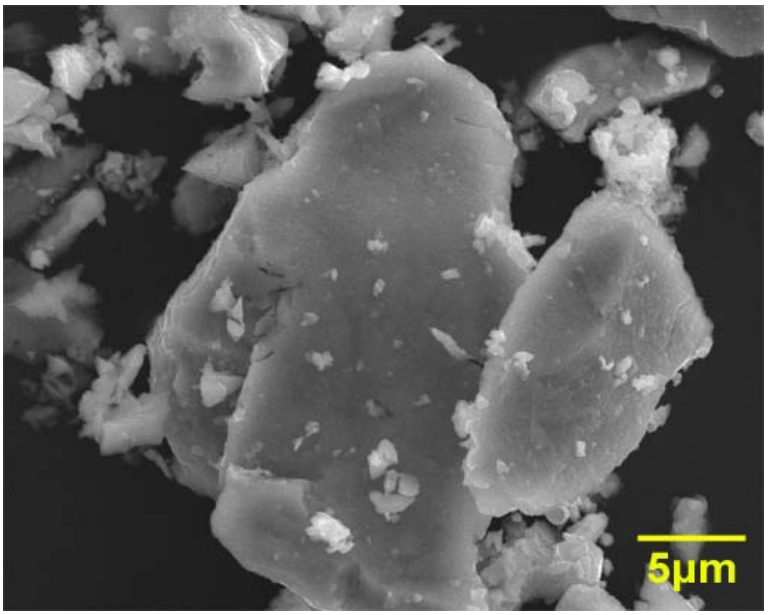

(a)

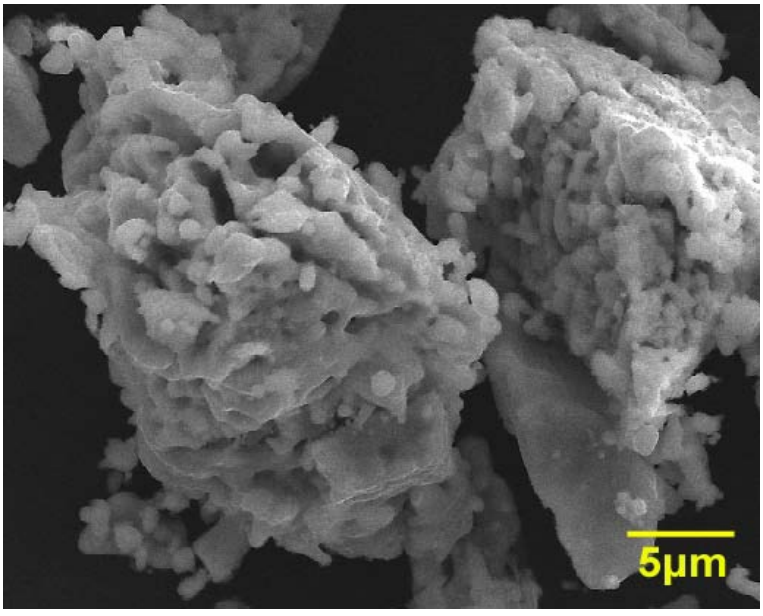

(b)

Figure 19. SEM micrographs: (a) 30% reduction after 5 seconds; (b) 100% reduction after 60 seconds. (T = 900^{o}C)

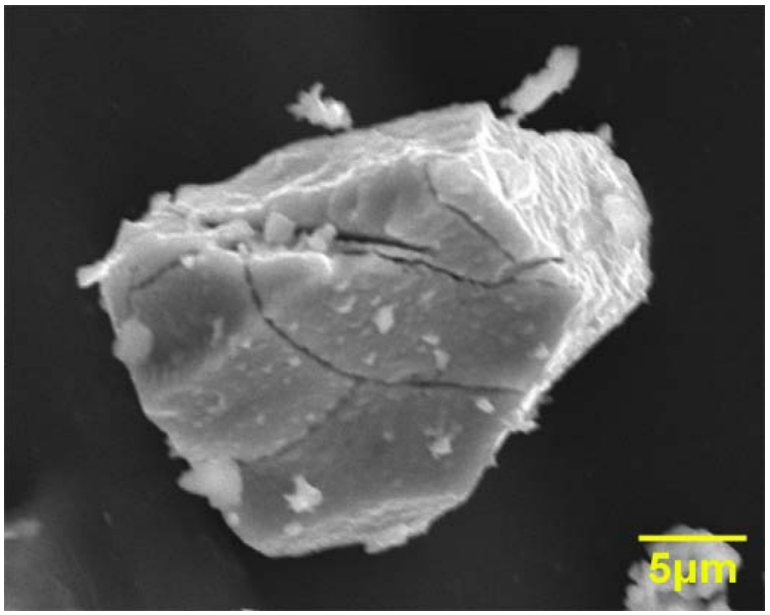

(a)

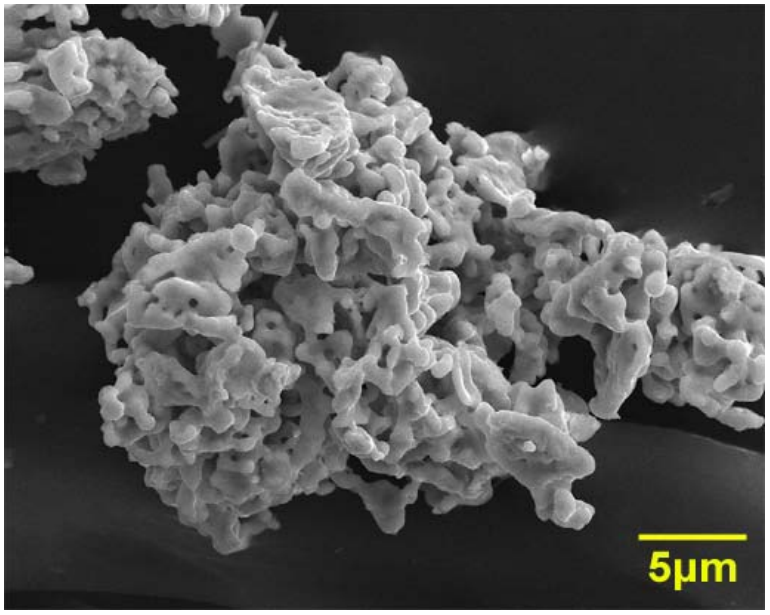

(b)

Figure 20. SEM micrographs: (a) 30% reduction after 2 seconds; (b) 100% reduction after 30 seconds. (T = 1000^{o}C)

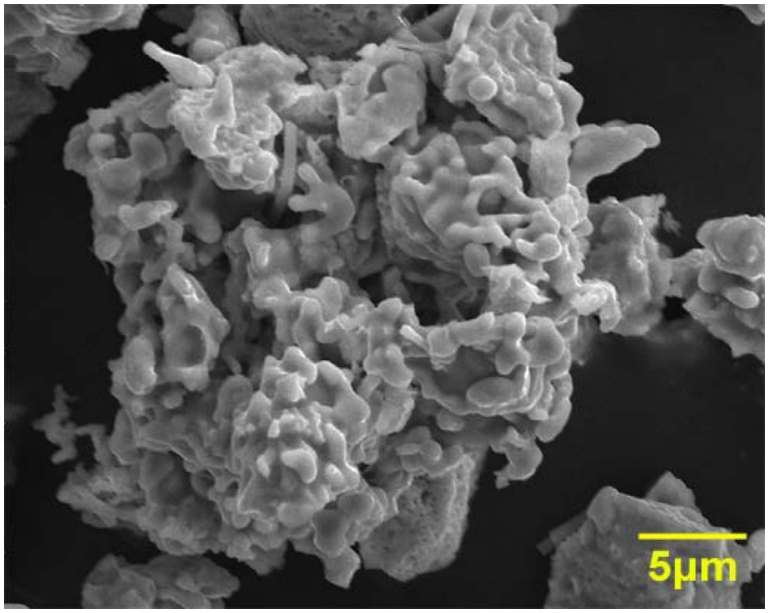

(a)

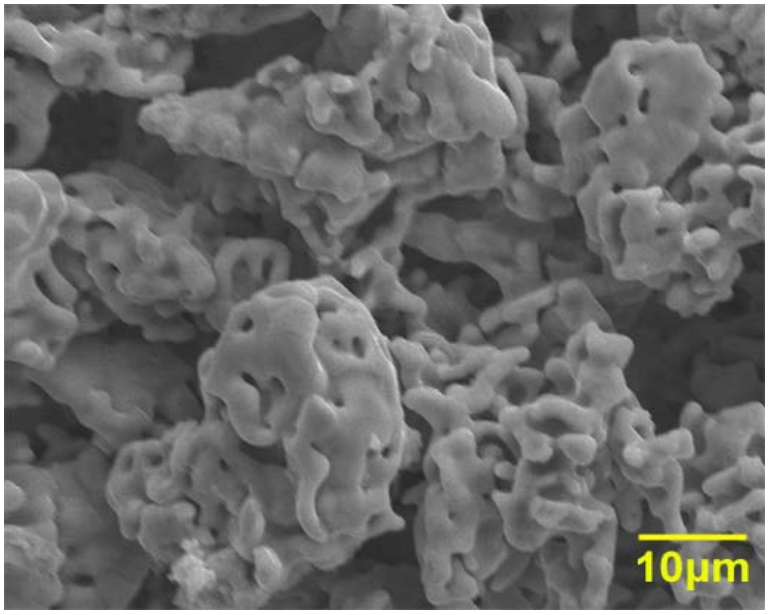

(b)

Figure 21. SEM micrographs: (a) 50% reduction after 2 seconds; (b) 100% reduction after 10 seconds. (T = 1100^{o}C)

the Kaowool bed, and the effect of minerals in Kaowool on the reactivity of iron oxide.

These measurements indicated that the reduction rate was indeed sufficiently rapid even at rather moderately high temperatures. They also provided an expectation that the rate would be higher at higher temperatures. The results, therefore, justified further measurements of accurate rate data over expanded ranges of conditions.

5.2 Kinetics Measurements

The major purpose of the hydrogen reduction rate measurements in the present study was the investigations on the kinetic feasibility of the proposed technology. Specifically, the rate measurements were mainly aimed at determining whether a high metallization degree can be obtained within a few seconds of residence time that is typically available in a suspension reduction process at a reasonable temperature and with an acceptable amount of excess hydrogen. While more comprehensive rate measurements including the entire conversion range versus time are continuing in this laboratory as an independent study, the following discussion is presented with an emphasis on the determination of the kinetic feasibility of the proposed ironmaking process.

5.2.1 Effect of Temperature

In the first series of experiments with the high temperature drop-tube reactor, over 90% reduction was attained in 1.6 seconds and the particles were almost completely reduced in 2.5 seconds at 1200^{o}C in large excess hydrogen, as shown in Figure 22. Because of the way of experiments were conducted, the residence time and % excess H_2 are directly coupled, i.e. the amount of iron oxide fed was kept the same and the hydrogen feed rate was varied. The residence time was varied by the flow rate of

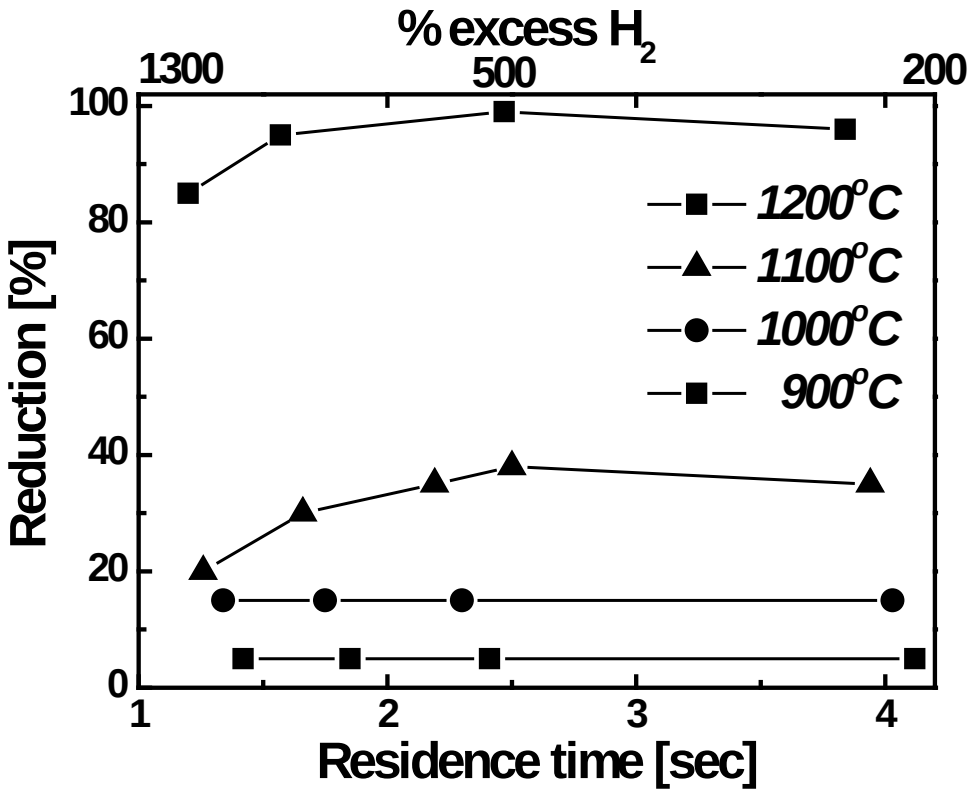

Figure 22. Hydrogen reduction rate of iron ore concentrate vs. residence time and % excess H_2 at 900-1200^{o}C. (particle size: 25-32 μm)

hydrogen.

As expected for thermally activated processes, increased temperature promotes a higher reduction rate. It is especially noted that there was a considerable increase in the hydrogen reduction rate when temperature was increased from 1100 to 1200^{o}C, which essentially establishes the lower limit of the process temperature of the suspension reduction process at approximately 1200^{o}C, given that the residence time in such a process would be in the same range.

At low excess H_2, the reduction rate decreased even in a longer residence time due to the effect of water vapor produced by the reduction reaction. Water vapor not only lowers the partial pressure of hydrogen but also decreases the thermodynamic reducing power of the gas due to the equilibrium limitation of the FeO-H_2 reaction system (K_{R2} = 0.88 at 1200^{o}C).[97] This point can be further understood by considering the following simplified global rate expression for iron oxide reduction:

$$R = k_{app} \cdot f\left(p_{H_2}, p_{H_2O}\right) = k_{app}\left(p_{H_2}^{m} - p_{H_2O}^{m} / K_{R2}^{m}\right) \tag{18}$$

Thus, the presence of water vapor lowers p_{H2} and also increases the negative term in the parentheses. In Equation (18), m represents the reaction order and the global apparent rate constant (k_{app}) includes the effect of internal structure development, especially the specific surface area, during the reduction, which is dependent on the sample and reaction conditions.

To determine whether external mass transfer has a significant effect on the experimentally determined reduction rate, an estimation of mass-transfer controlled rate

was performed. The overall process consists of chemical reaction at the interface between the unreacted core and the product layer and the diffusion of gaseous reactants and products through the product layer and through the boundary layer at the external surface of the solid. When the external mass transfer presents comparable resistances to the progress of reaction, the reduction rate of iron oxide by hydrogen where the final stage of the reduction, i.e. the reaction of FeO with H_2, is limited by equilibrium can be expressed as Equation (19).

$$\rho_O V_p \frac{dX}{dt} = bk_m A_p \left(p_{H_2} - p^e_{H_2} \right) \tag{19}$$

where all in consistent units, ρ_O = moles of oxygen atom per unit volume of the solid, V_p = volume of the solid, X = degree of reaction, t = reaction time, b = stoichiometric coefficient, k_m = mass transfer coefficient, A_p = surface area of the solid, p_{H2} = partial pressure of hydrogen, p^e_{H2} = partial pressure of hydrogen at equilibrium.

Assuming V_p and A_p remain unchanged by reaction, Equation (19) can be written as

$$\frac{dX}{dt} = \frac{3bk_m}{\rho_O r_p} \left(p_{H_2} - p^e_{H_2} \right) \tag{20}$$

where r_p = radius of the solid particle,

By integration, Equation (20) becomes

$$X = \frac{3bk_m \left(p_{H_2} - p^e_{H_2} \right)}{\rho_O r_p} t \tag{21}$$

Then, the time required for the complete reaction of the specimen (X = 1) can be calculated from Equation (22).

$$t\big|_{X=1} = \frac{\rho_O r_p}{3bk_m\left(p_{H_2} - p^e_{H_2}\right)} \tag{22}$$

When the particles are spherical and small enough to be entrained in the gas stream, the Sherwood number (Sh) can be taken to be its lower-limit value of 2. Then, the mass transfer coefficient (k_m) is expressed by Equation (23).

$$Sh = \frac{k_m\left(2r_p\right)}{D} = 2 \tag{23}$$

By combining Equations (22) and (23),

$$t\big|_{X=1} = \frac{\rho_O r_p^2}{3bD\left(p_{H_2} - p^e_{H_2}\right)} \tag{24}$$

The molar concentration of oxygen (ρ_O) in the solid Fe_3O_4 is 89.32 kmol/m^3. The radius of Fe_3O_4 sphere (r_p) is 15 μm. The stoichiometric coefficient b is 1 because one mole of oxygen atoms reacts with one mole of hydrogen molecules producing one mole of water vapor during the reduction of iron oxide. The binary diffusion coefficient of hydrogen and water vapor (D) is calculated with the aid of the Chapman-Enskog equation as 15.32 cm^2/s at 1200^{o}C.[91] At equilibrium, (p_{H2}-p^e_{H2}) becomes 40.3kPa, which is equivalent to 3.29 mol/m^3, considering the equilibrium constant value (K_e = 0.88) at

1200°C. Then, it is calculated that the reduction should be completed in 1.33 x 10^{-3} seconds if the reaction is limited by external mass transfer. However, it is far from the observation from the experiments.

To determine whether the diffusion of gaseous species through the product layer has a significant effect on the experimentally determined reduction rate, an estimation of diffusion-controlled rate was also performed.

When the reaction is limited by the diffusion, the conversion-*vs*-time relationship for an isothermal, first-order reaction of a nonporous solid which has the shape of a sphere can be expressed as[91]

$$\left(\frac{K_e}{1+K_e}\right)\frac{6bD_e p_{H_2}}{\rho_B r_p^2}t = 1-3(1-X)^{2/3}+2(1-X) \qquad (25)$$

where, K_e = equilibrium constant, b = stoichiometric coefficient, D_e = effective diffusivity of H_2-H_2O in porous iron, p_{H2} = partial pressure of hydrogen, ρ_B = molar density of solid B, r_p = radius of the solid particle, t = reaction time, X = degree of reaction.

For the reduction of iron oxide by hydrogen limited by equilibrium, the time required for the complete reaction of the specimen (X = 1) can be calculated from Equation (26).

$$t\big|_{X=1} = \frac{\rho_B r_p^2\left(1+1/K_e\right)}{6bD_e p_{H_2}} \qquad (26)$$

The molar density of Fe_3O_4 (ρ_B) is 22.33 kmol/m^3. The radius of Fe_3O_4 sphere (r_p) is 15 μm. The equilibrium constant (K_e) at 1200°C is 0.88. The stoichiometric coefficient

b in this case is 1/4 from Reaction (12). The effective diffusivity for H_2-H_2O in porous iron reduced (D_e) of 4 cm^2/s at 1200°C obtained by Turkdogan et al.[112] was used as an approximate value. By assuming the solid is reduced by pure hydrogen, p_{H2} becomes 86.1kPa, which is equivalent to 7.03 mol/m^3. Then, it is calculated that the reduction should be completed in 2.54 x 10^{-3} seconds if the reaction is limited by the diffusion, which is also far from the observation from the experiments.

These calculations demonstrate that the rate controlled by pore-diffusion + mass-transfer is much greater than the measured rates, i.e., under this condition a 30 μm particle would be fully reduced in milliseconds compared with a few seconds as observed in this study. Therefore, it is concluded that the reaction is not limited by pore diffusion or mass transfer.

Further experiments were performed at temperatures higher than 1200°C to obtain the temperature effects. Above 1300°C complete reduction was already accomplished in less than 1.1 seconds with large excess H_2, as shown in Figure 23, and even when excess hydrogen was lowered to 40% complete reduction was reached in less than 6.5 seconds. These results confirm that the rate is sufficiently fast for the reduction of currently available concentrate to be carried out in the suspension reduction process above 1200°C.

5.2.2 Effect of Percent Excess Hydrogen

In an industrial application, it would be advantageous to operate the reduction process at a high rate with lower excess hydrogen input. Thus, additional experiments were conducted at moderate excess hydrogen and residence time. As shown in Figure 24, about 87% and 63% reductions were achieved in 2.5 seconds with 550% and 224% excess hydrogen, respectively, at 1200°C. With 1100% excess hydrogen, the conversion

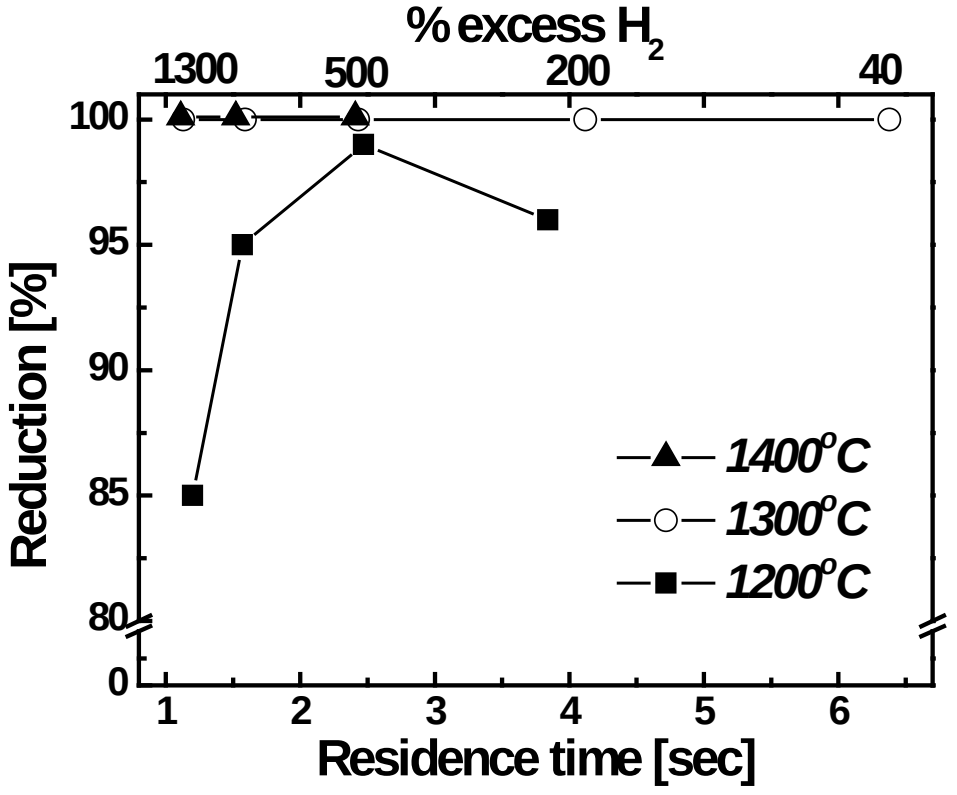

Figure 23. Hydrogen reduction rate of iron ore concentrate vs. residence time and % excess H_2 at 1200-1400^{o}C. (particle size: 25-32 μm)

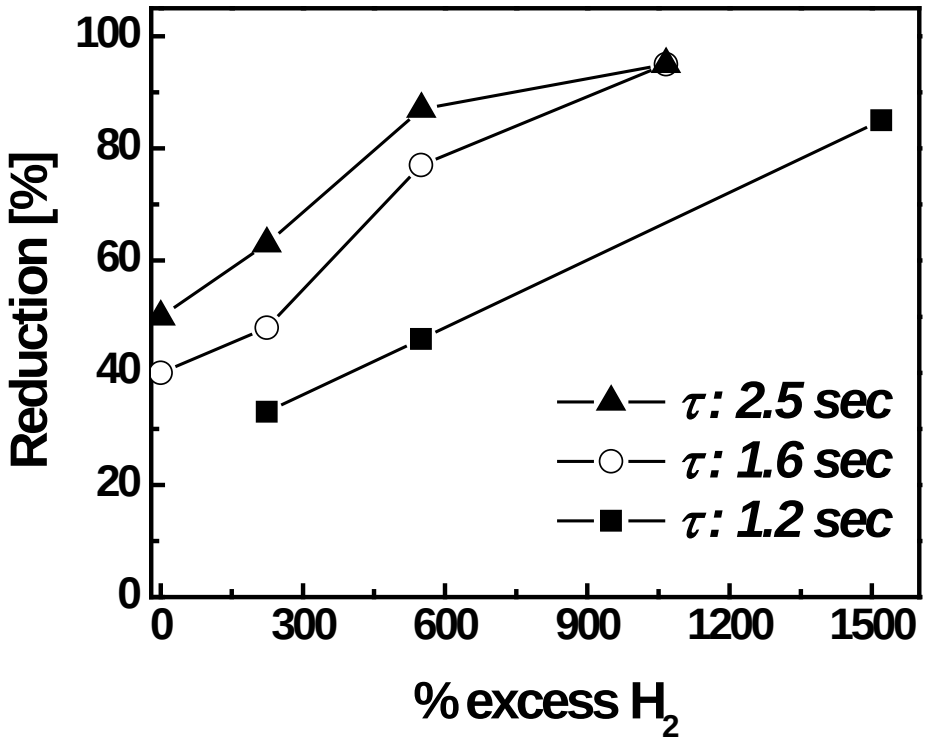

Figure 24. Hydrogen reduction rate of iron ore concentrate vs. % excess H_2 at 1200°C. (particle size: 25-32 μm)

increased to 95% in the same residence time. As the residence time decreased, the reduction degree decreased accordingly.

At 1300^{o}C, about 90% reduction was achieved in 2.4 seconds with 240% excess hydrogen, as shown in Figure 25, which was 25% higher than that at 1200^{o}C at the same residence time and % excess hydrogen. When the residence time was increased to 4.1 seconds with the same excess hydrogen, reduction was already completed meaning complete conversion was achieved between 2.4 and 4.1 seconds. When the residence time was further increased to 6.5 seconds, complete reduction began to be observed with only 24% excess hydrogen. At 1400^{o}C, reduction was almost completed in 2.4 seconds with 240% excess hydrogen, as shown in Figure 26. With the same % excess hydrogen, 94% and 75% reductions were achieved in 1.5 and 1.1 seconds, respectively.

Comparing the experimental data obtained at 1200^{o}C to those at 1400^{o}C, there was a clear temperature effect on the reduction rate such that at a higher temperature, the rate was faster with the same excess hydrogen or less excess hydrogen was needed to obtain the same reduction extent in the same residence time. However, the temperature increase to 1500^{o}C did not result in much increase in the reduction rate, comparing Figures 27 and 28. This is believed to be due to the melting of FeO (m.p. ~1380^{o}C) which prevents the formation of cracks in the particles seen at lower temperatures.

Reduced iron also forms a dense layer at this temperature rather than porous layer as at low temperatures. A weak dependence of the reduction rate on temperature may be expected if the chemical kinetics have become sufficiently rapid at these increased temperatures so that pore diffusion and mass transfer between the bulk gas and particle control the overall rate. As discussed in the previous section, however, the rate controlled by pore-diffusion + mass- transfer for the small iron oxide particles used in this work is

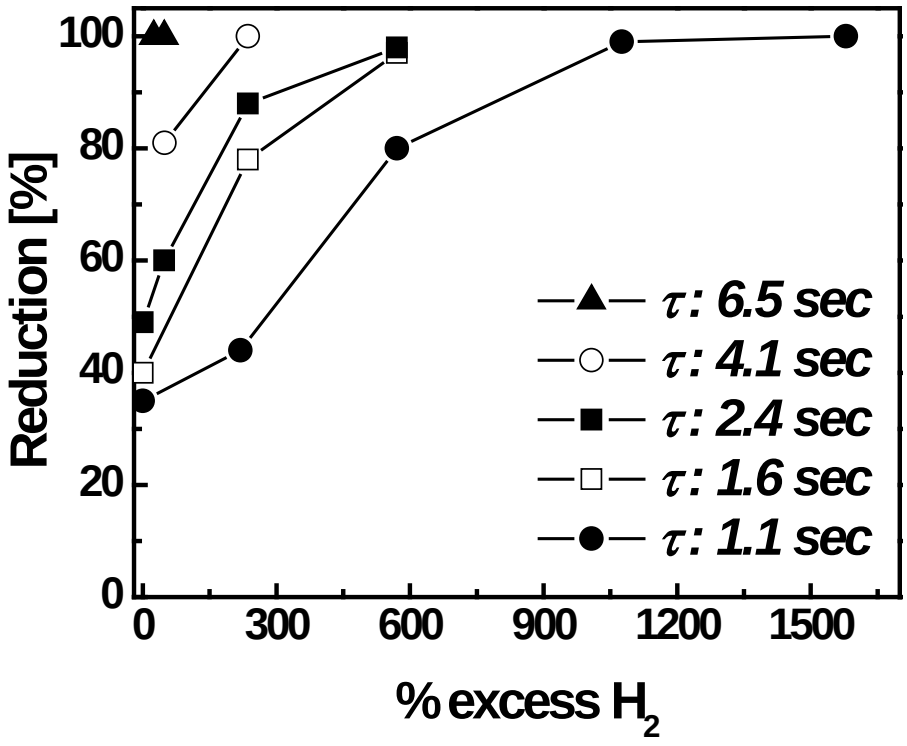

Figure 25. Hydrogen reduction rate of iron ore concentrate vs. % excess H_2 at 1300^{o}C. (particle size: 25-32 μm)

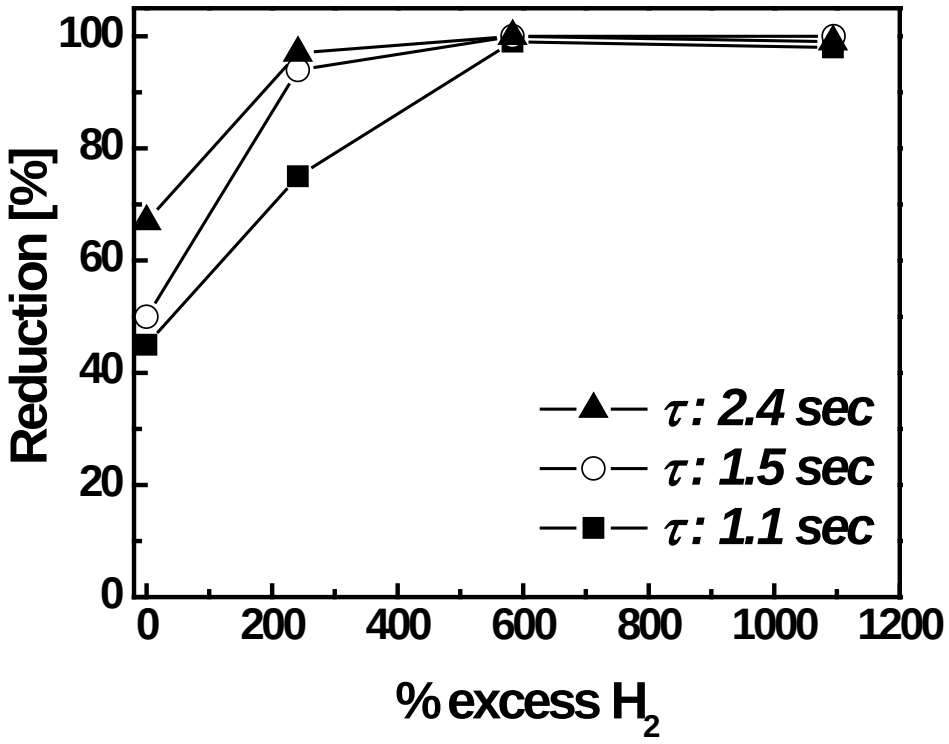

Figure 26. Hydrogen reduction rate of iron ore concentrate vs. % excess H_2 at 1400°C. (particle size: 25-32 μm)

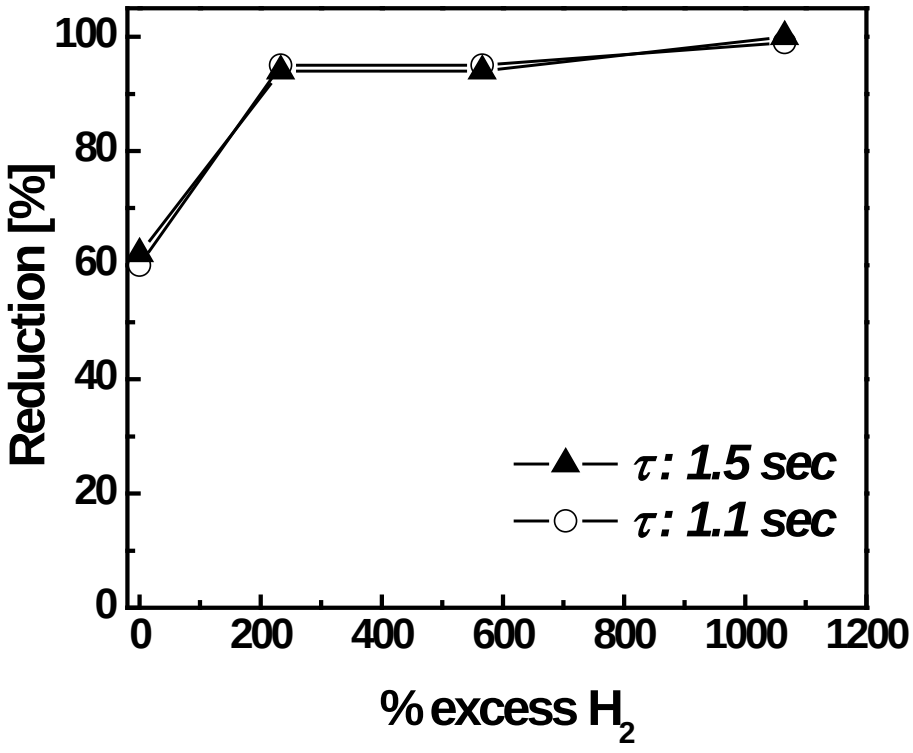

Figure 27. Hydrogen reduction rate of iron ore concentrate vs. % excess H_2 at 1500°C. (particle size: 25-32 μm)

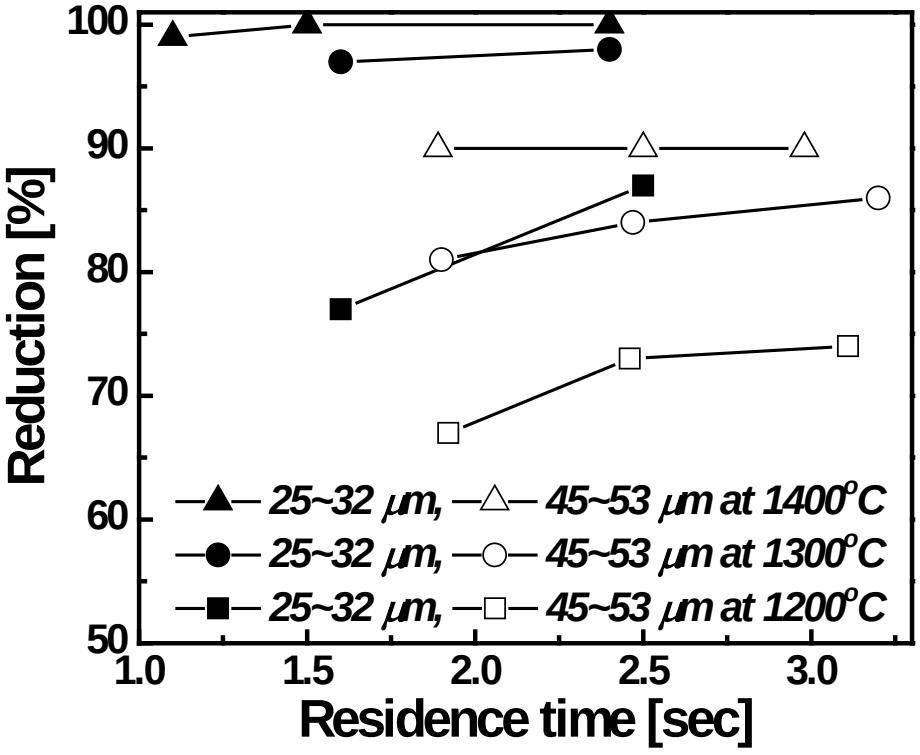

Figure 28. Hydrogen reduction rate of iron ore concentrate vs. residence time at different temperatures (1200-1400^{o}C) and particle sizes (25-32 μm and 45-53 μm) with pure hydrogen (excess hydrogen: ~550%).

much greater than the observation from the experiments, which indicates that the rate is controlled by the chemical reaction. Thus, the weak dependence of rate on temperature between 1400 and 1500^{o}C is attributed to the change in particle morphology during the reduction reaction, not because the reaction rate is controlled by mass transfer. Once the particle and intermediate product (m.p. of Fe_3O_4 = 1597^{o}C) form a fully molten phase at higher temperatures, the reduction rate is expected to increase with temperature more strongly.

5.2.3 Effect of Particle Size

Although the mean particle size of the entire concentrate was about 30 μm and thus the kinetic feasibility tests were performed with particles screened to 25-32 μm, almost half of the concentrate particles were between 30 and 100 μm, as shown in Figure 4. Therefore, further experiments were performed with larger concentrate particles (45-53 μm) at different temperatures to observe the effect of particle size on the reduction rate as shown in Figure 28. At 1400^{o}C, the larger particles reached 90% reduction in 1.9 seconds with ~550% excess hydrogen whereas the smaller particles reached almost complete reduction in 1.1 seconds. At 1300 and 1200^{o}C, the reduction extents of the larger ones ranged 81-86 and 67-74%, respectively, when the residence time was in the range from 2 to 3 seconds. With the smaller concentrate particles, reduction extents higher than 95 and 85% were achieved at 1300 and 1200^{o}C, respectively, in the same residence time range.

5.2.4 Particle Morphology

The SEM micrographs in Figures 2 and 29 show the variation of microstructure of iron ore concentrate during the reduction process. In Figure 2, the raw concentrate

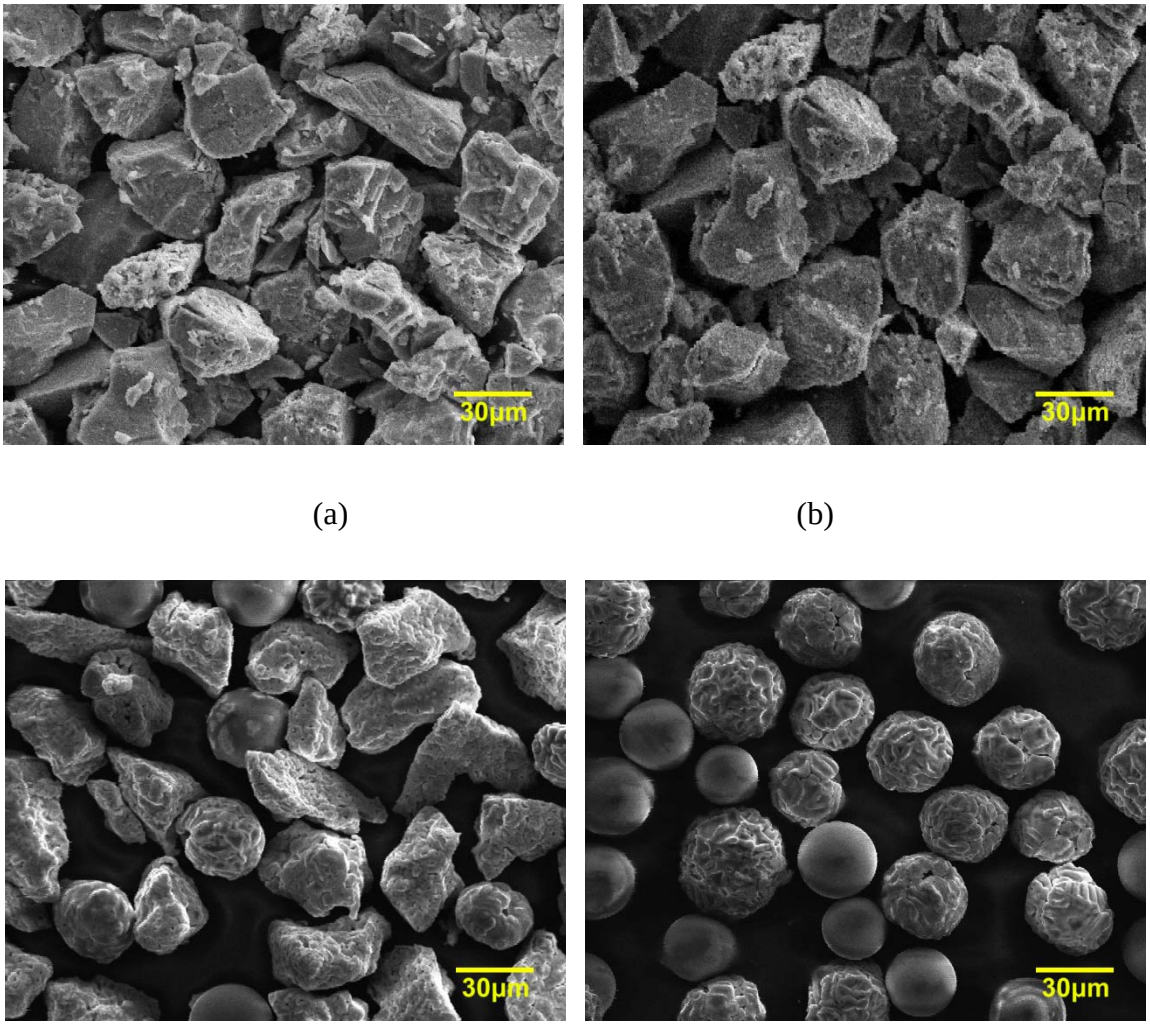

(a) (b)

(c) (d)

Figure 29. SEM photographs: (a) 25% reduction at 1100^{o}C; (b) 83% reduction at 1200^{o}C; (c) 100% reduced sample at 1300^{o}C; (d) 100% reduced sample at 1350^{o}C.

particles are irregular in shape. When the particles were reduced to 30% at 1100^{o}C (Figure 29-(a)), the size and shape remained relatively unchanged from those of the concentrate. After being 84% reduced at 1200^{o}C (Figure 29-(b)), they became porous without much change in size and shape. However, upon complete reduction at 1300^{o}C (Figure 29-(c)), most particles became more porous and some became spherical indicating the beginning of fusion. At 1350^{o}C (Figure 29-(d)), all of the particles became spherical either by melting or sintering and it is also noted that the presence of impurities like silica in the concentrate particles decreased the melting point further. From the EDAX analysis as shown in Figure 30, the spherical particles with smooth surfaces had larger amounts of silicon and oxygen which are expected to exist as silica. Thus, it is believed that the larger amount of silica decreased the melting point and these particles melted before being quenched.

Some agglomeration of concentrate particles were at times observed at low excess hydrogen and long residence time. Agglomeration in feed particles was avoided by completely drying the concentrate and increasing the flow rate of gaseous species. This dispersed the concentrate particles as soon as they came out of the powder feeding tube inside the reactor. The agglomeration of fine concentrate particles lowers the reaction rate and residence time and thus should be avoided. Turbulence of the gas-particle flow is expected to be much higher in a large scale operation. Thus, the problem of agglomeration would be less.

The findings from the kinetic measurement conclusively show that the proposed suspension reduction process is feasible at a temperature higher than 1200^{o}C with 90% or higher reduction degree within 1-7 seconds. A temperature higher than 1400^{o}C would lso be preferable from the viewpoint of kinetics and moderate % excess H_2. This would be

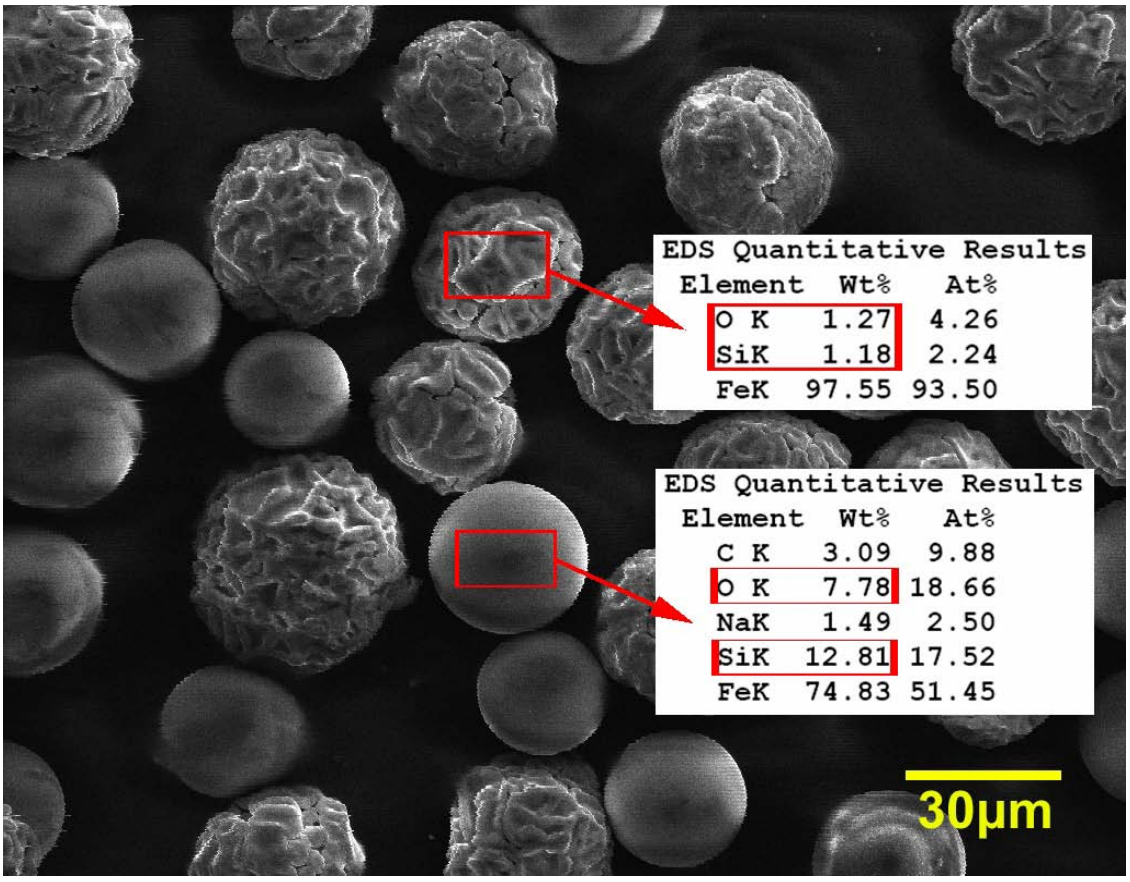

Figure 30. EDAX quantitative analysis of 100% reduced sample at 1350^{o}C.

required in any case if the reduced iron is collected as a liquid. Although there is the possibility of re-oxidation as the product is cooled during collection, the sintered or melted then solidified product, as shown in Figures 29-(c) and (d), has low specific surface area and thus low reactivity. During this work, no significant re-oxidation was observed.

5.3 Scale-Up Tests

Based on the results from the preliminary experiments and kinetic measurements, larger-scale suspension reduction tests were conducted as a step toward verifying the feasibility of the industrial application of the proposed process.

5.3.1 Reduction by Hydrogen

As shown in Figure 31, the extent of reduction with hydrogen was determined at three different nominal residence times; 3.5, 4, and 4.5 seconds in which the reduction extent was 21, 29 and 43%, respectively, with 0% excess H_2 and approached over 90% with 860% excess H_2 at 1150^{o}C. It is again noted that the maximum temperature obtained with the set-up was 1150^{o}C in the reaction zone limited by the reactor material. The reduction extent with a longer residence time was always higher and only 0.5 second difference made a notable change in the reduction rate.

Figure 32 shows that the extent of reduction significantly depends on the excess hydrogen. It is noted that the degree of reduction was relatively low with moderate excess % H_2 even though the residence time increased to 4.5 seconds. This is mainly due to the low reaction temperature in the present set-up and the kinetic measurements with the drop-tube reactor already showed that the reactivity was much faster at higher

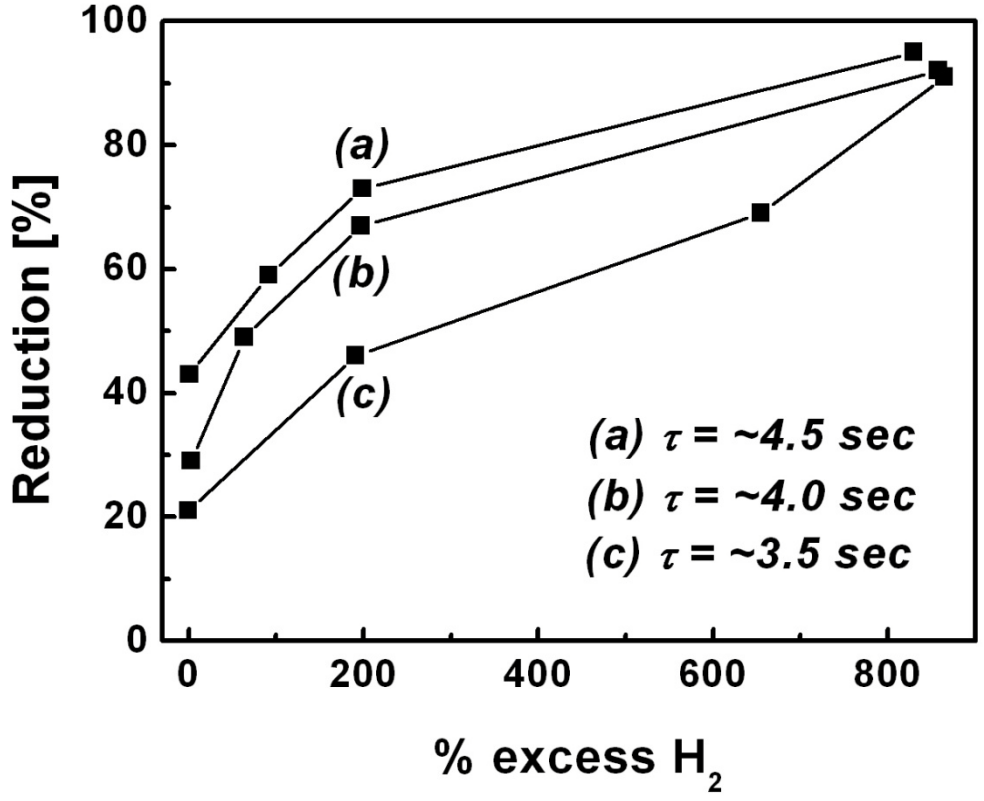

Figure 31. Reduction extent of iron ore concentrate vs. % excess H_2 in 3.5-4.5 seconds nominal residence time. (T=1150^{o}C)

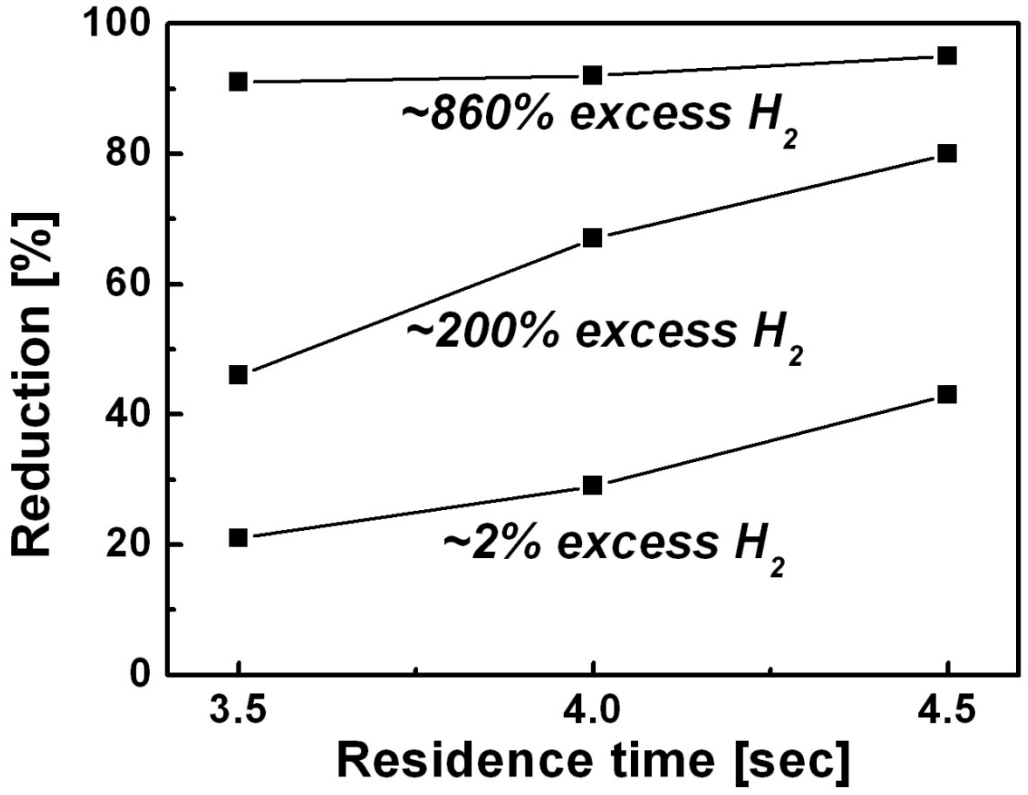

Figure 32. Reduction extent of iron ore concentrate vs. nominal residence time with 2-860% excess H_2. (T=1150^{o}C)

reaction temperatures. In an industrial operation, however, the size of furnace will be much larger than the current one, and thus the residence time is expected to be much longer. To demonstrate this opinion and better simulate the process in an industrial operation, additional experiments were conducted with moderate % excess H_2 from 50 to 100% and longer residence time from 5.0 to 5.5 seconds at 1150^{o}C. As shown in Figure 33, 64% and 71% reductions were reached in 5.0 and 5.5 seconds, respectively, with 100 % excess H_2 indicating the possibility of higher reduction rate even at moderate temperature and excess hydrogen in a industrial operation.

Based on the results from the kinetic measurements and the scale-up tests, it is apparent that the operating temperature of the facility needed to be increased to 1300-1400^{o}C to obtain a sufficiently high reduction rate with moderate excess hydrogen (0-50%) and with increased concentrate feed rate (1-5 kg/hr). A technical issue that must be overcome is the heat supply. The heat may be generated internally by burning a portion of the reducing agents, or supplied by plasma or burning of other fuels. These types of processes in which hot reducing gas environment is created internally are used in many industrial operations. Examples include the reforming of natural gas, coal gasification by partial combustion, and the Horsehead Flame Reactor Process for treating electric arc furnace (EAF) dusts. The main effort in the current study included addressing this issue in addition to determining the feasibility of achieving high degrees of reduction in a simulated suspension process. The fabrication and further scale-up tests with such an advanced facility are on-going in this laboratory as an independent study.

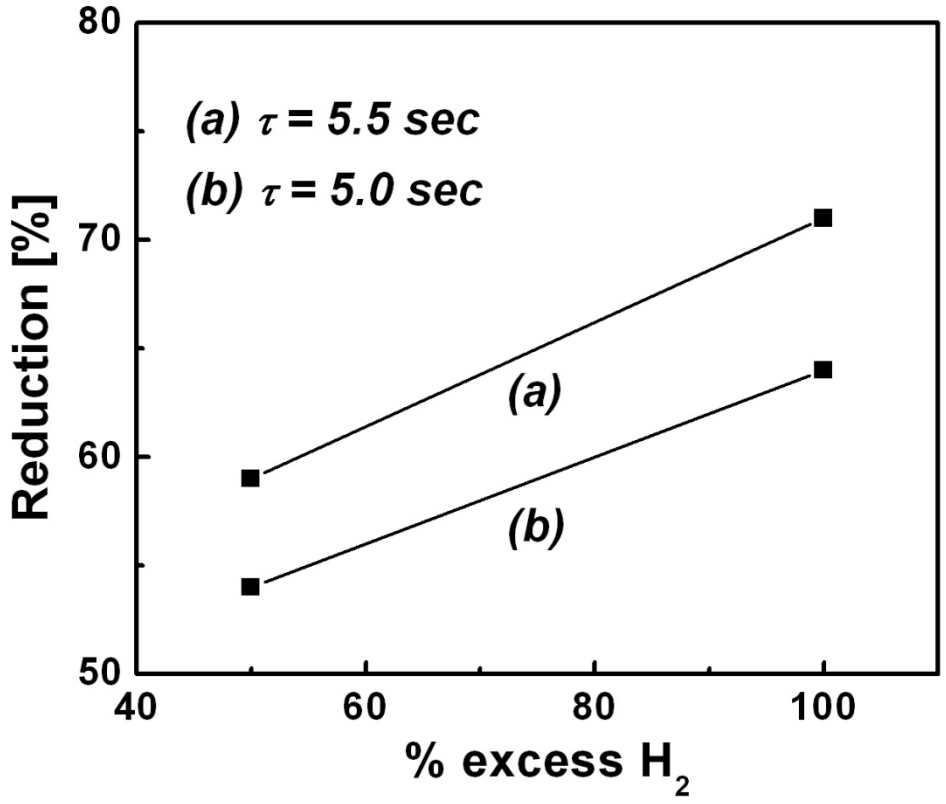

Figure 33. Reduction extent of iron ore concentrate vs. % excess H_2 in 5.0-5.5 seconds nominal residence time. (T=1150^{o}C)

5.3.2 Particle Morphology

SEM micrographs were obtained to examine the variation of microstructure of iron ore concentrate particles during the process of reduction. Figure 34 shows the microstructural changes with the degree of reduction increasing from 0% to 92%. From Figure 34-(a), it is seen that the raw concentrate particles are irregular both in shape and size. While the degree of reduction increases from 0% to 29%, cracks began to appear on the surface of particle as shown in Figure 34-(b). As the degree of reduction increased to 43% and 67% (Figures 34-(c) and (d)), more cracks and pores were formed. When the degree of reduction reached over 80% (Figures 34-(e) and (f)), the whole particle became porous. The porosity allows hydrogen to penetrate to the interior of the particles.

However, it is noted that reduction and morphological changes do not occur uniformly for all particles. In Figure 35-(a), the two particles with similar size and shape show different porosities. Sometimes, even smaller particles did not become porous while larger particles became highly porous, as seen in Figure 35-(b). This is because the gas carrying the particles was introduced as an expanding jet and thus particles had different trajectories inside the reactor, which had a certain temperature distribution. This caused the particles to experience different temperatures and residence times.

5.3.3 Reduction by Syngas

Although hydrogen is the best choice as a reductant and/or fuel from environmental and reduction kinetics viewpoints, it is currently expensive. Instead, syngas, which is mainly composed of H_2 and CO from the reforming of natural gas or coal gasification, has been used as a reducing gas mixture for the majority of direct reduction (DR) processes.[113,114] Thus, the use of syngas as a reductant was examined in

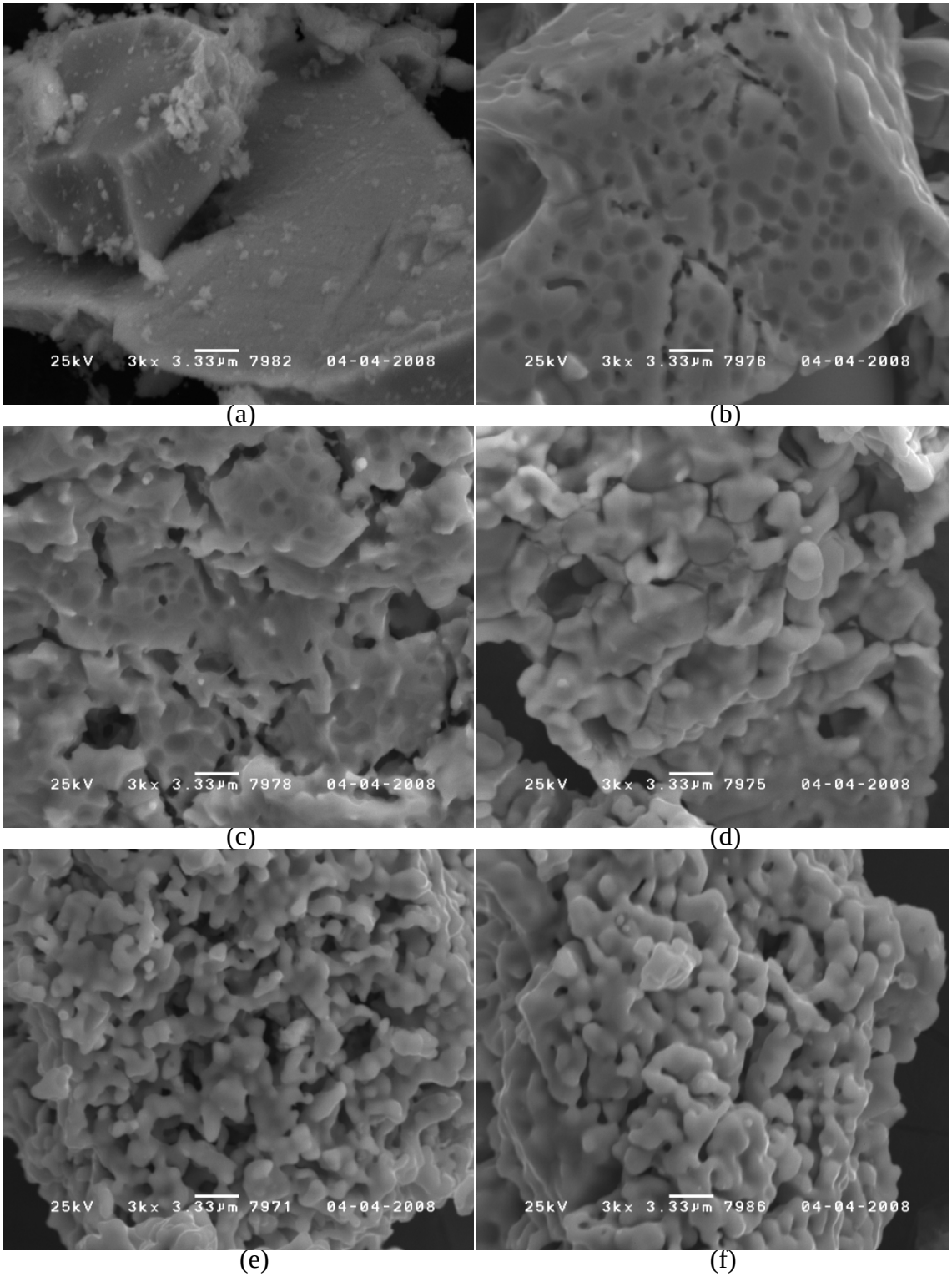

Figure 34. SEM micrographs of concentrate reduced by hydrogen at 1150^{o}C: (a) 0% reduction (as-received iron ore concentrate), (b) 29% reduction, (c) 43% reduction, (d) 67% reduction, (e) 80% reduction, and (f) 92% reduction.

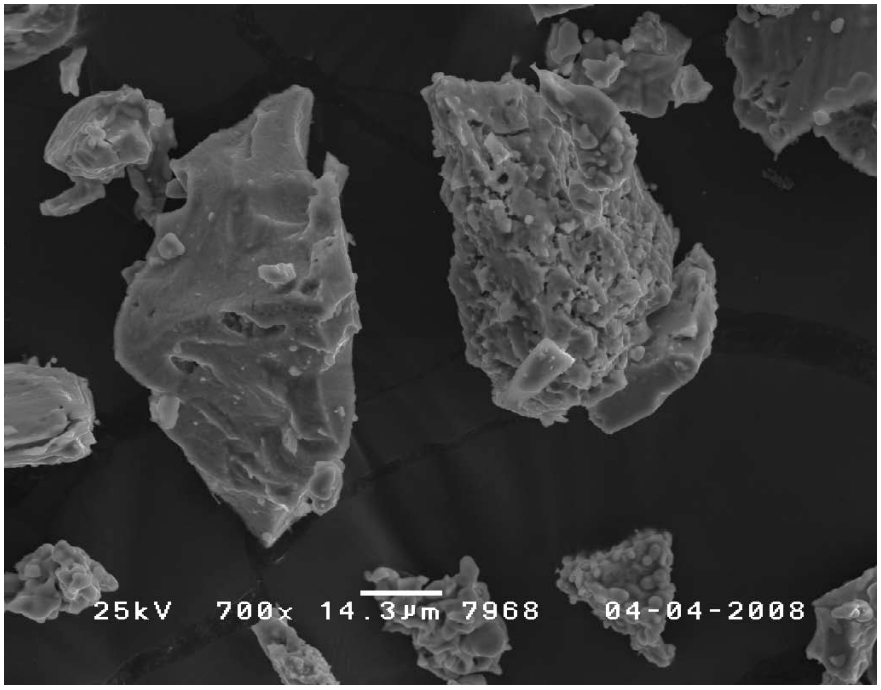

(a)

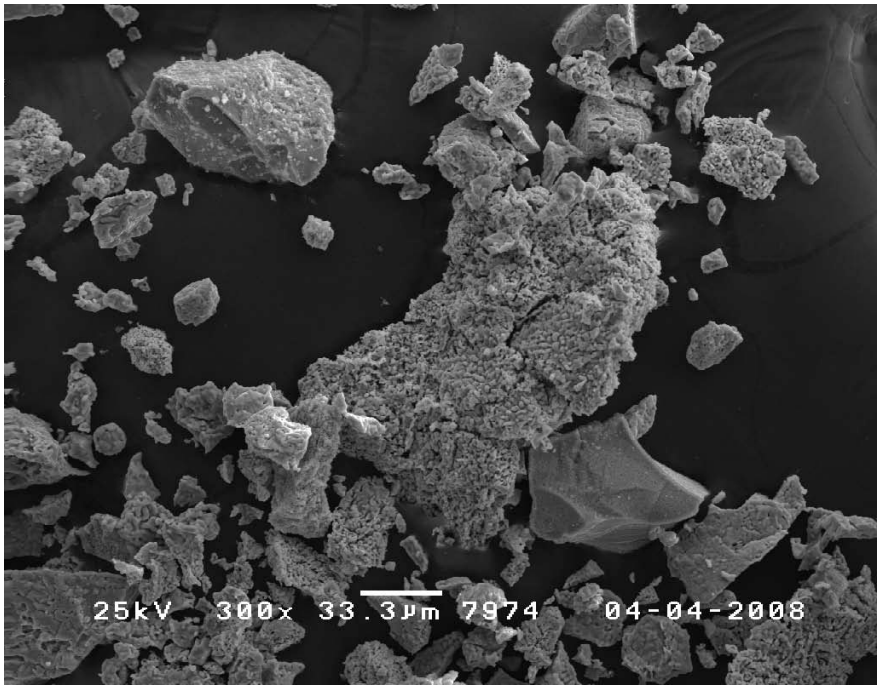

(b)

Figure 35. Lower-magnification SEM micrographs of samples illustrating the variation of particle paths: (a) 29% reduction and (b) 80% reduction. (T=1150^{o}C)

the same flash reactor used for the scale-up tests with hydrogen. The syngas was simulated with a mixture of H_2, CO, and N_2 while keeping the compositional ratio the same as that obtained by mixing hydrogen with a combustion gas from an internal burner. This approach was based on the results from the scale-up tests indicating that the heat supply is one of the most critical technical issues to obtain a sufficiently rapid reaction rate in a gas-solid suspension reduction with moderate excess hydrogen. Considering the currently available technologies to be applicable to overcome the hurdle, it was determined that generating heat internally by a gas burner and by burning a portion of the reducing agents or other fuels would be the most promising choice. Although burning hydrogen only as a heat source would be the simplest, there is no such burner available at present. Thus, the idea was adapted that hot reducing gas may be generated internally from the partial combustion of natural gas with oxygen, which is typical in many industrial operations. The only difference is to supply additional hydrogen for higher reactivity of the reducing gas.

The variation of the concentration of each gas at equilibrium in the hot reducing gas generated from the partial combustion of natural gas with oxygen was calculated at different temperatures with the Outokumpu's HSC software[98] as shown in Figures 36-39. The adiabatic temperatures of the flame and the equilibrium gas compositions are listed in Table 4. Considering the following factors - (1) the amount of O_2 remaining after the combustion, (2) the ratios of H_2 to H_2O and CO to CO_2, which should be large enough for the hot reducing gas from the partial combustion of methane to participate in the reduction process, (3) the adiabatic flame temperature, and (4) the temperature of the hot educing gas stream - 50% of stoichiometric amount O_2 system was determined to be the best as the input condition. Having determined the ratio between the fuel and the oxidant

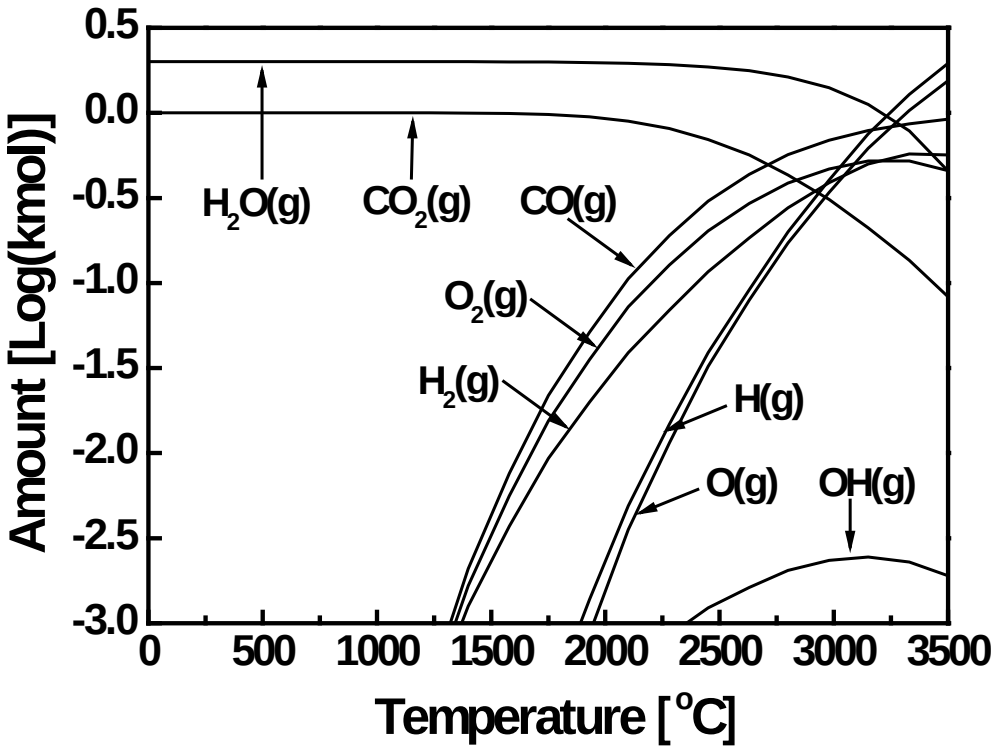

Figure 36. Equilibrium compositions of the combustion product gases at various temperatures with CH_4: O_2 = 1 kmol: 2 kmol (stoichiometric amount O_2).

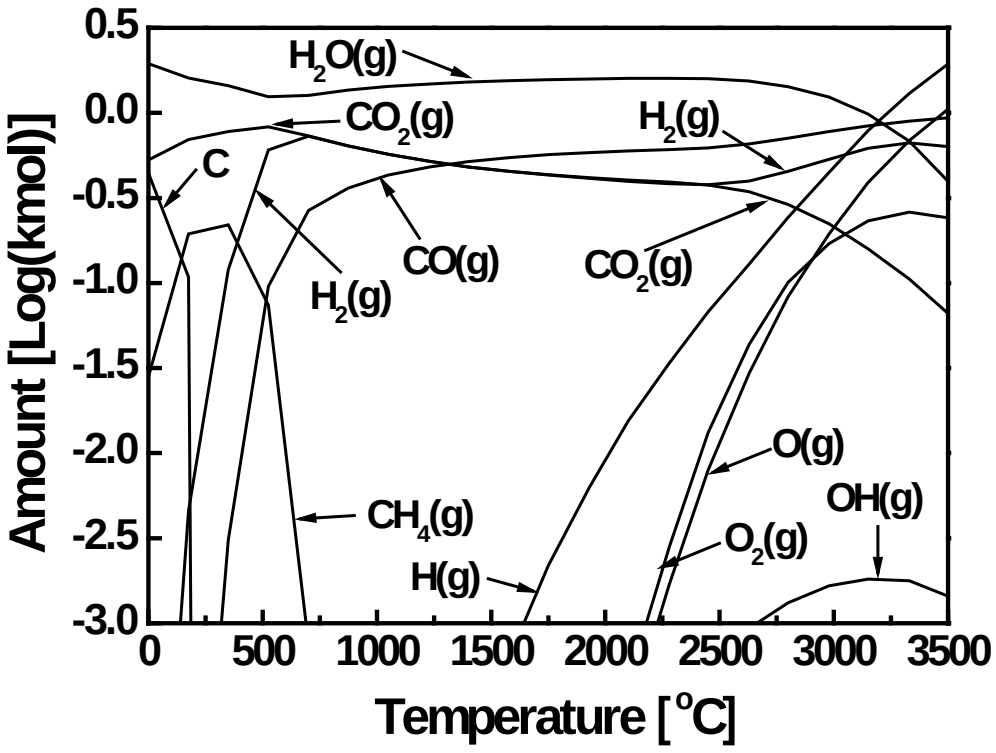

Figure 37. Equilibrium compositions of the combustion product gases at various temperatures with CH_4: O_2 = 1 kmol: 1.5 kmol.

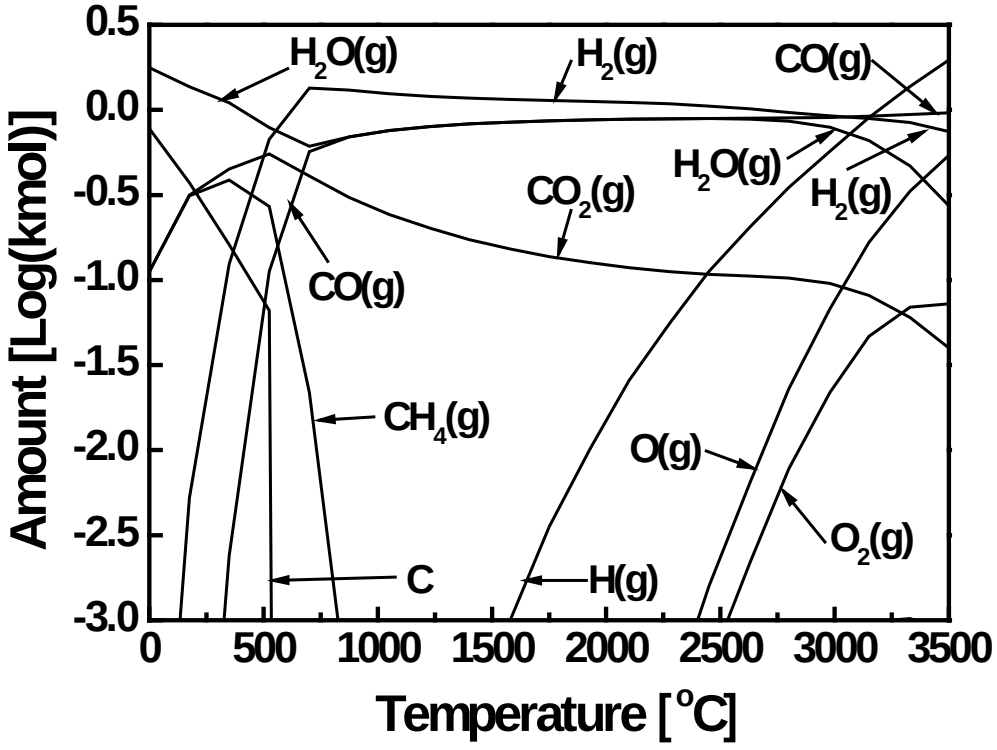

Figure 38. Equilibrium compositions of the combustion product gases at various temperatures with CH_4: O_2 = 1 kmol: 1 kmol.

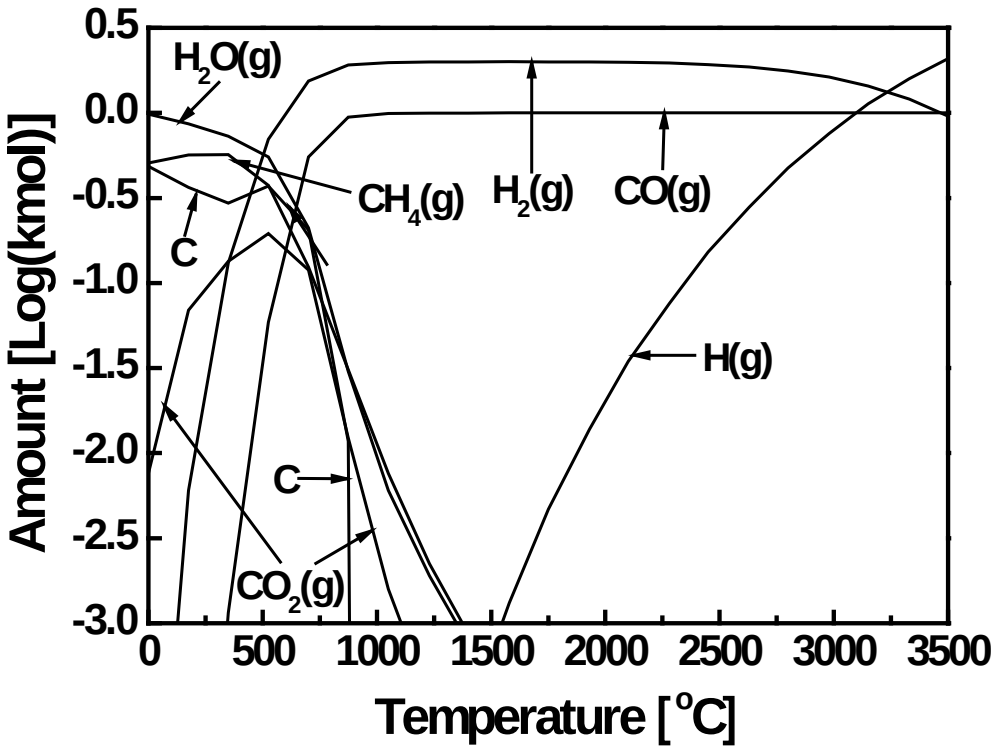

Figure 39. Equilibrium compositions of the combustion product product gases at various temperatures with CH_4: O_2 = 1 kmol: 0.5 kmol.

Table 4. Equilibrium compositions and adiabatic temperatures of product at different input conditions.

Input			Output					
CH_4 [kmol]	O_2 [kmol]	T [^oC]	H_2 [kmol]	CO [kmol]	H_2O [kmol]	CO_2 [kmol]	O_2 [kmol]	T [^oC]
1.0	2.0 (100)[a]	25	0.5	0.7	1.5	0.3	0.6	3100
1.0	1.5 (75)	25	0.7	0.8	1.3	0.2	0.2	3100
1.0	1.0 (50)	25	1.1	0.9	0.9	0.1	7.2×10^{-4}	2500
1.0	0.5 (25)	25	1.7	0.8	0.1	0.06	7.0×10^{-22}	770

a: % of stoichiometric amount of O_2

and assumed the concentrate feed rate at 0.1 mol/min, mass and energy balance calculations have been conducted to determine the amounts of additional hydrogen, the input of the gas burner (CH_4 and O_2) and the output of the burner (H_2, H_2O, CO, and CO_2). The temperatures before and after the reaction between the concentrate and the reducing gases were also calculated as shown in Table 5. The amount of additional hydrogen was calculated at 200% excess hydrogen, namely twice the stoichiometric amount of hydrogen to reduce Fe_3O_4 to Fe.

Based on the thermodynamic considerations, the actual experimental conditions with syngas for the scale-up tests were prepared. The reaction temperature was set to be 1150^oC which was the maximum temperature the flash reactor could reach and the same temperature as all the scale-up tests with hydrogen were performed. At a fixed feed rate of concentrate (1.5 g/min), the input amount of each component was calculated based on material and energy balances considering the preheated input gas temperature (500^oC), the heat of reaction between CH_4 and O_2 in the gas burner, and the heat absorbed by the room-temperature hydrogen added to improve the reduction rate. In the actual experiments, H_2O and CO_2 were replaced with N_2 since the effect of the ratio between H_2 and CO in the reducing gas stream was the major concern rather than the effect of the thermodynamic limitation by the ratio H_2/H_2O or CO/CO_2 on the iron oxide reduction. Once all the amounts of input materials were determined, the residence time of the concentrate was calculated.

A series of experiments showed that about 90% reduction was accomplished in 3.5 seconds at 860 % excess hydrogen (32.7 kPa H_2, 53.4 kPa N_2). The % reduction remained similar when 11.6 kPa of N_2 was replaced with the same amount of CO. When 10% (7.6 kPa) of H_2 was replaced with CO the conversion decreased from 90% to 80%

Table 5. Material and energy balance in the reduction with gas burner. (P=86.1 kPa)

Input (at 25 °C)		Gas burner system						T1[b]	T2[c]
		Input (at 25 °C)		Output (at 2500°C[a])					
Fe_3O_4	H_2	CH_4	O_2	H_2	H_2O	CO	CO_2		
23.2 [g/min] 1.4 [kg/h]	22.9 [L/min]	8.6 [L/min]	8.6 [L/min]	87.7 [L/min]	71.8 [L/min]	71.8 [L/min]	8.0 [L/min]	1425 [°C]	1331 [°C]

a: Flame temperature

b: Temperature of the mixture before reaction

c: Temperature after reduction reaction

even at about 4.5 seconds of nominal residence time. It was observed that there was a decrease in reduction rate by introducing syngas instead of H_2. The results are still of interest especially at higher operating temperatures where the reactivity of syngas toward iron oxide becomes higher.

5.3.4 Development of a New Bench Reactor

Encouraged by the promising results from the scale-up tests performed in this study, the development of a larger-scale test facility is in progress. The bench-scale reactor tests are necessary to overcome several technical difficulties before an industrially viable technology can be developed, such as the method of supplying the energy required to maintain the necessary temperature, the installation of proper refractory and insulation linings for the use of high temperatures, and the safe control of the facility. The new facility will produce DRI or molten iron directly from fine iron ore concentrate (10~100 μm) using hydrogen or natural gas as the fuel as well as the reductant in a closed cylindrical and vertical reaction chamber. In identifying the specific design and functional features necessary for the bench facility, the reactor heating system has been the key issue, which was the major limitation in the previous scale-up tests. The energy for the sensible heat of solid and gas feed materials and for the reduction reaction of iron oxide will be supplied by a single burner installed on top of the reduction chamber in combination with a plasma torch as a supplementary heat source. Although external preheating of the feed gases was also considered, the use of a hydrogen preheater was abandoned in favor of a plasma torch due to the fact that the maximum temperature to which large amount of hydrogen can be preheated with the commercial equipment may only be about 400^{o}C.

Figure 40 shows the conceptual diagram of the bench-scale test facility comprising several subsystems such as a burner, a powder feeder, gas delivery lines, detection and safety instrumentation, a powder collector, and an off-gas treatment system. A gas burner will generate a vertical flame inside the top part of the reaction chamber (0.81 m ID, 1.52 m high). Concentrate particles will be supplied through the burner so that they fall down through the highest temperature region in the flame and be preheated as quickly as possible, before being reduced. This flame will also be an energy source for the sensible heat for gaseous reducing agent and for the reduction reaction. For safety, the flame will be monitored by a flame detector and several thermocouples that are connected to the interlocking and control system of gas flow. If the flame would be extinguished, the system would immediately shut off the flammable gas feed lines of hydrogen and oxygen and open the purging gas lines of nitrogen to prevent possible explosion in the reactor. The gas analyzer will also keep measuring the concentrations of hydrogen and oxygen in the atmosphere near the facility and in the off-gas line. It will give a shut-off signal to the interlocking system when abnormally high concentration of either gas is detected. As an additional safety measure, a rupture disc will be installed on the top part of the reactor, which is an artificially-made weak point to be broken for pressure release if erratic burning or an unstable flame generates pressure peaks inside the reactor. More details on the safety system and procedure are explained in the Appendix. A powder collector will be installed at the bottom part of the reactor wherein the off-gas is separated from the reduced concentrates and then either combusted with air or recycled after being dehumidified.

As shown in Figures 41-43, three operating conditions with different % excess hydrogen have been examined for a basic design of the bench-scale reactor. The role of

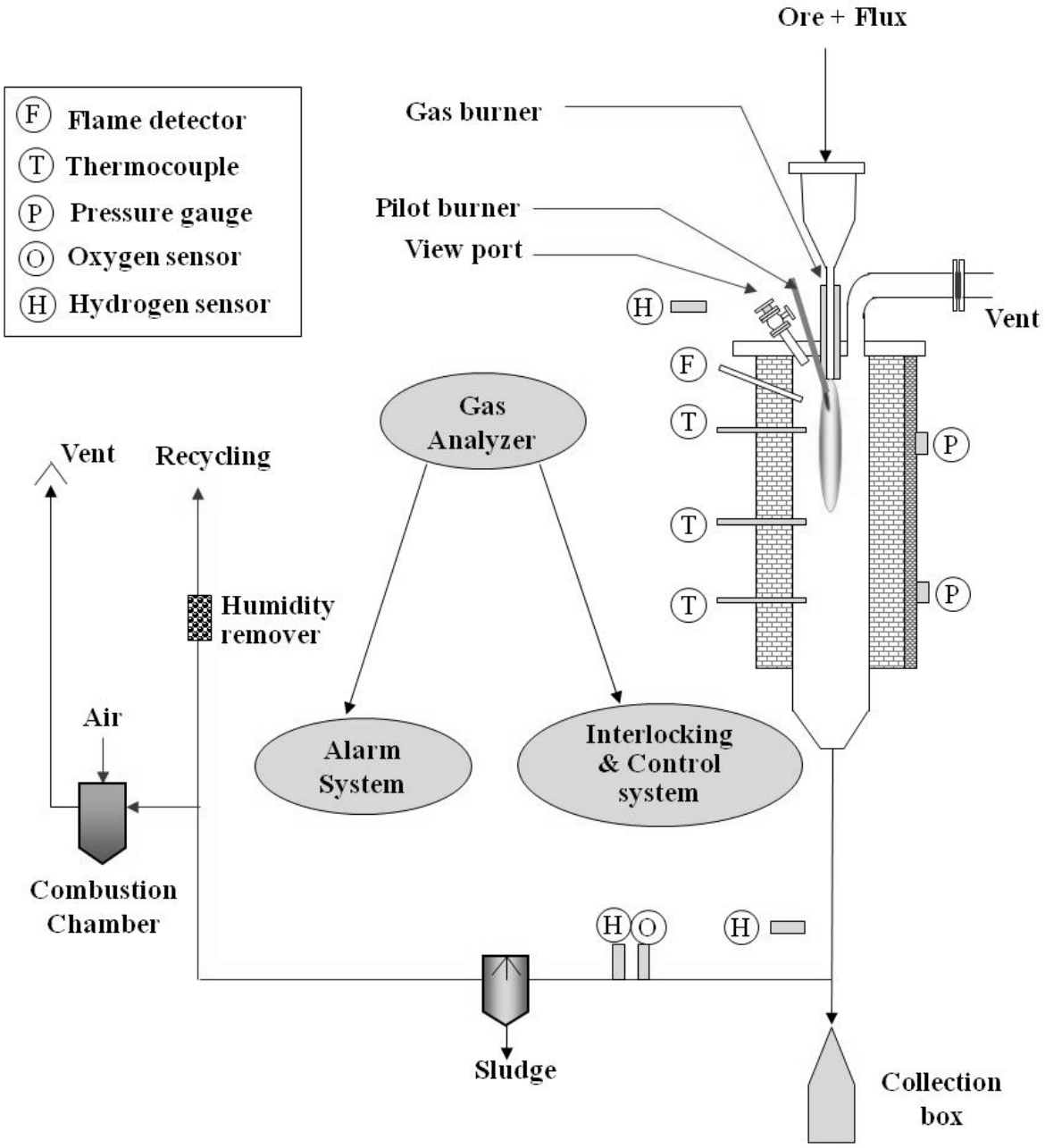

Figure 40. Conceptual diagram of a bench-scale test facility. (updated diagram of similar drawing in Ref. 115)

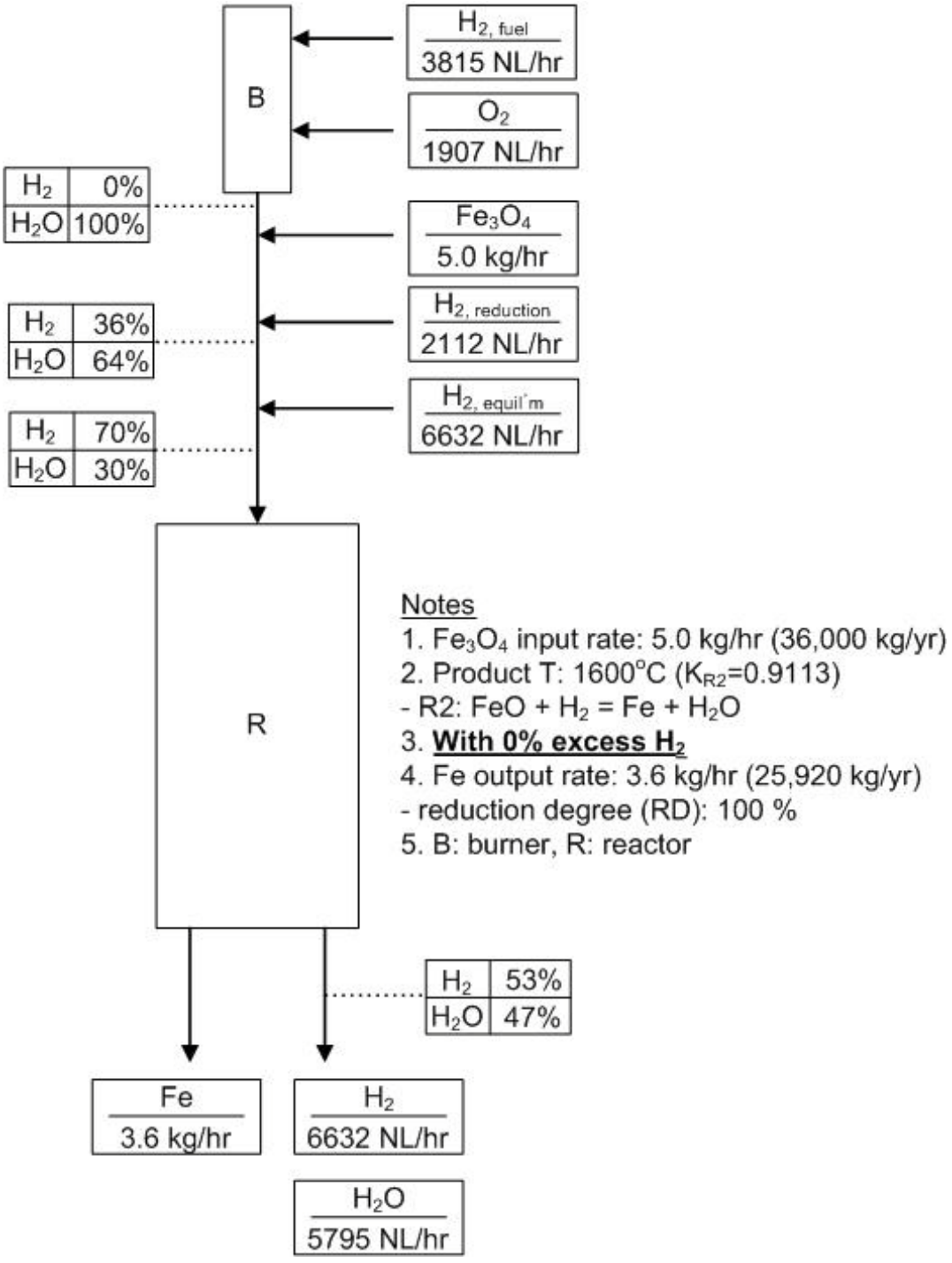

Figure 41. Operating conditions of bench reactor at 0% excess H_2.

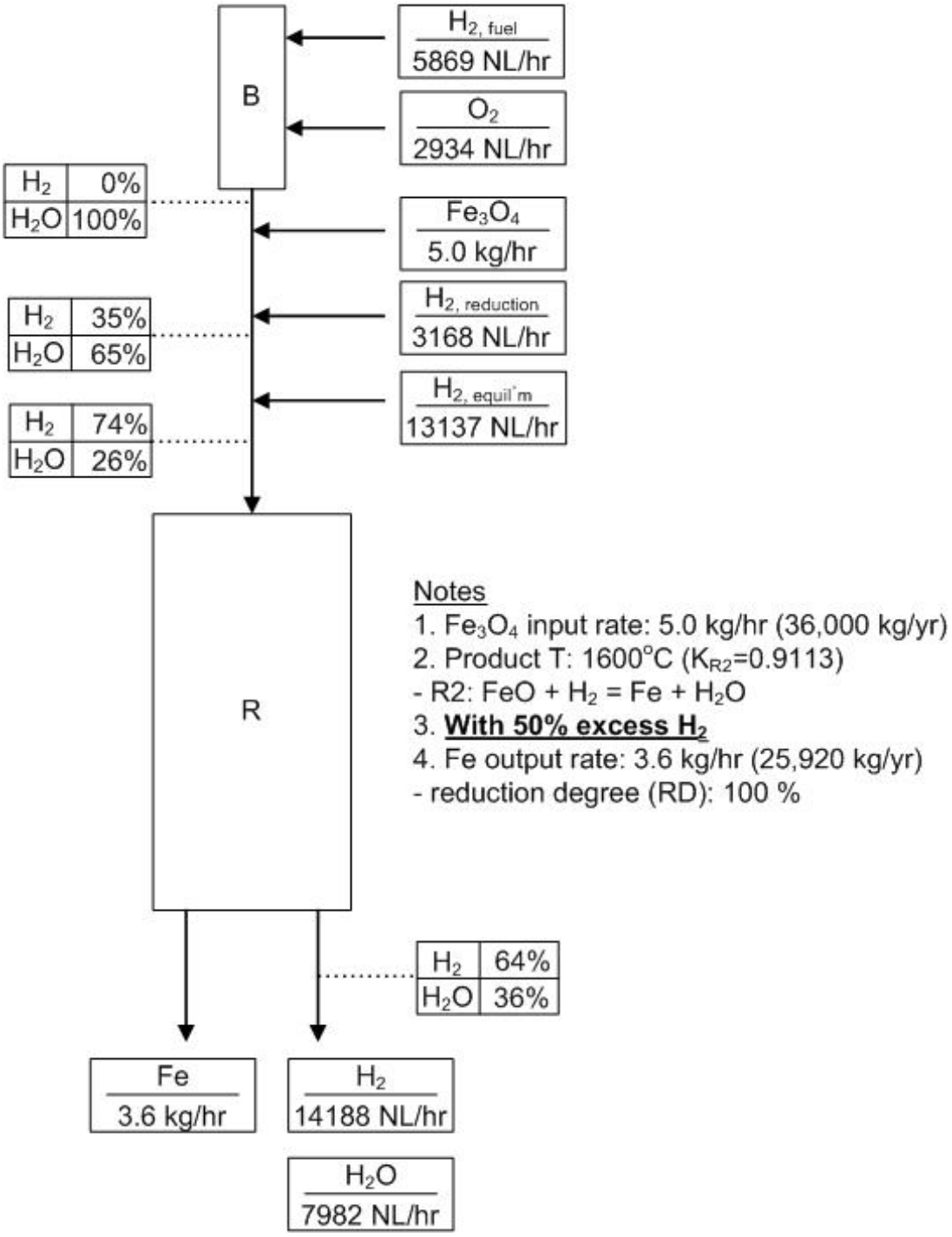

Figure 42. Operating conditions of bench reactor at 50% excess H_2.

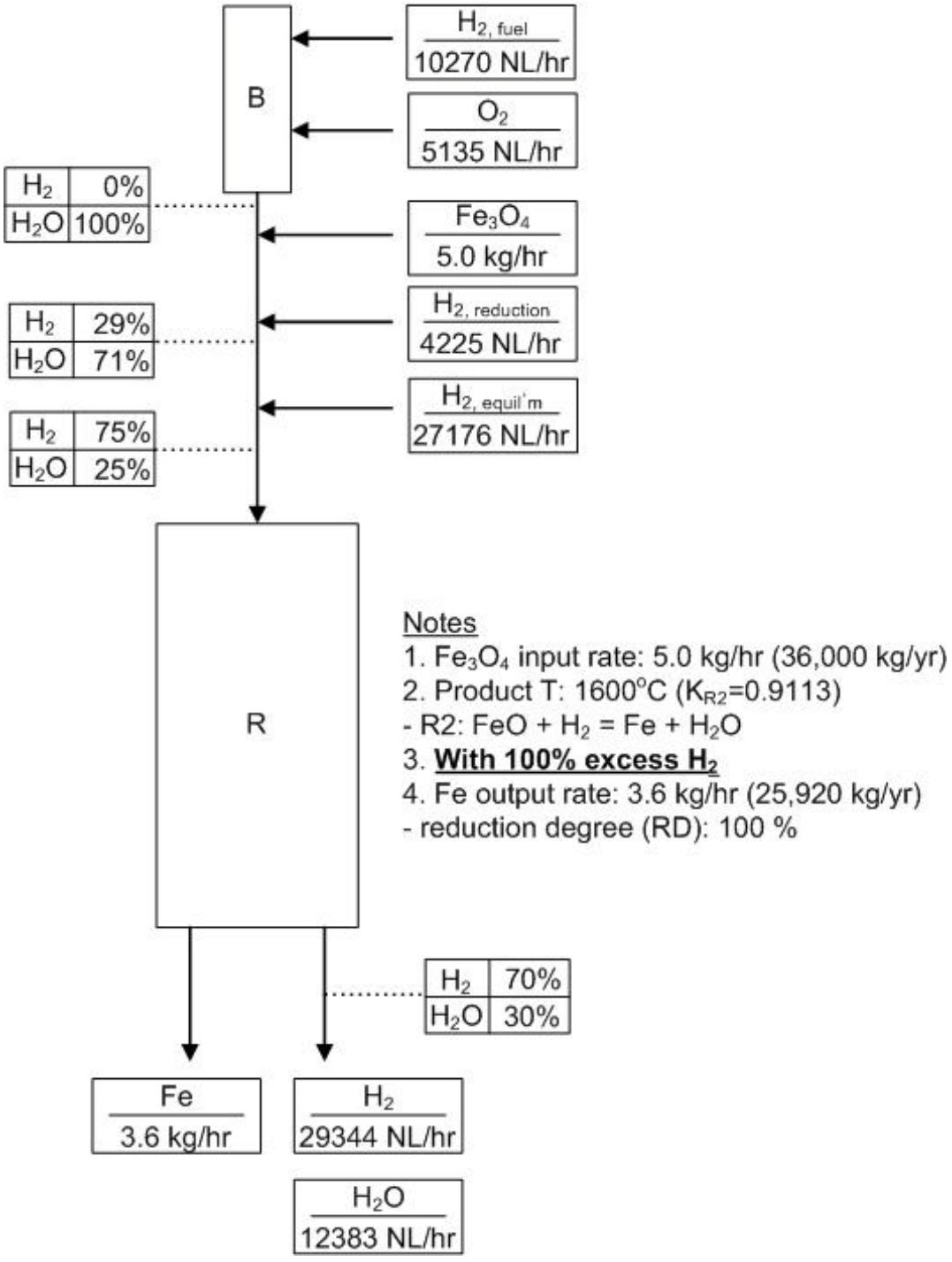

Figure 43. Operating conditions of bench reactor at 100% excess H_2.

hydrogen in this system can be divided into three categories; a fuel ($H_{2,fuel}$) to obtain necessary temperatures for reduction reaction, a reducing agent ($H_{2,reduction}$) needed to stoichiometrically convert the iron oxide to metallic iron, and an additional gas ($H_{2,equilibrium}$) to overcome thermodynamic equilibrium limit also guaranteeing the complete combustion of unreacted oxygen from the burner nozzle. A basic feed rate of iron ore concentrate in this scale is 5 kg/hr. In the diagrams, B and R represent H_2/O_2 burner and the reactor, respectively. The temperature in the main portion of the reactor is 1500 – 1600^{o}C, although there is some temperature gradient from about 3000^{o}C in the flame to 1000 ^{o}C near the gas exit.

CHAPTER 6

CONCLUSIONS AND FUTURE WORK

6.1 Conclusions

A novel green ironmaking technology is under development for producing iron directly from fine iron ore concentrates by a gas-solid suspension reduction that bypasses energy intensive and environmentally problematic cokemaking, pelletization, and sintering steps. The material and energy balance showed that the process would reduce energy consumption by about 40% of the amount required by the blast furnace and drastically lower environmental pollution, especially CO_2 emission, from the steel industry. The rate measurements of fine concentrate particles by hydrogen-containing gases were carefully designed and performed to form the most important basis for the new technology from the kinetics point of view. The findings from the kinetic measurements and scale-up tests showed that the reduction rate was fast enough to obtain 90-99% reduction within 1-7 seconds at 1200-1500^{o}C, depending on the amount of excess hydrogen supplied with iron oxide. This clearly indicates that a high metallization degree within a few seconds of residence time is feasible for a suspension process. The use of syngas from the reforming of natural gas or coal gasification as part of the reducing gas mixture was also considered, and the experimental tests showed that syngas was adequate as a reducing gas, especially at higher temperatures.

6.2 Future Work

Further scale-up tests are recommended focusing on the method of supplying the energy required to maintain the necessary temperature (1300-1600^{o}C) for a satisfactory degree of reduction with higher concentrate feed rates. The facility would produce direct reduced iron (DRI) or molten iron directly from fine concentrates (10-100 μm) using hydrogen, natural gas or syngas as the fuel as well as the reductant. The energy for the sensible heat of solid and gas feed materials and for the reduction reaction of iron oxide may be supplied by a single or multiple burners, or in combination with a plasma torch. External preheating of the feed gases is another alternative. Sophisticated material and energy balance calculations to construct process flowsheets are also recommended to establish process concepts on the bench-, pilot, and finally industrial-scale and to perform parametric studies and economic analyses. In addition, more comprehensive and systematic kinetic measurements and their CFD modeling would help to provide necessary information on the design and experimental conditions of scale-up facilities as well as the actual industrial reactor.

APPENDIX

SUMMARY OF SAFETY SYSTEM AND PROCEDURE OF NEW BENCH REACTOR

In the suspension reduction process, hydrogen is used as a fuel to provide necessary energy for the sensible heats of solid and gas feed materials as well as for the endothermic reduction of iron oxide. To burn the hydrogen, oxygen is provided to the reactor, which can put the experimental condition at a risk of explosion. Therefore, the safety specifications have been prepared as follows:[115]

1. Back flows of oxygen and hydrogen will be prevented with suitable vent stack designs, flashback arrestors, and check valves.
2. Pipes and vessels (reactor, combustion chamber) will be purged with an inert gas (nitrogen) before and after using hydrogen in the equipment.
3. Interlocking and sequence purging systems for safety on hydrogen and oxygen flow lines and on reactor will be operated appropriately.
4. Residual hydrogen and oxygen concentration will be measured at a number of locations within the system (the residual hydrogen concentration should be kept less than 3% and oxygen concentration less than 0.5%) before and after using hydrogen in the equipment.
5. A pilot burner will be used to prevent the flow of unburned hydrogen in the system, which could lead to explosion. A combustion chamber will be used to burn out the remained hydrogen in off-gas before emitting.
6. A detection system of hydrogen leakage near the connection parts such as flanges (gaskets) and valves (packing) will be installed in the site together with an alarm system.
7. A double valve system will be used for hydrogen and oxygen pipe lines to counteract in case of failure in the close/open operation or leakage through a valve.

8. Explosion-proof equipment will be used, especially for instrumentation systems, and the metallic materials to be used in the reactor should be resistant to hydrogen embrittlement.
9. An emergency-operation-stop button will be installed in an appropriate place to shutdown the plant safely in an emergency.
10. In handling of extremely fine DRI, the re-oxidation should be prevented because it can cause an ignition.

REFERENCES

1. World Steel Association, Steel Statistical Yearbook 2008, accessed 23 March 2010, http://www.worldsteel.org/pictures/publicationfiles/SSY2008[1].pdf

2. A. Chatterjee, *Beyond the Blast Furnace* (Boca Raton, FL: CRC press, 1993), pp. 1-6.

3. C. P. Manning and R. J. Fruehan, "Emerging Technologies for Iron and Steelmaking," *JOM*, 53 (10) (2001), pp. 36-43.

4. R. J. Fruehan, "Fruehan: Blast-Furnace Output Will Continue To Fall," *New Steel*, 14 (5) (1998), pp. 34-37.

5. A. Ritt, "Reaching for Maximum Flexibility," *New Steel*, 16 (1) (2000), pp. 20-26.

6. Lockwood Greene Technologies, "Ironmaking Process Alternatives Screening Study" (Report LG Job No. 010529.01, U.S. Department of Energy, 2000), accessed 23 March 2010, http://www1.eere.energy.gov/industry/steel/pdfs/ironmaking_process.pdf

7. H. Y. Sohn, "Suspension Ironmaking Technology with Greatly Reduced Energy Requirement and CO_2 Emission," *Steel Times International*, May/June (2007), pp. 68-72.

8. H. Y. Sohn, "Suspension Hydrogen Reduction of Iron Ore Concentrate" (Final Report TRP9953NonPropFinalReport, U.S. Department of Energy, American Iron and Steel Institute, 31 March 2008), available from Office of Scientific and Technical Information, P.O. Box 62, Oak Ridge, TN 37831, Tel: (865) 576-8401, Fax: (865) 576-5728, E-mail: reports@osti.gov, http://www.osti.gov/contract.html.

9. L. von Bogdandy and H. -J. Engell, *The Reduction of Iron Ores – Scientific Basic and Technology* (Berlin, Germany: Springer-Verlag, 1971), p. 230.

10. C. L. -O. Iheagwara, "Reduction of Taconite Concentrates in Plasma Reactors" (Ph.D. thesis, University of Minnesota, 1989).

11. M. Naito, "Development of Ironmaking Technology" (Nippon Steel Technical Report No. 94, July 2006).

12. M. D. Fenton, 2008 Minerals Yearbook - Iron and Steel, U.S. Geological Survey, accessed 23 March 2010, http://minerals.usgs.gov/minerals/pubs/commodity/iron_& _steel/

13. P. J. R. Chowdhury, "DRI - An Alternative Amongst Many," *International Conference on Alternative Routes of Iron and Steelmaking (ICARISM)*, ed. V. N. Misra and R. J. Holmes (Victoria, Australia: The Australasian Institute of Mining and Metallurgy, 1999), pp. 215-218.

14. H. U. Chang-qing, C. Li-yun, Z. Chun-xia, Q. Yuan-hong, and Y. Rui-yu, "Emission Mitigation of CO_2 in Steel Industry - Current Status and Future Scenarios," *Journal of Iron and Steel Research International*, 13 (6) (2006), pp. 38-42.

15. C. K. Gupta and D. Sathiyamoorthy, *Fluid Bed Technology in Materials Processing* (Boca Raton, FL: CRC Press, 1999), p. 171.

16. J. Feinman, "Chapter 11. Direct Reduction and Smelting Processes," *The Making, Shaping and Treating of Steel, 11th ed. - Ironmaking Volume*, ed. D. H. Wakelin (Pittsburgh, PA: The AISE Steel Foundation, 1999), pp. 741-779.

17. R. Cheeley, "Gasification and the MIDREX Direct Reduction Process" (Paper presented at 1999 Gasification Technologies Conference, San Francisco, CA, 17-20 October 1999).

18. R. Quintero, "Operational Results of HYL III Process," *Skillings' Mining Review* (April 1981), pp. 12-17.

19. W. O. Philbrook, "A Close Look at HYL III Process in Operation," *Iron and Steelmaker* (August 1982), pp. 12-14.

20. R. Quintero, "HYL III: Status and Trends" (Paper presented at Gorham/Intertech Conference on Iron & Steel Scrap, Scrap Substitutes and Direct Steel Making, Atlanta, GA, 21-23 March 1995).

21. R. Steffen, "The COREX Process: First Operating Results in Hot-Metal Making," *Metallurgical Plant and Technology*, 13 (2) (1990), pp. 20-23

22. R. B. Smith, "Alternative Ironmaking Technology," *Metals and Materials*, 8 (9) (1992), pp. 491-494.

23. S. Joo, M. K. Shin, M. Cho, S. D. Lee, J. H. Lee, and I. O. Lee, "Direct Use of Fine Iron Ore in the COREX Process," *Iron and Steelmaker* (July 1998), pp. 39-43.

24. A. Eberle, W. Bohrn, K. Milionis, G. Tessmer, and J. Reidetschläger, "Smelting

Reduction and Direct Reduction of Iron Ores VAI Technologies for Scrap Substitutes (COREX, FINMET, FINEX),” *International Conference on Alternative Routes of Iron and Steelmaking (ICARISM)*, ed. V. N. Misra and R. J. Holmes (Victoria, Australia: The Australasian Institute of Mining and Metallurgy, 1999), pp. 201-211.

25. S. Joo, H. G. Kim, I. O. Lee, J. L. Schenk, U. R. Gennari, and F. Hauzenberger, “FINEX: a New Process for Production of Hot Metal from Fine Ore and Coal,” *Scandinavian Journal of Metallurgy*, 28 (4) (1999), pp. 178-183.

26. I. O. Lee, M. K. Shin, M. Cho, H. G. Kim, and H. G. Lee, “Energy and Pollutants Reducing Technologies in New Ironmaking Processes at POSCO,” *ISIJ International*, 42 (2002), pp. S33-S37.

27. K. Wieder, C. Böhn, J. Wurm, and B. Vuletic, “Confronting the Coke Shortage with the COREX and FINEX Technology,” *Berg- und Huettenmaennische Monatshefte (BHM)*, 149 (11) (2004), pp. 379-384.

28. F. Hauzenberger, J. Reidetschläger, J. L. Schenk, and H. Mali, “Methods for Assessing the Properties of Fine Iron Ores for Reduction Processes,” *Berg- und Huettenmaennische Monatshefte (BHM)*, 149 (11) (2004), pp. 385-392.

29. G. Peer, “FINMET and FINEX: Fluidized-Bed Applications for Iron Production,” *Industrial Fluidization South Africa (IFSA)*, ed. A. Luckos and P. Smit (Johannesburg, South Africa: South African Institute of Mining and Metallurgy, 2005), pp. 245-255.

30. A. D. Brent, P. L. J. Mayfield, and T. A. Honeyands, “The Port Hedland FINMET Project - Fluid Bed Production of High Quality Virgin Iron for the 21st Century,” *International Conference on Alternative Routes of Iron and Steelmaking (ICARISM)*, ed. V. N. Misra and R. J. Holmes (Victoria, Australia: The Australasian Institute of Mining and Metallurgy, 1999), pp. 111-114.

31. A. Hassan, R. Whipp, K. Milionis, and S. Zeller, “Development of an Improved Fluid Bed Reduction Process,” *Proceedings of the Annual ISS Ironmaking Conference* (Warrendale, PA: The Iron & Steel Society, 1994), pp. 481-490.

32. W. Bresser, P. Weber, and J. Bonestell, “Circored and Circofer: State-of-the-Art Technology for Low Cost Direct Reduction,” *68th Annual Meeting of the Minnesota Section, SME* (Duluth, MN: University of Minnesota, Center for Professional Development, 1995), pp. 17-27.

33. R. W. von Bitter, R. Husain, P. Weber, and H. Eichberger, “Experiences with Two New Fine Ore Reduction Processes - Circored and Circofer,” *International Conference*

on New Developments in Metallurgical Process Technology (Dusseldorf, Germany: Verein Deutscher Eisenhuettenleute, 1999), pp. 9-16.

34. R. Husain, S. Sneyd, and P. Weber, "Circored and Circofer Two New Fine Ore Reduction Processes," *International Conference on Alternative Routes of Iron and Steelmaking (ICARISM)*, ed. V. N. Misra and R. J. Holmes (Victoria, Australia: The Australasian Institute of Mining and Metallurgy, 1999), pp. 123-129.

35. T. J. Considine, C. Jablonowsk, and D. M. M. Considine, "The Environment and New Technology Adoption in the US Steel Industry" (Report National Science Foundation & Lucent Technologies Industrial Ecology Research Fellowship BES-9727297, 2001)

36. M. Komatina and H. -W. Gudenau, "The Sticking Problem during Direct Reduction of Fine Iron Ore in the Fluidized Bed," *Metalurgija – Journal of Metallurgy (MJoM)*, 10 (4) (2004), pp. 309- 328.

37. A. Morrison, S. Hietkamp, and D. S. van Vuuren, "Direct Reduction Process Using Fines and With Reduced CO_2 Emission," *Ironmaking and Steelmaking*, 31 (4) (2004), pp. 285-290.

38. T. Sharma, R. C. Gupta, and B. Prakash, "Swelling of Iron Ore Pellets by Statistical Design of Experiment," *ISIJ International*, 32 (12) (1992), pp. 1268-1275.

39. T. Sharma, R. C. Gupta, and B. Prakash, "Effect of Firing Condition and Ingredients on the Swelling Behaviour of Iron Ore Pellets," *ISIJ International*, 33 (4) (1993), pp. 446-453.

40. T. Sharma, "Swelling of Iron Ore Pellets under Non-Isothermal Condition," *ISIJ International*, 34 (12) (1994), pp. 960-963.

41. M. Singh and B. Björkman, "Swelling Behaviour of Cement-Bonded Briquettes-Proposed Model," *ISIJ International*, 44 (3) (2004), pp. 482-491.

42. J. D. Jorgenson, 2007 Minerals Yearbook - Iron Ore, U.S. Geological Survey, accessed 23 March 2010, http://minerals.usgs.gov/minerals/pubs/commodity/iron_ore/

43. J. D. Jorgenson, 2010 Mineral Commodity Summaries - Iron Ore, U.S. Geological Survey, accessed 23 March 2010, http://minerals.usgs.gov/minerals/pubs/commodity/iron_ore/

44. J. J. Poveromo, "Chapter 8. Iron Ores," *The Making, Shaping and Treating of Steel, 11th ed. - Ironmaking Volume*, ed. D.H. Wakelin (Pittsburgh, PA: The AISE (Association

of Iron and Steel Engineers) Steel Foundation, 1999), pp. 547-642.

45. Mineral Information Institute, “Iron Ore: Hematite, Magnetite & Taconite,” accessed 23 March 2010, http://www.mii.org/Minerals/photoiron.html

46. J. J. Poveromo, “Chapter 5. Iron-Bearing Raw Materials for Direct Reduction,” *Direct Reduced Iron – Technology and Economics of Production and Use*, ed. J. Feinman and D. R. MacRae (Warrendale, PA: The Iron & Steel Society, 1999), pp. 59-79.

47. S. C. T. Trang, “Environmental Assessment of Iron Ore Agglomeration Processes,” *Green Processing Conference* (Victoria, Australia: The Australasian Institute of Mining and Metallurgy, 2006), pp. 155-161.

48. K. Yamaguchi, H. Ueno, M. Naito, and K. Tamura, “Maximum Injection Rate of Fine Ore into Blast Furnace through Tuyeres,” *ISIJ International*, 31 (7) (1991), pp. 677-684.

49. I. F. Kurunov, “Prospects for the Use of Non-Agglomerated Iron-Bearing Materials in the Blast Furnace,” *Metallurgist*, 47 (5-6) (2003), pp. 179-191.

50. W. -K. Lu, “The Search for an Economical and Environmentally Friendly Ironmaking Process,” *Metallurgical and Materials Transactions B*, 32B (5) (2001), pp. 757-762.

51. Commission of the European Communities, *Direct Reduction of Iron Ore – A Bibliographical Survey* (London, UK: The Metals Society, 1979), pp. 316-325.

52. N. J. Themelis and B. Zhao, “Flash Reduction of Metal Oxides,” *Flash Reaction Processes*, ed. T. W. Davies (Dordrecht, Netherlands: Kluwer Academic Publishers, 1995), pp. 273-293.

53. R. W. Bartlett, “Flash Melting and Partial Reduction of Iron Ore Concentrates,” *Flash Reaction Processes*, ed. D. G. C. Robertson, H. Y. Sohn, and N. J. Themelis (Rolla, MO: University of Missouri-Rolla, The Center for Pyrometallurgy, 1988), pp. 391-404.

54. P. R. Taylor, M. Abdel-latif, and R. W. Bartlett, “Reduction of Taconite Concentrates in a Cyclone Reactor,” *Minerals and Metallurgical Processing*, 11 (4) (1994), pp. 203-209.

55. T. W. Johnson and J. Davison, “Reduction of Iron Ore by the Flame-Smelting Process,” *Journal of the Iron and Steel Institute*, 202 (1964), pp. 406-419.

56. P. E. Cavanagh, “Method for Jet Smelting,” U.S. Patent 2,951,756 (6 September 1960).

57. R. L. Cavanagh, “Progress in the Development of the Jet Smelting Process,” *Iron Ore*

Reduction, Proceedings of a Symposium of the Electrochemical Society, ed. R. R. Rogers (Oxford, UK: Pergamon Press, 1962), pp. 221-240.

58. In Ref. 51, pp. 531-537.

59. G. Kazonich, T. P. Gribben, J. W. Walkiewicz, and A. E. Clark, "Reduction of Iron Oxides in a Novel Reactor Utilizing Rocket Technology," *The Paul E. Queneau International Symposium, Extractive Metallurgy of Copper, Nickel and Cobalt*, ed. R. G. Reddy and R. N. Weizenbach (Warrendale, PA: The Minerals, Metals & Materials Society, 1993), pp. 1125-1132.

60. J. A. Burgo, "Chapter 10. The Manufacture of Pig Iron in the Blast Furnace," *The Making, Shaping and Treating of Steel, 11th ed. - Ironmaking Volume,* ed. D. H. Wakelin (Pittsburgh, PA: The AISE Steel Foundation, 1999), pp. 699-739.

61. L. Barreto, A. Makihira, and K. Riahi, "The Hydrogen Economy in the 21st Century: A Sustainable Development Scenario," *International Journal of Hydrogen Economy*, 28 (3) (2003), pp. 267-284.

62. U.S. Department of Energy and U.S. Department of Transportation, "Hydrogen Posture Plan - An Integrated Research, Development and Demonstration Plan" (2006), accessed 23 March 2010, http://www.hydrogen.energy.gov/pdfs/hydrogen_posture_plan_dec06.pdf

63. A. Pineau, "Kinetics of Reduction of Iron Oxides by H_2 Part I: Low Temperature Reduction of Hematite," *Thermochimica Acta*, 447 (2006), pp. 89-100.

64. W. -K. Lu, "The Impact of the Environmental Concerns on the Development of Ironmaking Technology," *Acta Metallurgica Sinica*, 33 (2) (1997), pp. 207-212.

65. T. R. Karl, J. M. Melillo, and T. C. Peterson, *Global Climate Change Impacts in the Unites States* (Cambridge, NY: Cambridge University Press, 2009), accessed 23 March 2010, http://globalchange.gov/publications/reports/scientific-assessments/us-impacts/full-report

66. T. Emi and S. Seetharaman, "Future Steelmaking Plant with Minimized Energy Consumption and Waste Evolution," *Scandinavian Journal of Metallurgy*, 29 (2000), pp. 185-193.

67. Y. Kim and E. Worrell, "International Comparison of CO_2 Emission Trends in the Iron and Steel Industry," *Energy Policy*, 30 (2002), pp. 827-838.

68. D. Gielen, "CO_2 Removal in the Iron and Steel Industry," *Energy Conversion and*

Management, 44 (2003), pp. 1027-1037.

69. K. -H. Tacke and R. Steffen, "Hydrogen for the Reduction of Iron Ores - State of the Art and Future Aspects," *Stahl und Eisen*, 124 (4) (2004), pp. 45-52.

70. K. Meijer, M. Denys, J. Lasar, J. -P. Birat, G. Still, and B. Overmaat, "ULCOS: Ultra-Low CO_2 Steelmaking," *Ironmaking and Steelmaking*, 36 (4) (2009), pp. 249-251.

71. D. Burchart-Korol, "New Technologies to Reduce CO_2 Emissions from Steel Plants," *Hutnik-Wiadomości Hutnicze*, 76 (9) (2009), pp. 708-712.

72. In Ref. 9, pp. 251-253.

73. S. Luidold and H. Antrekowitsch, "Hydrogen as a Reducing Agent: Thermodynamic Possibilities," *JOM*, 59 (10) (2007), pp. 58-62.

74. T. Uetani and N. Bessho, "Ironmaking and Steelmaking Technologies as Fundamentals for the Steel Production," *Kawasaki Seitetsu Giho*, 32 (3) (2000), pp. 183-190.

75. J. A. Turner, "Sustainable Hydrogen Production," *Science*, 305 (5686) (2004), pp. 972-974.

76. International Atomic Energy Agency, "Hydrogen as an Energy Carrier and Its Production by Nuclear Power" (Report IAEA-TECDOC-1085, 1999).

77. L. Walters, D. Wade, and D. Lewis, "Transition to a Nuclear/Hydrogen Energy System," *Nuclear Energy*, 42 (1) (2003), pp. 55-62.

78. J. M. Ogden, "Hydrogen as an Energy Carrier: Outlook for 2010, 2030 and 2050," (Paper presented at The Pew Center/NCEP 10-50 Workshop, Washington, DC, 25 March 2004).

79. C. W. Forsberg, "Future Hydrogen Markets for Large-Scale Hydrogen Production Systems," *International Journal of Hydrogen Energy*, 32 (2007), pp. 431-439.

80. D. Lewis, "Hydrogen and Its Relationship with Nuclear Energy," *Progress in Nuclear Energy*, 50 (2008), pp. 394-401.

81. W. Wenzel, "Ironmaking with the Aid of Nuclear Energy," *Proceedings of the International Conference on Science and Technology of Iron and Steel* (Tokyo, Japan: Iron and Steel Institute of Japan, 1971), pp. 206-212.

82. M. -Y. Cho, "POSCO Aims to Halt CO_2 via Hydrogen Steelmaking," *Reuters* (27 November 2009), accessed 23 March 2010, http://www.reuters.com/article/

idUSSEO205120091127

83. H. Park, “POSCO CO_2 Breakthrough Solutions Towards Sustainable Steel Industry” (Presented at New Earth 2008 - International Symposium on Technologies for Mitigating Global Warming, Osaka, Japan, 27 November 2008), accessed 23 March 2010, http://www.rite.or.jp/Japanese/kicho/ne2008kekka/05Park.pdf

84. M. H. Chang, S. K. Sim, and D. J. Lee, “SMART Behavior under Over-Pressurizing Accident Conditions,” *Nuclear Engineering and Design*, 199 (2000), pp. 187-196.

85. S. W. Lee, S. H. Kim, and Y. J. Chung, “Development and Steady State Level Experimental Validation of TASS-SMR Core Heat Transfer Model for the Integral Reactor SMART,” *Annals of Nuclear Energy*, 36 (2009), pp. 1039-1048.

86. N. J. Themelis and W. H. Gauvin, “A Generalized Rate Equation for the Reduction of Iron Oxides,” *Transactions of the Metallurgical Society of AIME*, 227 (1963), pp. 290-230.

87. N. J. Themelis and W. H. Gauvin, “Reduction of Iron Oxide in Gas-Conveyed Systems,” *AIChE Journal*, 8 (4) (1962), pp. 437-444.

88. E. G. Davis and I. L. Feld, “Flash Reduction of Iron Ore” (Report of Investigation 7627, U.S. Department of the Interior and Bureau of Mines, 1972).

89. H. Y. Sohn, University of Utah, Salt Lake City, Utah, personal communication, 2004.

90. S. Y. M. Ezz and R. Wild, “The Gaseous Reduction of Fine Iron Ores,” *Journal of the Iron and Steel Institute*, 194 (1960), pp. 211-221.

91. J. Szekely, J. W. Evans, and H. Y. Sohn, *Gas-Solid Reactions* (New York, NY: Academic Press, 1976), 400 pp.

92. M. Fuji, K. Otsuka, A. Yoshizhwa, and T. Soma, “Hydrogen Reduction of Ferric Oxide Powders in Dilutely Gas-Conveyed System,” *Journal of the Faculty of Engineering, the University of Tokyo*, A (10) (1972), pp. 62-63.

93. S. Hayashi and Y. Iguchi, “Hydrogen Reduction of Liquid Iron Oxide Fines in Gas-Conveyed Systems,” *ISIJ International*, 34 (7) (1994), pp. 555-561.

94. Y. Nomura, H. Nakagawa, T. Maeda, K. Nishioka, and M. Shimizu, “Rapid Reduction of Fine Iron Ore Transported with CH_4 Gas,” *Journal of the Iron and Steel Institute of Japan*, 91 (6) (2005), pp. 521-527.

95. N. Takeuchi, Y. Nomura, K. Ohno, T. Maeda, K. Nishioka, and M. Shimizu, “Kinetic

Analysis of Spherical Wüstite Reduction Transported with CH_4 gas," *ISIJ International*, 47 (3) (2007), pp. 386-391.

96. C. O. Bounds and J. F. Pusateri, "EAF Dust Processing in the Gas-Fired Flame Reactor Process," *Lead-Zinc '90, Proceedings of a World Symposium on Metallurgy and Environmental Control, 119th TMS Annual Meeting*, ed. T. S. Mackey and R. D. Prengaman (Warrendale, PA: The Minerals, Metals & Materials Society, 1990), pp. 511-528.

97. J. M. Svoboda, "Plasma and Flame Reactor Treatment of Electric Arc Furnace Dust," *Transactions of the American Foundrymen's Society*, 99 (1991), pp. 405-409.

98. Outokumpu HSC Chemistry 5.1 for Windows – Chemical Reaction and Equilibrium Software with Extensive Thermochemical Database (Pori, Finland: Outokumpu Research Oy)

99. H. Hiebler and J. F. Plaul, "Hydrogen Plasma Smelting Reduction - An Option for Steelmaking in the Future," *Metalurgija*, 43 (3) (2004), pp. 155-162.

100. Energetics, Inc., "Energy and Environmental Profile of the US Iron and Steel Industry" (Report DOE/ EE-0229, U.S. Department of Energy, 2000), accessed 23 March 2010, http://www1.eere.energy.gov/industry/steel/pdfs/steel_profile.pdf

101. L. Price, J. Sinton, E. Worrell, D. Phylipsen, H. Xiulian, and L. Ji, "Energy Use and Carbon Dioxide Emissions from Steel Production in China," *Energy*, 27 (2002), pp. 429-446.

102. G. Wingrove, B. Keenan, D. Satchell, and C. van Aswegen, "Developments in Ironmaking and Opportunities for Power Generation" (Paper presented at 1999 Gasification Technologies Conference, San Francisco, CA, 17-20 October 1999).

103. J. Stubbles, "Energy Use in the U.S. Steel Industry: An Historical Perspective and Future Opportunities" (U.S. Department of Energy, September 2000), accessed 23 March 2010, www1.eere.energy.gov/industry/steel/pdfs/steel_energy_use.pdf

104. R. J. Fruehan, O. Fortini, H. W. Paxton, and R. Brindle, "Theoretical Minimum Energies to Product Steel for Selected Conditions" (U.S. Department of Energy, May 2000), accessed 23 March 2010, http://www1.eere.energy.gov/industry/steel/pdfs/theoretical_minimum_
energies.pdf

105. H. G. Mcllvried and F. E. Massoth, "Effect of Particle Size Distribution on Gas-

Solid Reaction Kinetics for Spherical Particles," *Industrial & Engineering Chemistry Fundamentals*, 12 (2) (1973), pp. 225-229.

106. J. Szekely and N. J. Themelis, *Rate Phenomena in Process Metallurgy* (New York, NY: Wiley-Interscience, 1971), pp. 606-608.

107. F. Durst, S. Ray, B. Ünsal, and O. A. Bayoumi, "The Development Lengths of Laminar Pipe and Channel Flows," *Transactions of the ASME*, 127 (6) (2005), pp. 1154 – 1160.

108. H. Y. Sohn, "The Coming-of-Age of Process Engineering in Extractive Metallurgy," *Metallurgical Transactions B*, 22B (1991), pp. 737-754.

109. M. Pérez-Tello, "Experimental Investigation and Computer Simulation of the Continuous Flash Converting Process of Solid Copper Mattes" (Ph.D. thesis, University of Utah, 1999).

110. International Standard, *Direct Reduced Iron - Determination of Metallic Iron - Bromine-Methanol Titrimetric Method, ISO 5416, 3rd ed.*, (Geneva, Switzerland: International Organization for Standardization, 2006).

111. In Ref. 9, p. 36.

112. E. T. Turkdogan, R. G. Olsson, and J. V. Vinters, "Gaseous Reduction of Iron Oxides: Part II. Pore Characteristics of Iron Reduced from Hematite in Hydrogen," *Metallurgical Transactions*, 2 (1971), pp. 3189-3196.

113. C. G. Davis, J. F. McFarlin, and H. R. Pratt, "Direct-Reduction Technology and Economics," *Ironmaking and Steelmaking*, 9 (3) (1982), pp. 93-129.

114. H. B. Lüngen, K. Knop, and R. Steffen, "State of the Art of the Direct Reduction and Smelting Reduction Processes," *Stahl und Eisen*, 126 (7) (2006), pp. 25-40.

115. H. Y. Sohn, "Gas-Solid Suspension Ironmaking Technology" (Annual Report, American Iron and Steel Institute, 23 January 2009).